METHODOLOGY FOR MITIGATION OF SEISMIC HAZARDS IN EXISTING UNREINFORCED MASONRY BUILDINGS

PHASE I

S. A. Adham

R. D. Ewing

March 1978

Prepared under
National Science Foundation Contract No. C-AEN77-19829

AGBABIAN ASSOCIATES
El Segundo, California

50272-101

REPORT DOCUMENTATION PAGE	1. REPORT NO. NSF/RA-780131	2.	3. Recipient's Accession No. PB287898

4. Title and Subtitle Methodology for Mitigation of Seismic Hazards in Existing Unreinforced Masonry Buildings, Phase 1	5. Report Date March 1978
	6.
7. Author(s) S.A. Adham, R.D. Ewing	8. Performing Organization Rept. No.
9. Performing Organization Name and Address Agbabian Associates El Segundo, California 90245	10. Project/Task/Work Unit No.
	11. Contract(C) or Grant(G) No. (C) AEN7719829 (G)
12. Sponsoring Organization Name and Address Applied Science and Research applications (ASRA) National Science Foundation 1800 G Street, N.W. Washington, DC 20550	13. Type of Report & Period Covered
	14.

15. Supplementary Notes

16. Abstract (Limit: 200 words) A multiphased program is initiated to develop a methodology for the mitigation of seismic hazards in existing unreinforced masonry (URM) buildings. The present research, part of Phase 1, identifies trends in the seismic response of the components of URM buildings and determines what studies and testing are necessary to arrive at a methodology that can be used nationwide. The response of plywood, diagonal-sheathed, and straight-sheathed diaphragms, represented by lumped-mass mathematical models, was studied. Experimental data on static loading and unloading were used. Both local and distant earthquake ground motions were used as inputs. The results show a strong dependence of the diaphragm response on the long-period content of the input. The response of masonry walls subjected to in-plane earthquake ground motion was also studied. The analytical results show that the model used can reasonably predict the response of the wall as a function of its height-to-width ratio and of the stiffness of the supporting soil. The report evaluates methods for selecting earthquake ground-motion input at a site in the United States and describes analysis methods that can be used to determine the response of URM buildings to earthquake forces.

17. Document Analysis a. Descriptors

Earthquakes
Earthquake resistant structures
Seismology
Mathematical models
Earth movements
Masonry
Hazards

b. Identifiers/Open-Ended Terms

Seismic hazards
Unreinforced masonry (URM)

c. COSATI Field/Group

18. Availability Statement	19. Security Class (This Report)	21. No. of Pages
NTIS		93
	20. Security Class (This Page)	22. Price

(See ANSI-Z39.18) See Instructions on Reverse

OPTIONAL FORM 272 (4-77)
(Formerly NTIS-35)
Department of Commerce

ACKNOWLEDGMENTS

This research effort has been supported by the National Science Foundation under Contract No. C-AEN77-19829. The support is gratefully acknowledged.

Primary contributors to this work were R.D. Ewing, Principal Investigator, and S.A. Adham, Project Engineer. Staff members from Agbabian Associates who also supported the work were H.S. Ts'ao, K.T. Dill, and E.M. Dombourian. J.D. Radler edited the final report, and M.S. Agbabian and R.W. Anderson contributed suggestions throughout the program.

SUMMARY

Existing unreinforced masonry (URM) buildings are considered the largest single earthquake hazard today. Nevertheless, no nationally accepted structural engineering standards provide guidelines for retrofitting these buildings to improve their earthquake resistance. The National Science Foundation has therefore initiated a multiphased program to develop a methodology for the mitigation of seismic hazards in existing URM buildings.

The present research, part of Phase I, has concentrated primarily on identifying trends in the seismic response of the components of URM buildings; and on determining what studies and testing are necessary to arrive at a methodology that can be used nationwide.

The response of plywood, diagonal-sheathed, and straight-sheathed diaphragms, represented by lumped-mass mathematical models, was studied. Experimental data on static loading and unloading were used. Both local and distant earthquake ground motions were used as inputs. The results show a strong dependence of the diaphragm response on the long-period content of the input.

The response of masonry walls subjected to in-plane earthquake ground motion was also studied. The analytical results show that the model used can reasonably predict the response of the wall as a function of its height-to-width ratio and of the stiffness of the supporting soil.

The report evaluates methods for selecting earthquake ground-motion input at a site in the United States and describes analysis methods that can be used to determine the response of URM buildings to earthquake forces.

This part of Phase I, combined with the interrelated studies of two other investigators, lays a foundation for the more specific experimental and analytical studies recommended for Phase II.

CONTENTS

CONTENTS (CONTINUED)

ILLUSTRATIONS

ILLUSTRATIONS (CONTINUED)

ILLUSTRATIONS (CONTINUED)

ILLUSTRATIONS (CONCLUDED)

TABLES

SECTION 1

INTRODUCTION

1.1 STATEMENT OF THE PROBLEM

Unreinforced masonry (URM) construction has been widely used throughout the United States. The majority of such buildings existing today were constructed more than 50 years ago, some before the turn of the century. Evaluation of overall damage from high intensity earthquakes indicates that existing URM buildings constitute the greatest single-hazard category. Concern for the safety of these structures in seismically active regions has been increasing as public agencies and the private sector become more conscious of the potential hazards when such structures are subjected to earthquake shaking and of the potential liability of injury or loss of life. The socioeconomic implications of property damage and the resulting disruption and dislocation are also significant cause for concern.

It was hoped that normal attrition would slowly reduce the hazards presented by the existing URM buildings. In recent years, however, it has become apparent that an increase in the salvaging and retrofitting of existing URM buildings for further use has slowed the attrition rate of these hazards.

Some of the existing URM buildings have suffered earthquake damage. Others, experiencing an identical intensity of shaking, have been unscathed. As a result, governing agencies and the building owners differ considerably in their opinions about the need for increasing the seismic resistance of such structures.

The formulation of design methods and criteria is needed for determining (1) which structures actually require hazard mitigation and (2) what methods of retrofit should be used. Even in areas of the United States where no mandatory regulations for earthquake protection exist, the concern is rising for some definition of the minimum level of protection in zones of differing seismic activity. The City of Long Beach, California, passed an ordinance that requires evaluation of old concrete masonry structures and regulation of new concrete masonry construction. A preliminary survey of existing buildings in the City of Los Angeles indicates that approximately 10,000 URM buildings need to be evaluated for seismic hazards.

Research has been conducted on the strength and material behavior of existing URM construction to develop a better understanding of variations in strength and stiffness that can be expected in this type of construction.

Research on modeling masonry structures and determining their dynamic response to high-intensity earthquakes is in its early stages.

Major efforts have been launched by several agencies to establish criteria for seismic risk and seismic design input for different types of buildings in various zones of the United States.

Full-scale tests of existing buildings under low-amplitude vibrations have been conducted. These tests are being extended to high-amplitude vibrations. An attempt is being made to correlate the results obtained by analytical modeling with the response of structures during large shaking tests or actual earthquake events.

The National Science Foundation (NSF) has initiated a program to develop methodology for mitigation of seismic hazards in existing unreinforced masonry buildings. The overall objectives of this multiphase program are (1) to evaluate the current state of the art for mitigating the seismic hazards of existing URM buildings, (2) to develop a methodology for mitigation of these hazards, (3) to evaluate the methodology, and (4) to conduct a utilization plan for disseminating the information assembled by the total program effort.

1.2 PURPOSE AND SCOPE OF RESEARCH PROGRAM

In October 1977, three of the contracts awarded by the NSF for a Phase I program were given to Agbabian Associates (AA), S.B. Barnes and Associates (SB&A), and Kariotis, Kesler, and Allys (KK&A). With NSF's concurrence, the three firms planned an interactive six-month effort to fulfill the following tasks:

a. Evaluate the current state of the art for seismic-hazard mitigation in existing URM buildings.

b. Conduct a nationwide survey of different types of existing masonry construction.

c. Determine what studies and testing are necessary to arrive at a methodology that can be used nationwide for mitigating seismic hazards in existing URM buildings and to develop structural and economic criteria for any required retrofitting of existing masonry buildings.

The three firms conducted weekly meetings to collaborate in all studies conducted for Phase I. However, each firm assumed the prime responsibility of some tasks. For example, SB&A developed an experimental and analytical program for studying selected retrofit methods. KK&A categorized types of existing URM construction in various seismic zones of the United States, and investigated material properties, critical building components, and current structural alteration methods. AA was primarily concerned with the development of earthquake input ground motions, the selection of seismic-response analyses methods, and the development of an experimental and analytical program for studying static and dynamic behavior of critical components of URM buildings.

Phase I has been essentially an exploratory program. The data base resulting from this phase will guide the more specific experimental and analytical work to be proposed for the Phase II program.

1.3 SUMMARY OF RESULTS

During Phase I, the research effort has been primarily directed towards identifying trends in seismic response of components of URM buildings and identifying areas that need more experimental and analytical work, therefore warranting further studies. It was concluded that ATC-3* provides the state-of-the-art tool for describing the ground shaking at various sites in the United States. (However, an ensemble of time-history records, rather than elastic response spectra, should be selected for sites to be studied in Phase II of this program.) Earthquake ground-motion input at a site is discussed and analysis methods used to determine the response of buildings to earthquake forces are described. It was concluded that the STARS† computer program should be used for this study.

The response of plywood, diagonal-sheathed, and straight-sheathed wood diaphragms was studied using a lumped parameter model. Experimental data on monotonic loading and unloading of wood diaphragms were idealized. A hysteretic stress/strain relationship was included in the model and viscous damping was added to the analyses of some cases. Local and distant earthquake input ground motion were represented by the 1971 Castaic and 1940 El Centro records, respectively. Both records were scaled to the 0.40 g level specified for ground shaking in the Los Angeles area and were applied to the model. The model is described in detail and the analyses results are discussed.

These example analyses show three particularly important trends. First, the wood diaphragms have relatively long periods. Second, the response of these diaphragms strongly depends on the long-period content of the input earthquake motions. Third, straight-sheathed diaphragms tend to attenuate earthquake motions, as compared to the plywood and diagonal-sheathed diaphragms.

---

*The Applied Technology Council's 1977 report *Recommended Comprehensive Seismic Design Provisions for Buildings.*

†STARS is a lumped parameter computer program developed by Agbabian Associates for the dynamic analysis of nonlinear structural systems (*User's Guide for STARS Code*, R-6823-999, Agbabian-Jacobsen Associates, Los Angeles, 1969).

The response of masonry walls, supported on soil to in-plane earthquake ground motions was studied using a lumped parameter model. Results from the analyses, detailed in Section 5, show a particularly important trend: walls with height-to-width ratios equal to or greater than 1, on soft soil, would amplify the input earthquake motions.

Phase I represents only the first step in the development of a general methodology for carrying out analyses and evaluation of various components of existing URM buildings. Possible subsequent steps of Phase II are (1) selecting an ensemble of time histories for the analyses that relate to ATC-3 standard spectra, (2) extending and refining the diaphragm and wall-overturning analyses of Phase I, (3) conducting an experimental program on diaphragms to include both pseudo-static and -dynamic input (these tests would provide data for correlation with the results of the analyses of Phases I and II), (4) studying the effect of out-of-plane forces on the response of URM walls of different height-to-depth ratios, (5) evaluating the torsional capabilities of diaphragms, and (6) applying the methodology to a single and multistory URM building and evaluating the results.

1.4 REPORT ORGANIZATION

This report is organized in seven sections. Section 2 summarizes significant studies of masonry buildings. The consideration leading to the choice of design earthquake and the related capabilities of the buildings is given in Section 3. The analytical methods used to determine the response of buildings to earthquake forces are given in Section 4. Example analyses of diaphragms and masonry-wall rocking due to earthquake excitation are given in Section 5. Conclusions reached from the Phase I study and recommendations for a Phase II study are given in Section 6. The report concludes with the references listed in Section 7.

SECTION 2

PRIOR STUDIES OF MASONRY BUILDINGS

During Phase I of this program, a brief review of prior studies of masonry buildings was conducted to (1) evaluate the current state of knowledge in this area, and (2) use this information in the planning and development of the present research program including a Phase II proposal and utilization plan. Procedures and results from these studies are briefly summarized in this section. Comprehensive surveys of the available literature relevant to the mechanics of concrete masonry assemblies can be found in References 1 and 2.

Two separate major research programs were recently conducted to investigate the earthquake response of concrete-masonry buildings. The first program was conducted as a consortium research effort under the sponsorship of the National Science Foundation (NSF). The host institution for this program is the University of California, San Diego (UCSD). Participating institutions during the first phase were San Diego State University, Weidlinger Associates, and Agbabian Associates. The second program was conducted at the University of California, Berkeley (UCB), and was jointly sponsored by NSF and the Masonry Institute of America.

The preliminary investigations that preceded the research program at UCSD included a study of two multistory concrete-masonry buildings, constructed in San Diego County (Refs. 3, 4). The purpose of the study was to provide the predicted behavior of these buildings when subjected to earthquake ground motions and to determine whether these structures would experience severe damage if subjected to earthquake ground motion of a strength consistent with that which could reasonably be expected to occur during the planned life of the structure.

The first building had a relatively symmetric shape while the second building was highly asymmetric. A large eccentricity existed between the mass center and the center of rigidity of the asymmetric building. The transverse section of the first building and the plan of the second building are shown in Figures 2-1 and 2-2. All walls, with minor exceptions, were constructed of 8-in. reinforced concrete masonry, generally fully grouted up to the ninth floor.

A large-capacity digital computer program for two- and three-dimensional analysis of structural systems using the finite element approach was used to obtain the dynamic response of the two buildings to earthquake excitation. The analysis results indicated that the structures are stiff and walls would be subjected to several cycles of overstress. It was concluded that these walls would be badly damaged and would probably collapse if subjected to the seismic loads considered in the study. The results of this study indicated that more research is needed to provide better understanding of the behavior of concrete masonry in highly seismic zones. The study also indicated that some provisions of the present concrete masonry codes should be carefully evaluated.

The UCSD program (Refs. 5 and 6) involved a series of laboratory experiments designed to determine the linear and nonlinear behavior of reinforced and unreinforced concrete masonry blocks and joints (i.e., triplets, Fig. 2-3), and assemblies of blocks (i.e., panels, Fig. 2-4). These tests include static, quasi-static, and dynamic cyclic load histories and are intended to yield data that can be used to identify failure modes in concrete masonry and to develop constitutive relations.

In this program, a biaxial panel test that provides a globally homogeneous state of stress was developed. In this test, in contrast to conventional test methods (Ref. 2), the determination of material properties is not prejudiced by boundary constraint; further in contrast to the direct methods (Ref. 1), extraction of biaxial failure states does not necessitate a conjecture of isotropic linear elastic material behavior prior to macro-cracking (Ref. 7). The test system shown in Figure 2-5 is capable of creating simple shear deformation.

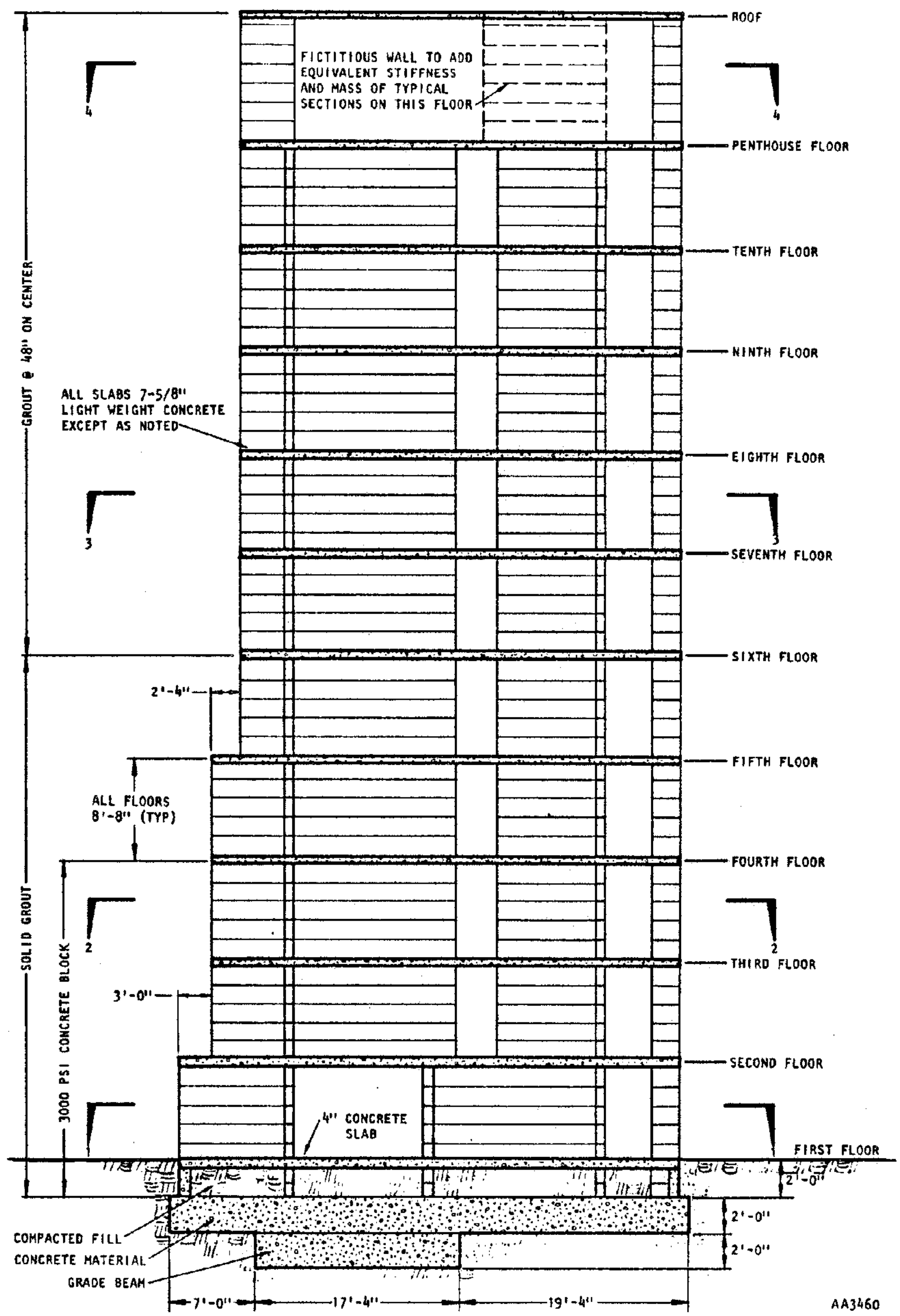

FIGURE 2-1. TYPICAL TRANSVERSE SECTION USED FOR ANALYSIS--SYMMETRIC BUILDING (Ref. 3)

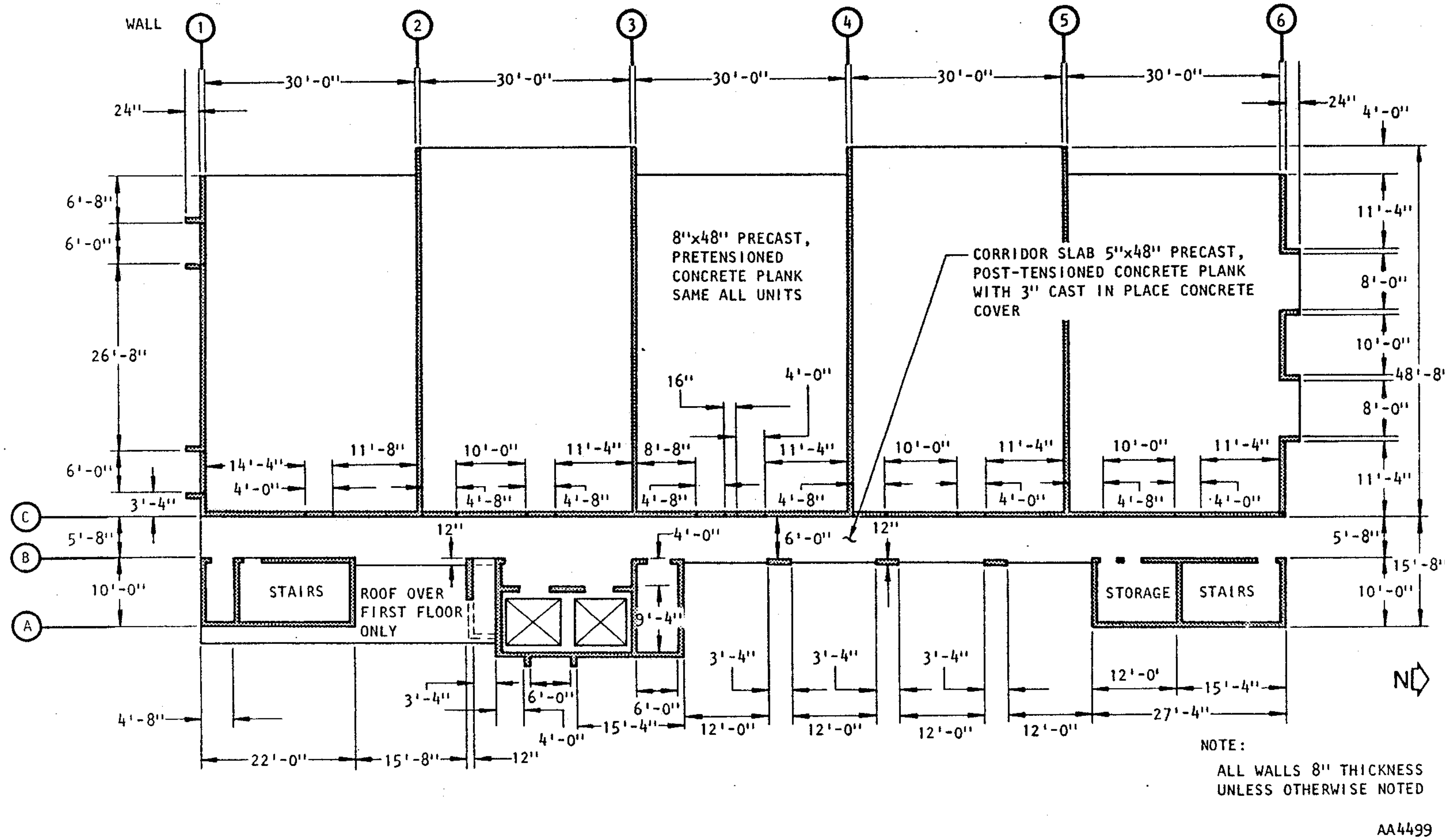

FIGURE 2-2. PLAN VIEW OF SECOND THROUGH THIRTEENTH FLOOR OF CONDOMINIUM--ASYMMETRIC BUILDING (Ref. 3)

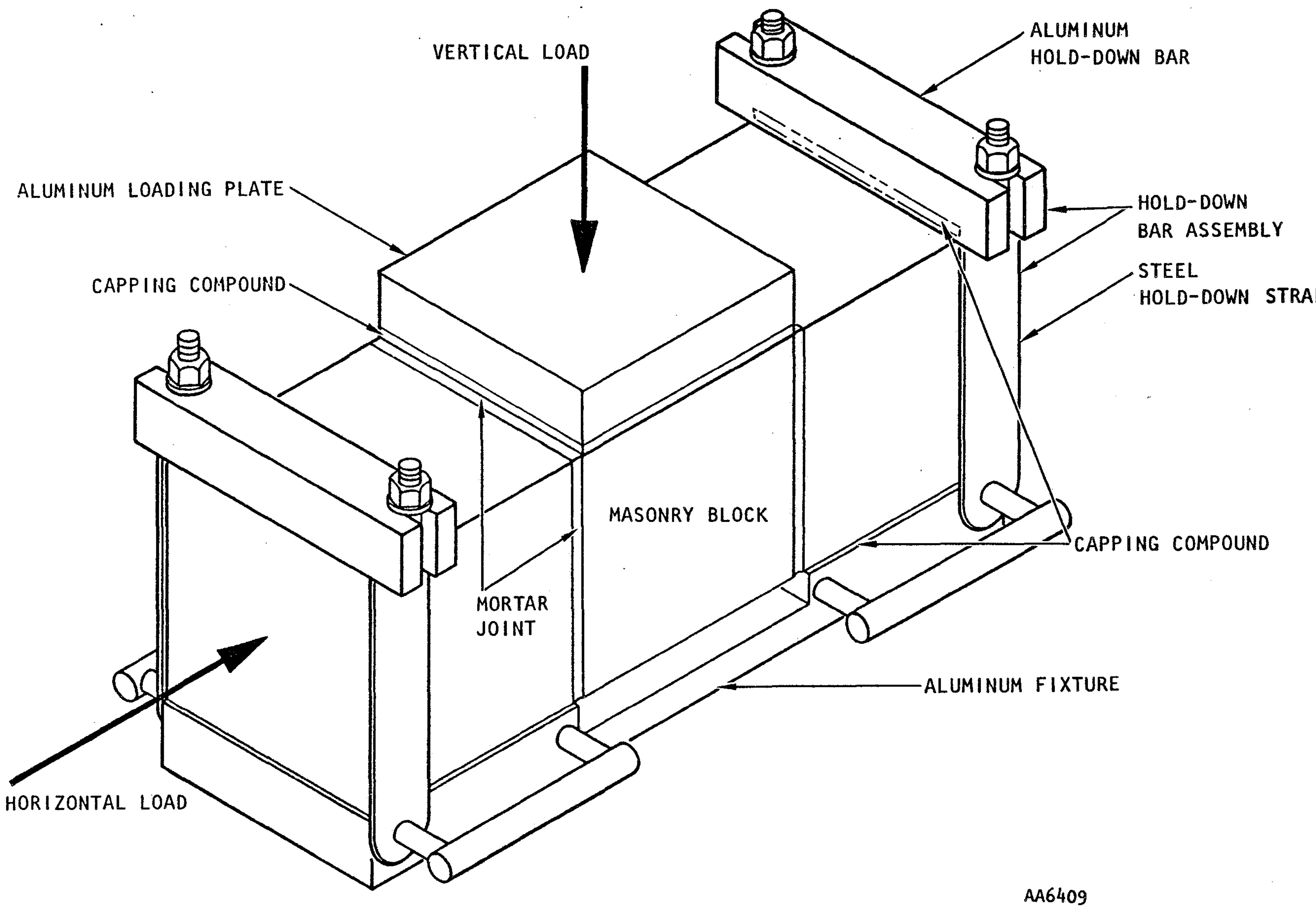

FIGURE 2-3. MASONRY BED-JOINT TRIPLET SPECIMEN AND FIXTURE (Ref. 6)

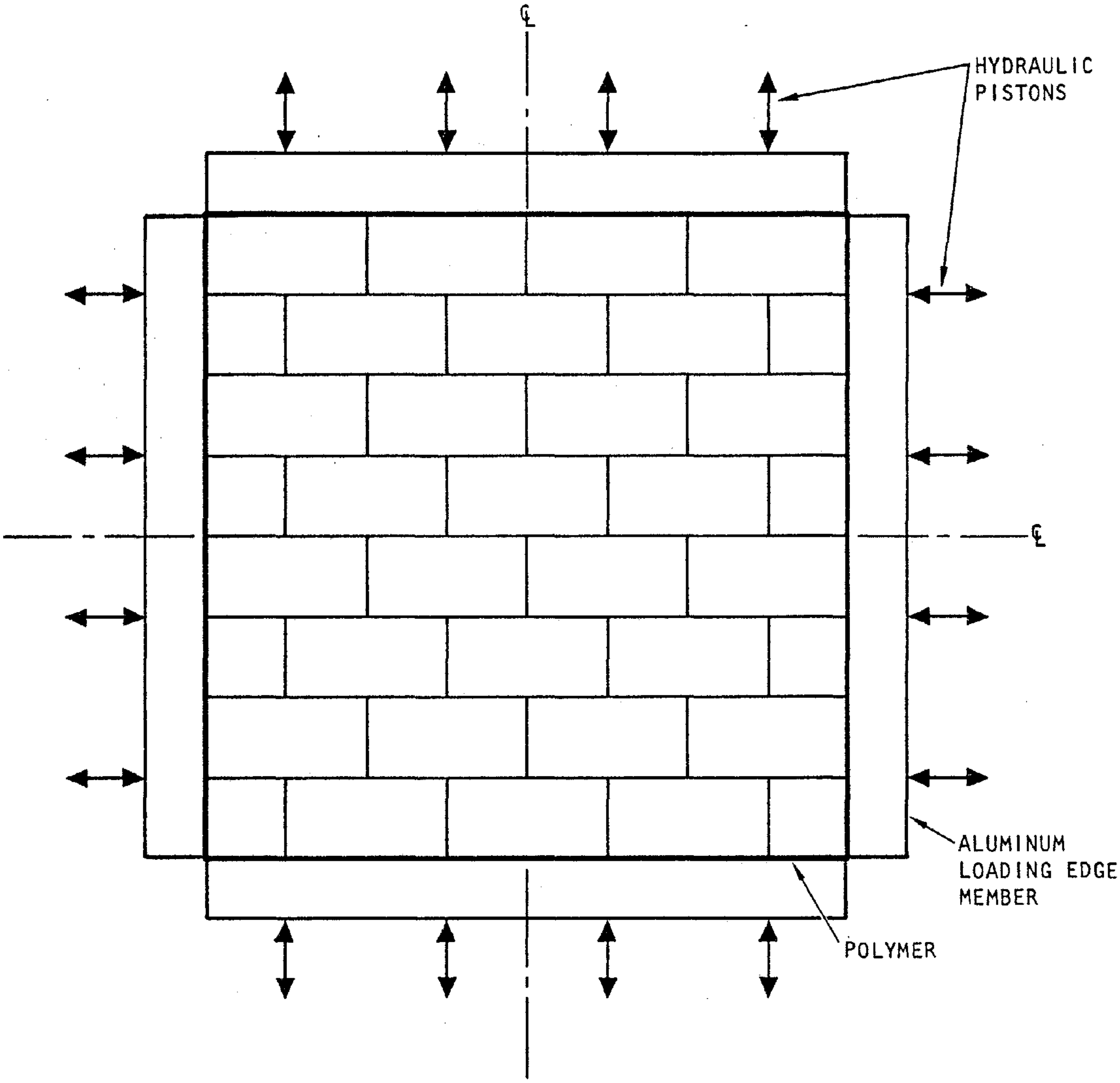

FIGURE 2-4. MASONRY PANEL SPECIMENS AND LOADING MEMBERS (Ref. 5)

The diagonal compression test (Fig. 2-6) is actually an indirect biaxial test (Ref. 1). Under concentrated diagonal compressive loads, the central portion of the specimen is subjected to a biaxial stress state, which is reasonably uniform over a characteristic length (area). In this test, the shear stress on the planes intersecting diagonals vanishes from symmetry. Failure occurs by induced tensile stresses on the vertical plane of symmetry (Fig. 2-7).

The curves in Figure 2-8 represent several macroscopic, analytical failure models considered to date. The dotted curve, shown for batch 6, is based upon the premise that failure occurs when a principal stress reaches either the tensile strength or the compressive strength associated with a uniaxial, 0 deg lay-up test. The solid curves result from the premise that the failure envelope in principal stress space is linear in the tension-compression zone, as illustrated in Figure 2-9 for plain concrete under biaxial stress states. This model is seen to provide a more accurate description of material behavior. The two solid curves in Figure 2-8 correspond to estimated (from prism tests) compressive strengths, and measured (from 0 deg lay-up panels) uniaxial tensile strengths for two groups of specimens. Note that only two experiments are necessary for construction of this failure model: (1) the uniaxial tensile strength and (2) the uniaxial compressive strength. The dashed curve represents a modification of the solid curve for batch 6 to account for the anisotropy discussed below (Ref. 7). Agbabian Associates participated in the first phase of the work at UCSD and contributed to the experimental program and analytical studies (Ref. 6).

The program at UCB (Ref. 8) involved a series of quasi-static and dynamic tests on double-piered elements (Fig. 2-10). These elements provide the primary shear resisting capacity for multistory reinforced-masonry buildings. Understanding the earthquake behavior of these elements would assist in developing a more realistic model of an entire perforated shear wall and, in addition, will aid in understanding the behavior of the coupled

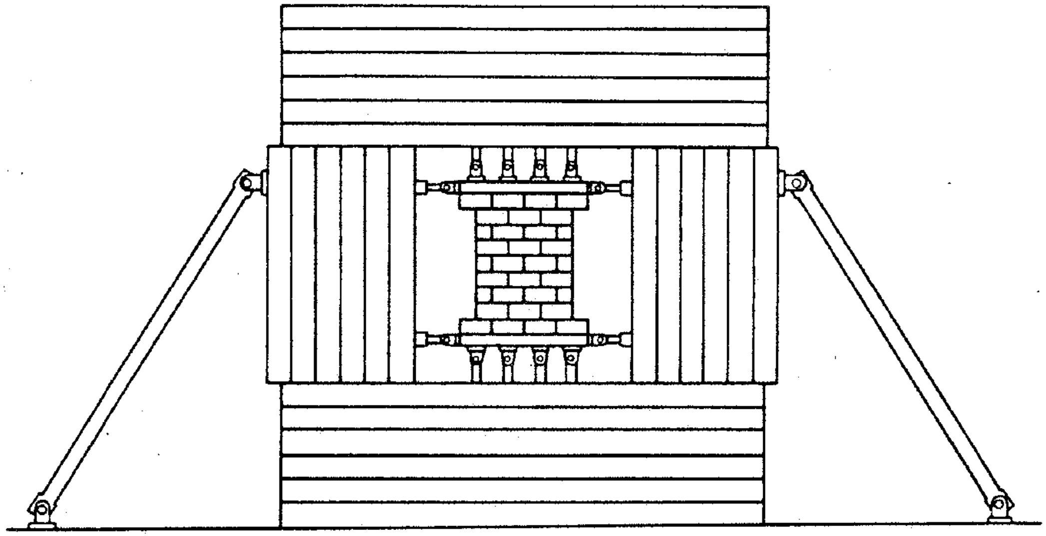

FIGURE 2-5. PANEL SHEAR TEST (Ref. 7)

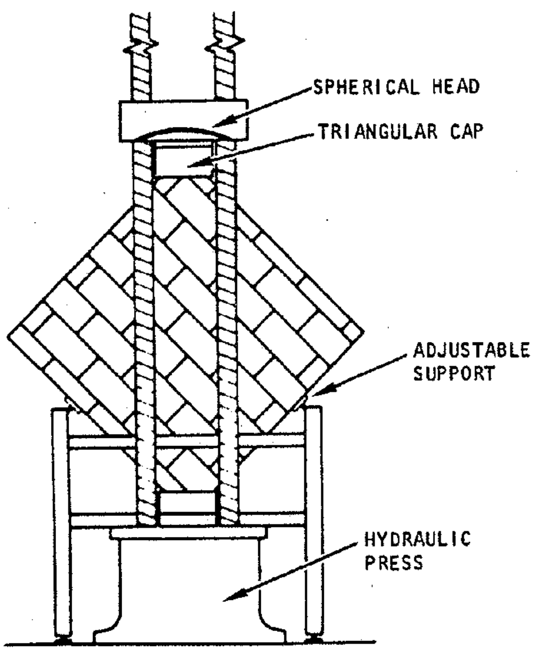

FIGURE 2-6. DIAGONAL COMPRESSION TEST (Ref. 7)

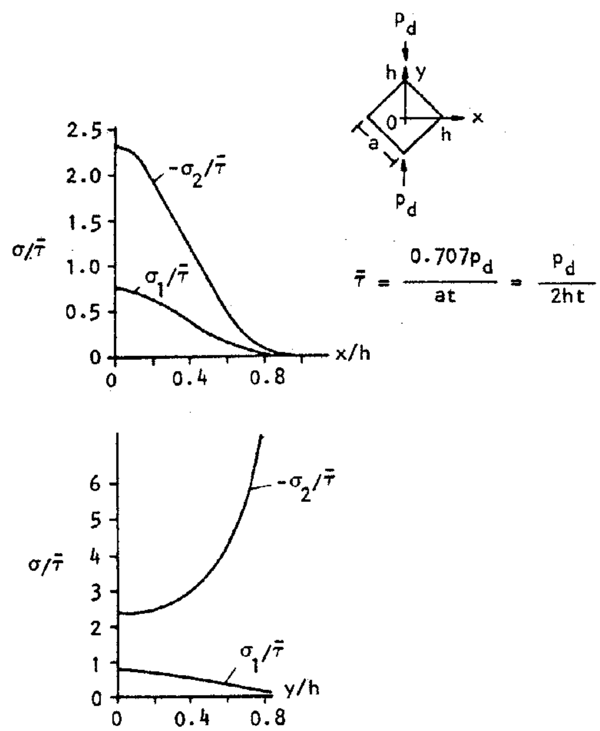

FIGURE 2-7. DIAGONAL COMPRESSION TEST: PRINCIPAL STRESS DISTRIBUTION ON THE PLANES y = 0 AND x = 0 (Ref. 7)

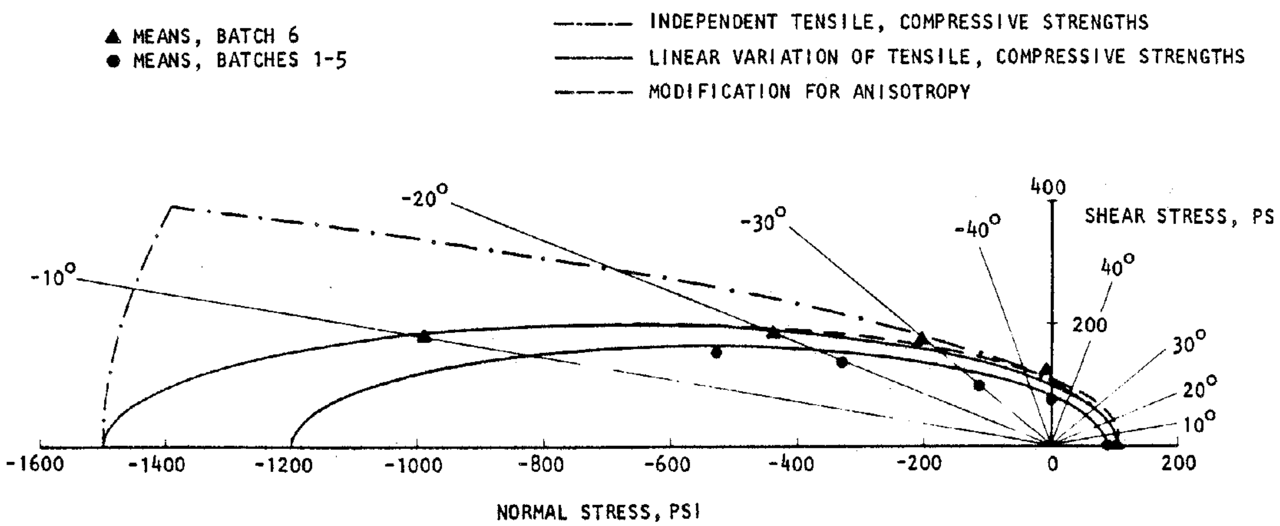

FIGURE 2-8. FAILURE ENVELOPE FOR ZERO HEAD JOINT NORMAL STRESS (Ref. 7)

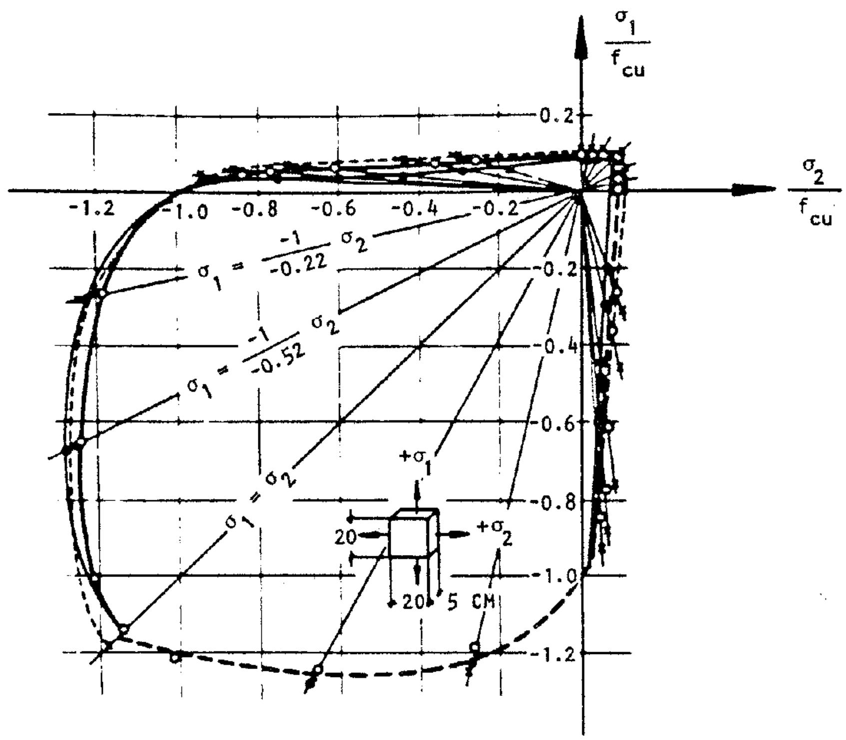

FIGURE 2-9. BIAXIAL STRENGTH OF CONCRETE (Ref. 7)

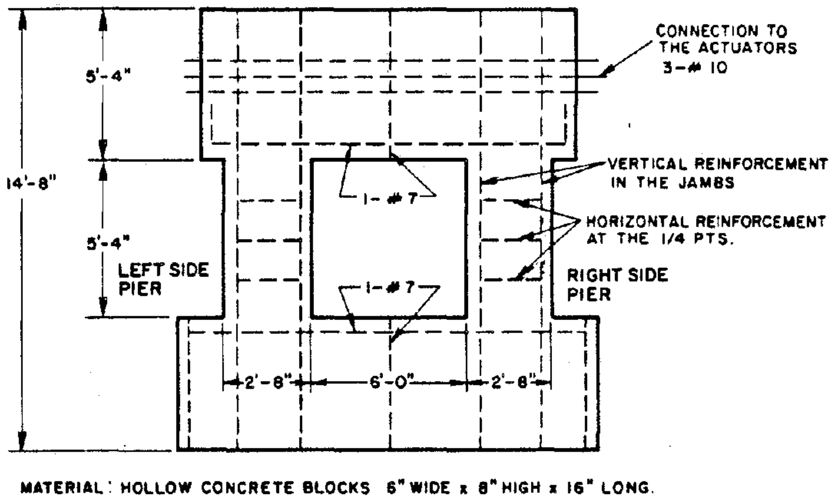

FIGURE 2-10. TYPICAL PANEL DIMENSIONS (Ref. 8)

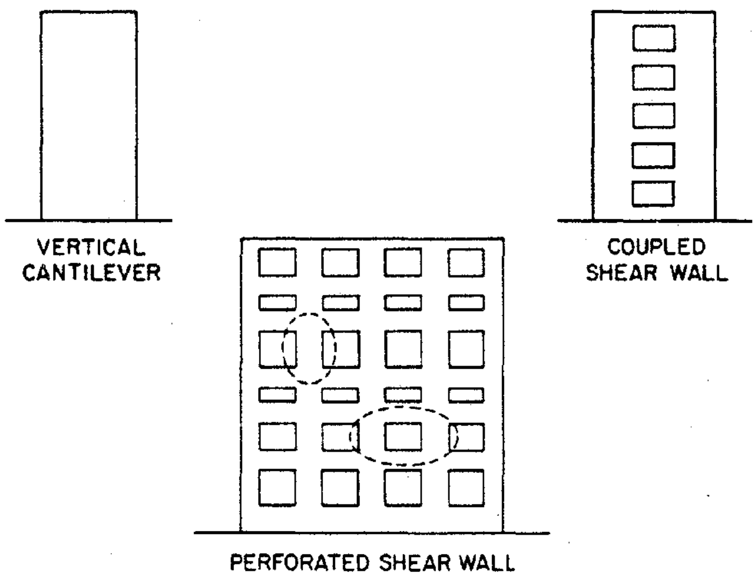

FIGURE 2-11. TYPES OF SHEAR WALLS (Ref. 8)

and cantilever shear walls (Fig. 2-11). The variables included in these tests are the frequency of load application, the quantity and distribution of reinforcement, the vertical bearing stress, and partial grouting. The ultimate strength, shear mode failure, combined shear and flexure modes of failure, full and partially grouted, horizontal and vertical reinforcement, and ductility of these piers were also investigated. It was found that partial grouting produces elastoplastic force deflection for piers failing in shear mode. It was also observed that piers which failed in the shear mode had pseudostatic ultimate strength less than the corresponding dynamic strength. Piers that failed in the flexural mode had pseudostatic ultimate strength greater or almost equal to the corresponding dynamic strength. It was also found that stiffness increased significantly by increasing the bearing stress. It was concluded from this work that the ultimate shear strength of masonry assemblages, and the validity of determining the allowable UBC strength as a function of the ultimate compressive strength, f'_m, of a prism must be further evaluated.

A program for testing of half-scale models of typical single-story masonry dwellings has been completed at UCB. The objective of the program was to determine design and construction requirements for such structures in Seismic Zone 2 of the United States. Shaking table tests were performed on these models to accomplish this objective. The project was supported by the Department of Housing and Urban Development.

Currently, a collaborative research program is being supported by the National Science Foundation to study structural identification, which includes both damage assessment and system identification. Several dynamic experiments will be performed on the EERC shake table at UCB, and these test data will be analyzed for damage assessment and system identification at Purdue University and UCB, respectively.

The behavior of masonry panels framed by reinforced-concrete members under alternating loads was studied by Esteva (Ref. 9). Both solid and hollow 3 m x 3 m panels were subjected to in-plane loads. These loads were applied in an alternating form along each diagonal, up to 70 cycles and reaching strains as high as 0.03 in./in. Elastic, cracking, and post-cracking behaviors were studied. Stress/strain curves were developed.

The structural performance of masonry walls under compression and flexure was studied by Fattal and Cattaneo (Ref. 10). Prisms and walls of brick, concrete block, and composite brick and block masonry construction were tested under various combinations of compressive and transverse loads. Constitutive relations for masonry were developed from test results. The report shows that prism strength can be predicted on the basis of linear behavior at failure. It was also shown that wall strength can be predicted on the basis of prism strength when an appropriate allowance is made for the effect of wall slenderness on sectional capacity.

Mayes and Galambos (Ref. 11) conducted a study of an existing full-scale contemporary reinforced-concrete building with infilled brick walls in St. Louis, Missouri. The test building was an approximately 40 ft x 40 ft square eleven-story tower structure. The building was subjected to large amplitude dynamic excitation. The effect of this excitation on the behavior of this building was observed. The work consisted of (1) survey of material and dimensional properties of the building, (2) small amplitude dynamic excitation to determine the dynamic characteristics of the structure as it existed before the large amplitude tests, (3) large amplitude dynamic tests to study the change of dynamic characteristics as the building was progressively damaged. The results indicate that there were large changes in the period of the building in most of the modes. The largest changes occurred in the first translational modes. The changes in the period associated with the large amplitude tests were permanent. The changes in mode shapes associated with the large changes in period were generally small. The most significant changes were in the first translational mode. There was a significant increase in damping as the input force level increased.

Blume, et al. (Refs. 12, 13) performed a structural dynamic investigation of 15 school buildings subjected to simulated earthquake motion. The study included detailed consideration of the short-period range of the earthquake spectrum. The study concluded that major elements of school buildings such as roof or floor diaphragms should be designed so that natural periods of such elements are 0.15 sec or less in order to avoid dangerous response to peak spectral values, which generally occur at around 0.25 sec. However, these results are limited to ambient vibrations under low amplitude forcing functions. Lower frequencies and longer periods would be expected during the inelastic response of the building to actual intensive earthquake motions.

A dynamic test program was conducted on an old school building by Rea, et al. (Ref. 14). The building had three basic modes of vibration that have been designated transverse, longitudinal, and flexure of the roof diaphragm. The resonant frequencies of transverse and longitudinal modes ranged from 7 to 10 Hz, and the associated damping capacities from 3% to 4%. The resonant frequencies of the flexure modes of the roof diaphragm ranged from 6 to 10 Hz and the associated damping capacities from 1% to 3%. These tests are also limited to ambient vibrations and would overestimate the frequencies of the diaphragms during an intensive earthquake shaking.

Static tests of full-scale lumber and plywood sheathed diaphragms were conducted by several investigators (Refs. 15 to 28). The series of test programs conducted by Stillinger (Ref. 22) included lumber-sheathed and plywood sheathed diaphragms 20 ft x 60 ft in size in order to determine the strength and stiffness at various load levels. The summary of test results indicates that the strength and stiffness of roof diaphragms can be appreciably influenced by altering any of the test variables included in this testing program. However, these tests did not include a load reversal cyclic loading and unloading.

The previous discussion indicates that most of the research programs have been directed toward studying masonry for new construction. Research programs for mitigation of earthquake hazard in existing unreinforced-masonry buildings are meager and still in the early stages.

The survey conducted in this study revealed that there is a large number of diaphragms of wood construction (girder-planking system) in older existing unreinforced-masonry buildings. The effectiveness of these diaphragms is an important consideration to how the building is modeled and analyzed. The response of the supporting masonry walls and foundation wall to in-plane seismic forces needs further evaluation.

No data are available on the dynamic behavior of diaphragms under earthquake loading. Low amplitude testing results of full-scale buildings would not necessarily provide adequate information on the dynamic properties of these buildings under intensive earthquake excitations.

SECTION 3

CONSIDERATION LEADING TO CHOICE OF DESIGN EARTHQUAKE AND RELATED BUILDING CAPABILITY

3.1 INTRODUCTION

This section provides background information on earthquake hazards and the current methods for selecting design earthquake motions for structures.

3.2 EARTHQUAKES

Earthquakes are normally caused by the release of stored energy during sudden displacement in the earth's crustal rock along a specific fault or by rupture of the rock (Fig. 3-1). This sudden motion of the crustal rock generates stress waves that propagate outward from the fault length along which the energy was released, resulting in an earthquake. It is the ground shaking induced by the passage of the stress wave that causes much of the earthquake damage, not the actual surface rupture of the fault.

Faults are considered active or potentially active according to evidence of past geologic activity. Also, an earthquake can occur along a fault that may have been permanently inactive, or a new fault may be produced. An example of this is the fault that generated the February 9, 1971 San Fernando earthquake. Few geologists knew of its existence in the San Gabriel Mountains behind Los Angeles until it ruptured, registering 6.4 to 6.6 magnitude on the logarithmic Richter scale. Parts of the mountain were vertically displaced eight feet. There was severe ground shaking in the surrounding area, lasting 10 to 12 sec. The earthquake resulted in the death of 64 persons; 1000 buildings were demolished or badly damaged, including 3 hospitals; 5 highway overpasses collapsed; and utilities were disrupted. It is interesting to compare this earthquake with the 8.3 magnitude earthquake that destroyed San Francisco in 1906. The energy released in the 1906 earthquake was 350 times the energy generated by the

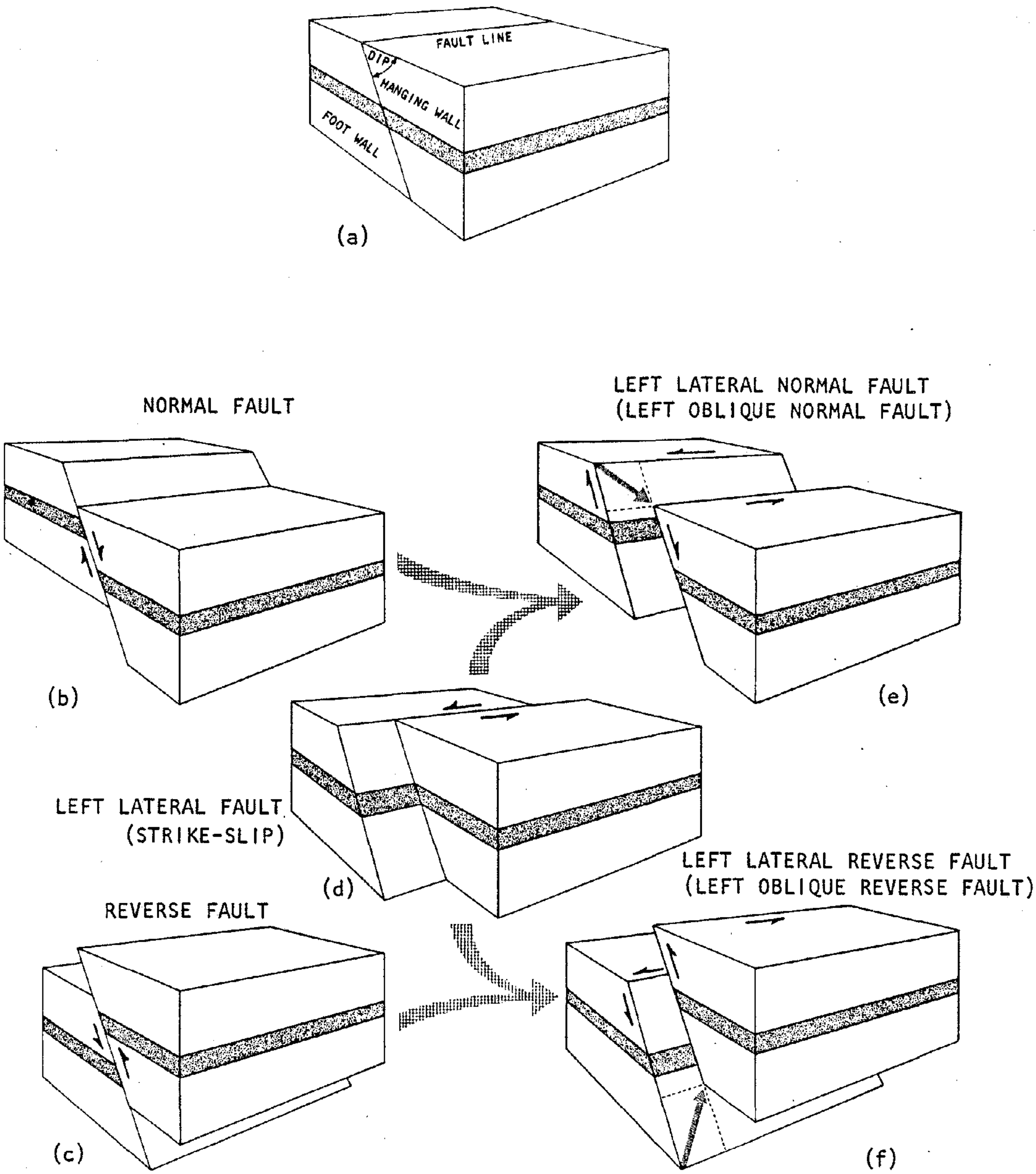

FIGURE 3-1. FAULT TYPES (Ref. 29)

1971 San Fernando earthquakes. Figure 3-2 shows the variation of earthquake magnitude with equivalent energy release expressed in tons of TNT, comparing the energies released by well-known earthquakes, as well as those released by nuclear weapons.

3.3 EARTHQUAKE PREDICTION

Earthquake-prediction technology in the United States has accelerated in recent years as more data have been acquired from an expanding network of instrumentation along active faults, such as is shown in Figure 3-3. Predictions for the Pacific Coast states, principally Alaska and California, are being emphasized, since they are especially vulnerable to earthquakes and related disaster. However, nearly every state in the nation faces some degree of risk from future earthquakes. Because of limitations on available moneys to support earthquake-prediction research, it has been necessary to restrict fault-monitoring activity to only a few locations along active and potentially damaging faults.

3.4 MODES OF EARTHQUAKE DAMAGE

Modes of failure associated with seismic events include ground shaking, ground failure, and water flooding.

3.4.1 GROUND SHAKING

Ground shaking is probably the most damaging effect of an earthquake because such a large area is subjected to the shaking.

3.4.2 GROUND FAILURE

Ground failure is the result of seismic activity on earth materials and includes landsliding, surface rupture, liquefaction, and compaction and subsidence.

a. Landsliding is a common geologic process normally associated with hilly or mountainous terrain and depends on the inability

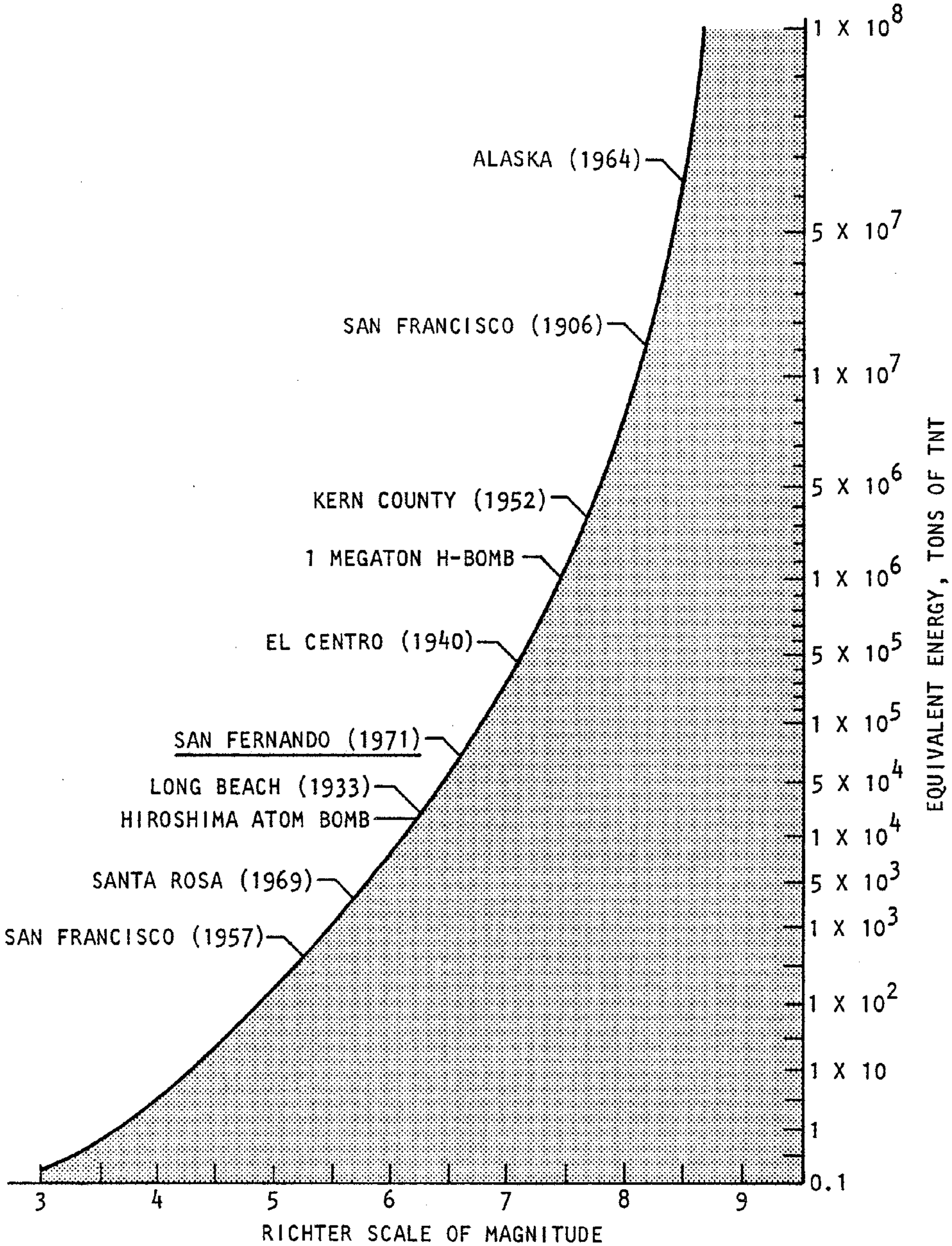

FIGURE 3-2. COMPARISON OF RICHTER SCALE MAGNITUDE VS. EQUIVALENT ENERGY OF TNT (Ref. 30)

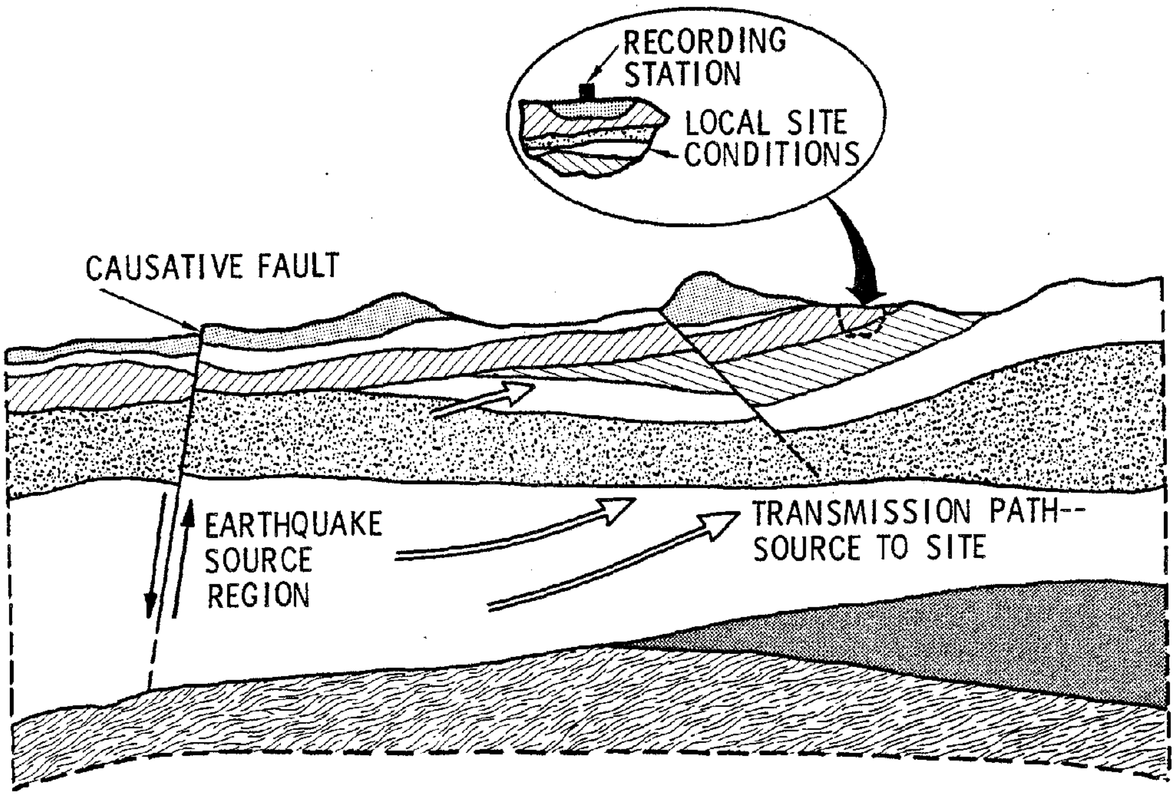

FIGURE 3-3. GENERATION AND TRANSMISSION OF SEISMIC WAVES (Adapted from Ref. 31)

of a slope of soil or rock to resist moving downhill. Earthquakes can trigger slides in areas prone to landsliding, depending on the stability of the slope. This will be influenced by rock-type and geologic structure; slope gradient, precipitation, or moisture penetration; and ground shaking from earthquakes.

b. Surface rupture (faulting, fissures, cracking, and fracturing) normally occurs in close proximity to the fault zone as the result of a seismic event on these faults.

c. Liquefaction is the sudden loss of strength of soils under saturated conditions, due to earthquake shock. It involves a temporary transformation of material into a fluid mass.

d. Compaction and subsidence of low-density alluvial material can result from ground shaking, depending on the physical properties of the material.

Landsliding could cause serious building damage due to foundation failure. Liquefaction may cause building foundations to settle or slide. Compaction of material may cause settlement of the foundations.

3.4.3 FLOODING

Flooding is a potential earthquake hazard at some sites, should hillside water reservoirs above the sites fail as a result of ground shaking or ground failure.

3.5 EARTHQUAKE THREAT TO BUILDINGS

3.5.1 EARTHQUAKE DAMAGE

The 1971 San Fernando earthquake occurred on the fringe of the very large metropolitan area of Los Angeles and provided the first really comprehensive test of modern U.S. building code provisions. It occurred also within the boundary area of a large network of strong-motion accelerographs. These are instruments developed for derivation of engineering data rather than of seismological data. These instruments (more than 250 in number), installed in buildings and on the ground, recorded in this one earthquake more useful data on the parameters of strong ground motion and facility response to this motion than the total of all records previously made by such instruments worldwide.

Seismograms from the San Fernando earthquake indicate a background acceleration level of from 0.35 to 0.5 g, with a maximum spike of acceleration at one location of more than 1.0 g. Coupled with this high level of ground acceleration, large ground displacements and surface faulting occurred. The time duration of violent ground motion lasted only from 10 to 12 sec, whereas in a magnitude 8.0+ earthquake, it would approximate 30 to 40 sec in the epicentral area.

3.5.2 EARTHQUAKE-RESISTANT DESIGN

Building codes intend to provide minimum requirements for lateral force resistance to prevent building collapse under the conditions of the most probable severe earthquake to which the structure would be subjected.

The damage experienced during the 1971 San Fernando earthquake demonstrated that, in general, modern structures designed according to the minimum requirements of the building codes received only architectural damage in areas where the accelerations were 20% g or less. There was minor-to-appreciable structural damage in the 20% to 30% g range, and the damage to buildings of minimum design varied from appreciable damage to collapse in the area of very strong shaking. Had the shaking endured longer, as it would have in a larger earthquake, the damage would have been more severe and more modern structures would have collapsed.

The San Fernando earthquake experience leads to the conclusion that the building codes of the time could not have been expected to produce a uniform structural performance or earthquake resistance in all buildings because of the many variables that influenced design such as architectural plan, structural system, and engineering judgment. In addition, the quality of design and construction differs greatly from one building to another. Many of the studies and reports of the San Fernando earthquake have concluded that improvements should be made in seismic code requirements relating to building design and construction. Most West coast code agencies and other advisory and regulatory bodies have already revised their code requirements or are currently in the process. For example, the 1976 edition of the Uniform Building Code and the 1974 Recommended Code of Practice of the Structural Engineering Association of California incorporate new earthquake design provisions more stringent than those of previous codes.

Building codes that have been revised since the 1971 San Fernando earthquake are now requiring the use of considerably higher coefficient values for computing lateral forces. These new values represent lateral forces that are closer to actual measured earthquake motion loadings determined from measured records. The direction is also toward the requirement for an analysis of building response that considers the time variation of ground motion to validate maximum equivalent static design coefficients. The importance of the critical "use" or "occupancy" of a building is now being recognized in the seismic code requirements. Also, more attention is being paid to nonstructural building components and systems.

3.6 DESIGN EARTHQUAKE EVENT

3.6.1 INTRODUCTION

The earthquake criteria for earthquake-resistant design discussed in this phase of the study is based on the design philosophy that

a. For moderate intensity earthquakes, little structural damage should result, but some damage to nonstructural elements in the building would be allowable.

b. For very high intensity earthquake ground motion, some structural damage could occur, but there should be no possibility of structural collapse. These very high intensity earthquake ground motions would be generated by the design earthquake event.

3.6.2 DEFINITION OF DESIGN EARTHQUAKE EVENT

A design earthquake event specifies the maximum values of certain characteristic parameters that may reasonably be expected to occur over the design life of the struture, or, in the case of a seismic safety plan for existing buildings, over the remaining life of the structure. This design earthquake generally specifies the maximum ground displacements, velocities, and accelerations that are likely to occur. Some measure of the time duration of the ground motions is also included. An important tool used to represent design earthquake motions is the response spectrum, which actually represents the peak response of a series of simple (single-degree-of-freedom) structures to given ground motions. Each earthquake ground-motion history produces a unique spectrum, and the design spectrum is usually a composite average, or envelope, of such spectral records that are appropriate for the site of the proposed facility. Development of criteria for a specific site generally requires consideration of major geological features; tectonics for the site, i.e., the types, locations, and arrangement of faults; seismic history including records of intensity and ground motion, if available; and local soil conditions. Engineering judgment and, in some cases, ground-motion calculations, provide the basis for selecting the required design earthquake event.

3.6.3 GOVERNING EARTHQUAKE CONDITIONS AT THE SITE

Earthquake threat to a site may come from different conditions. In many cases, two earthquake conditions govern the design at the site. The first corresponds to a nearby earthquake. The second condition corresponds to a distant event. Frequency content and duration of the record vary from one condition to the other, and one condition may be more detrimental to a certain building than the other condition.

3.7 EARTHQUAKE INPUT CRITERIA

3.7.1 INTRODUCTION

The earthquake input ground motion at the site that corresponds to the design earthquake event can be estimated by different methods. The geologic features that affect the ground shaking at the site can be related to the source mechanism, source site transmission path, and local soil conditions (Ref. 32). These factors are considered in the following methods.

3.7.2 SOIL-RESPONSE ANALYSES

This analysis requires constructing a mathematical model for the soil profile at the site. Well defined soil properties obtained from the geotechnical investigation of the site are used to define the material properties of the model. A selection is made of an ensemble of rock-outcrop motions for use as input to the computations. This ensemble is selected at the site to correspond to the intensity level that corresponds to the design earthquake event developed for the site. The ensemble of rock-outcrop motions is selected based on the following: (1) the motions must be taken from accelerograph stations that are underlain by rock materials; (2) the earthquake magnitude, source mechanism, and causative-fault distances should be as close as possible to that of the design earthquake event; and (3) where possible, the peak acceleration of the rock-outcrop records should be reasonably close to the peak acceleration specified for the design earthquake event.

The SHAKE code (Ref. 33) is used for the analysis of soil profiles that can be modeled as infinite horizontal layers. However, for inclined layers, a two-dimensional analysis should be used. The results of soil response analyses are used to develop composite response spectra for the site. The mean and mean-plus-one standard deviation spectrum can be developed from these results.

3.7.3 SITE-MATCHED RECORDS

Site-matched records (Ref. 34) should be selected to represent conditions comparable to those of the actual site, based on consideration of such features as magnitude, distance, local soil conditions, tectonic province, and fault mechanism. These records are scaled to the criterion for the site, and composite spectra corresponding to the mean statistical levels can be developed.

3.7.4 SEED-UGAS-LYSMER SPECTRUM SHAPES

Seed et al. (Ref. 35) have developed standardized spectrum shapes developed from statistical analyses of 106 spectra normalized to a 0-period acceleration of 0.10 g and categorized according to local soil conditions of the various accelerograph sites.

3.7.5 COMPARISON OF SPECTRA DEVELOPED BY DIFFERENT METHODS

The spectra developed by using site-soil response analyses, site-matched ensemble, and the Seed-Ugas-Lysmer method are compared and a final design spectrum can be selected for the site.

3.8 PROCEDURE OUTLINED BY ATC-3 (REF. 36) FOR SPECIFICATION OF EARTHQUAKE GROUND SHAKING AND DEFINITION OF SEISMIC HAZARD INDEX

3.8.1 INTRODUCTION

Two earthquake ground shaking regionalization maps were developed by ATC-3. These maps are based on the following: (1) the design lateral force and the period of a structure should take into account the distance from anticipated earthquake sources; (2) the probability of exceeding the design ground shaking should, as a goal, be roughly the same in all parts of the country; and (3) the regionalization maps should not attempt to delineate microzones. Any such microzonation should be done by experts who are familiar with localized conditions.

3.8.2 DESIGN EARTHQUAKE GROUND MOTIONS

ATC-3 defines the "design ground shaking" for a location as the ground motion that an architect or engineer should have in mind when he designs a building that is to give proper protection to life safety. A smoothed elastic response spectrum for single degree-of-freedom system (Ref. 37) was proposed.

3.8.3 GROUND MOTION PARAMETERS

The intensity of design ground shaking is represented by two parameters. These parameters are called the effective peak acceleration (EPA) and effective peak velocity (EPV). The EPA is proportional to spectral ordinates for periods in the range of 0.10 to 0.5 sec, while the EPV is proportional to spectral ordinates at a period of about 1 sec. The constant of proportionality (for the 5% damped spectra) is set at a standard value of 2.5 in both cases.

For a specific actual ground motion of normal duration, EPA and EPV can be determined as illustrated in Figure 3-4. The 5% damped spectrum for the actual motion is graphed and fitted by straight lines at the periods mentioned above. The ordinates of the smoothed spectrum are then divided by 2.5 to obtain EPA and EPV.

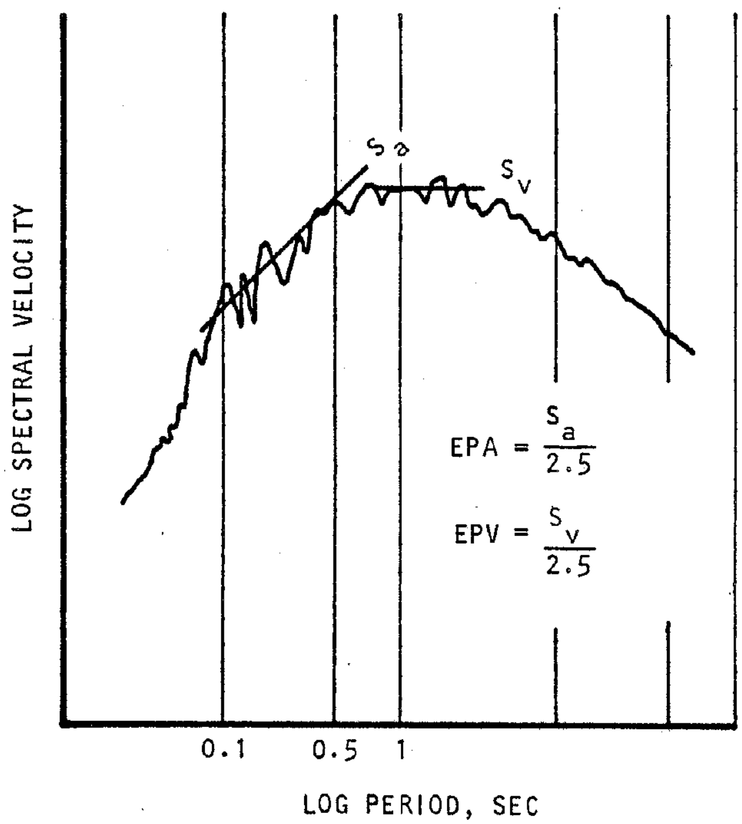

FIGURE 3-4. (Ref. 36)

3.8.4 DESIGN ELASTIC RESPONSE SPECTRA

The EPA and EPV maps are shown in Figures 3-5 and 3-6 (see Ref. 36 for a complete description of these maps) and have four contours whose associated values of EPA or EPV are as follows:

Contour	EPA Map 1	EPV Map 2
1	0.05g	1.5 in./sec
2	0.10g	3
3	0.20g	6
4	0.40g	12

For simplicity in application and to avoid the need for interpretation between contours, the maps for both EPA and EPV have been divided along county boundaries into seven levels of motion (Ref. 36). A seismic hazard index, which reflects the ability of different types of construction to withstand the effects of earthquake motions, was also included.

Spectral shapes representative of the different soil conditions discussed in Reference 36 were selected on the basis of statistical studies (Fig. 3-7). These spectra were simplified to a family of three curves by combining the spectra for rock and stiff soil conditions leading to the normalized spectral curves shown in Figure 3-8.

Recommended ground motion spectra for 5% damping for the different map zone levels are thus obtained by multiplying the normalized spectra values shown in Figure 3-8 by the values of effective peak ground acceleration. Soil profile factors were also derived for the above response spectra.

ATC-3 represents a state-of-the-art workable tool for describing the design ground shaking as a smoothed elastic response spectrum. However, the smoothed elastic response spectrum is not necessarily the ideal means for

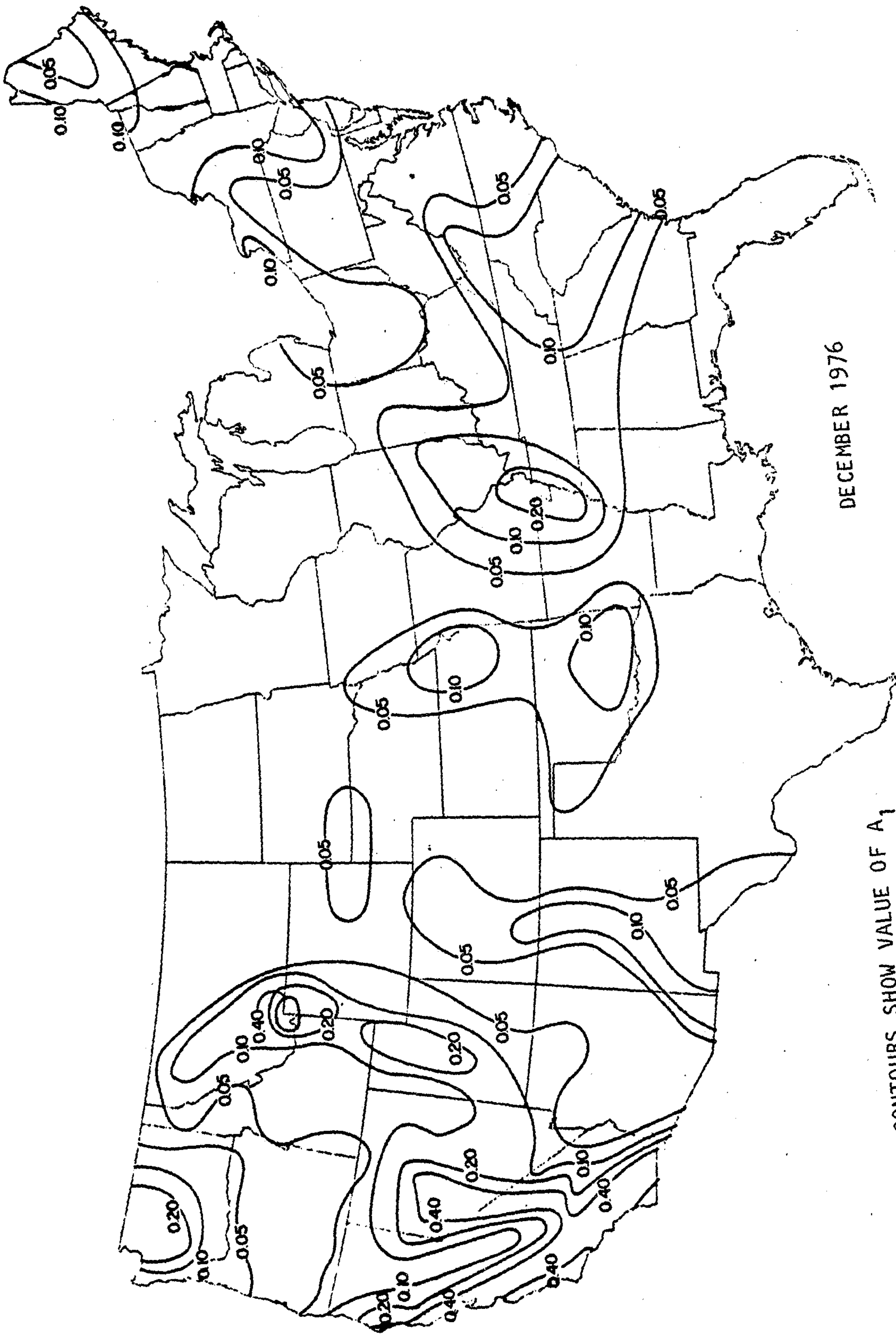

DECEMBER 1976

NOTE: CONTOURS SHOW VALUE OF A_1

FIGURE 3-5. EFFECTIVE PEAK ACCELERATION MAP (Ref. 36)

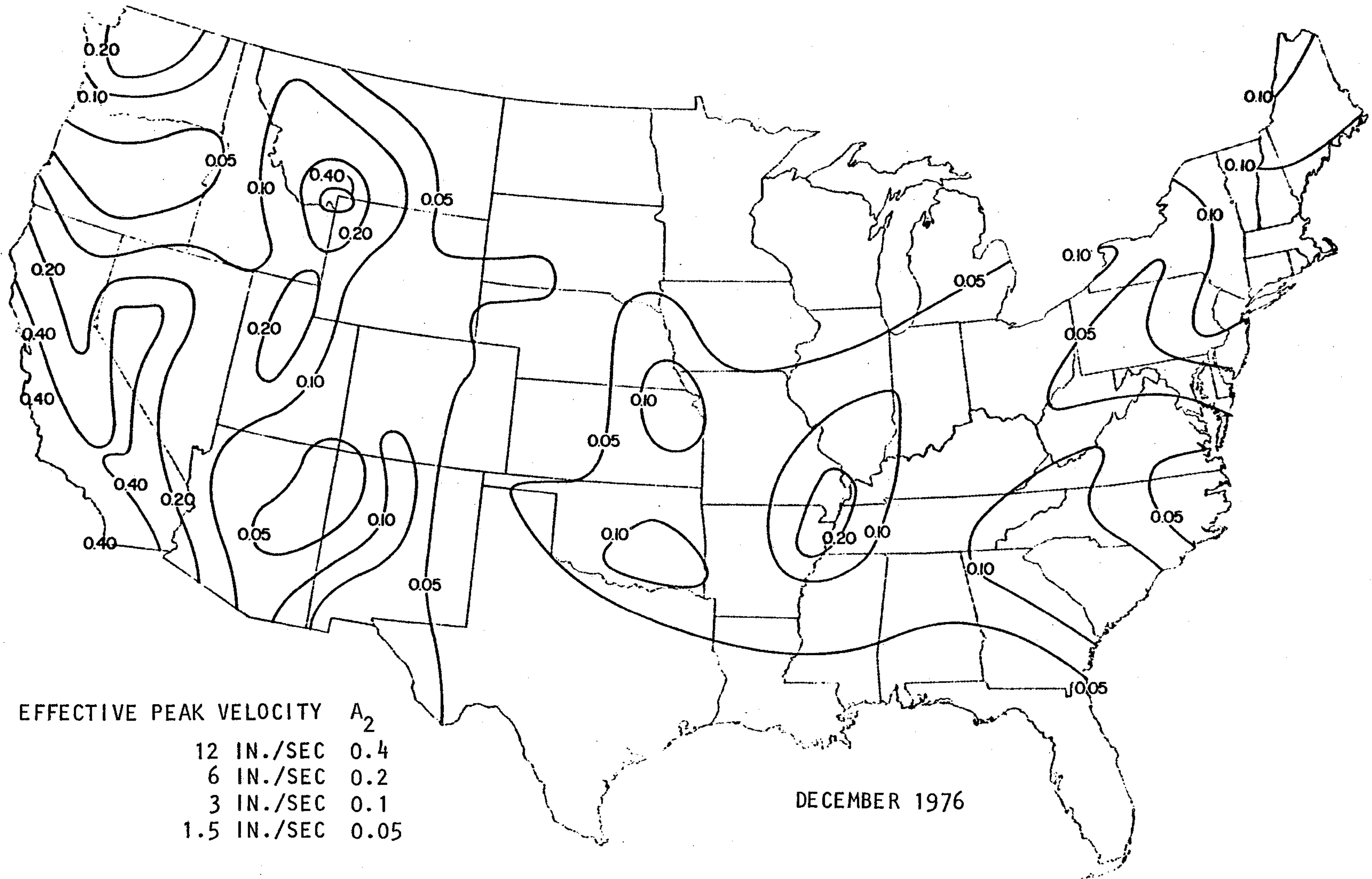

EFFECTIVE PEAK VELOCITY A_2

12 IN./SEC	0.4
6 IN./SEC	0.2
3 IN./SEC	0.1
1.5 IN./SEC	0.05

NOTE: CONTOURS SHOW VALUE OF A_2

FIGURE 3-6 EFFECTIVE PEAK VELOCITY MAP (Ref. 36)

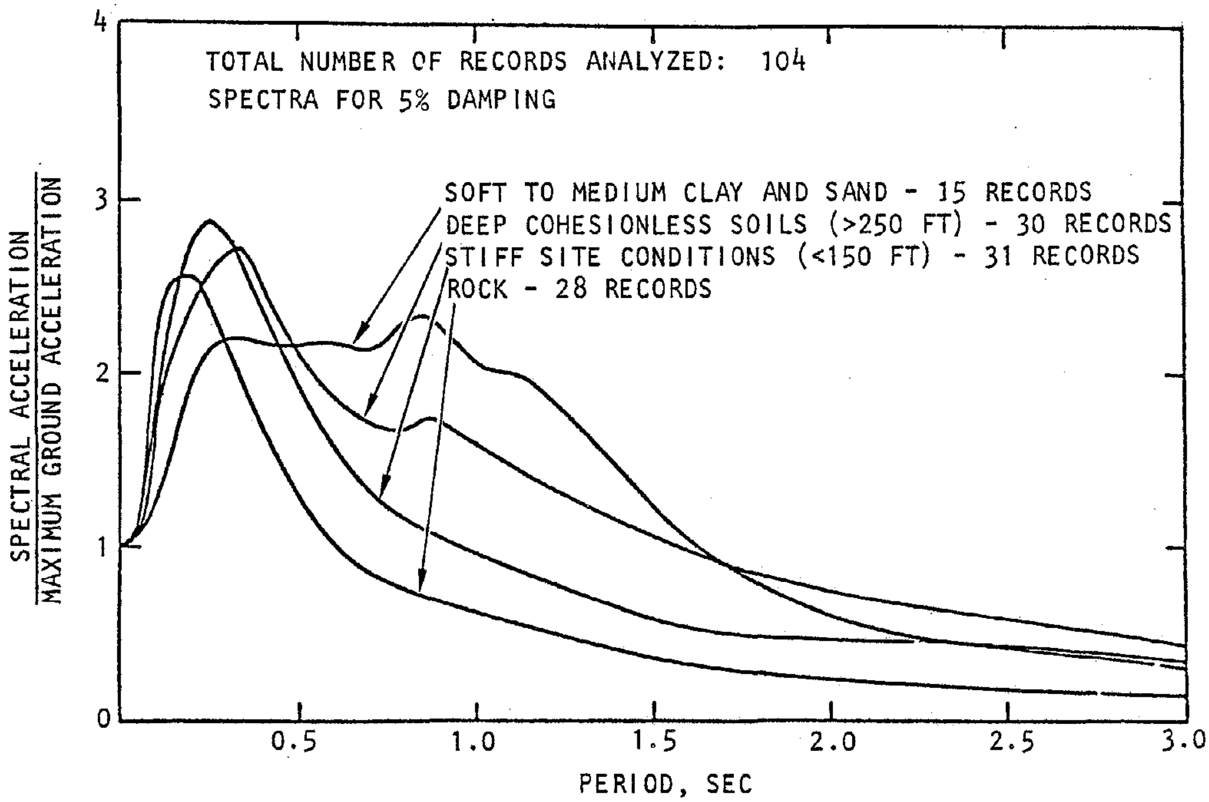

FIGURE 3-7. AVERAGE ACCELERATION SPECTRA FOR DIFFERENT SITE CONDITIONS

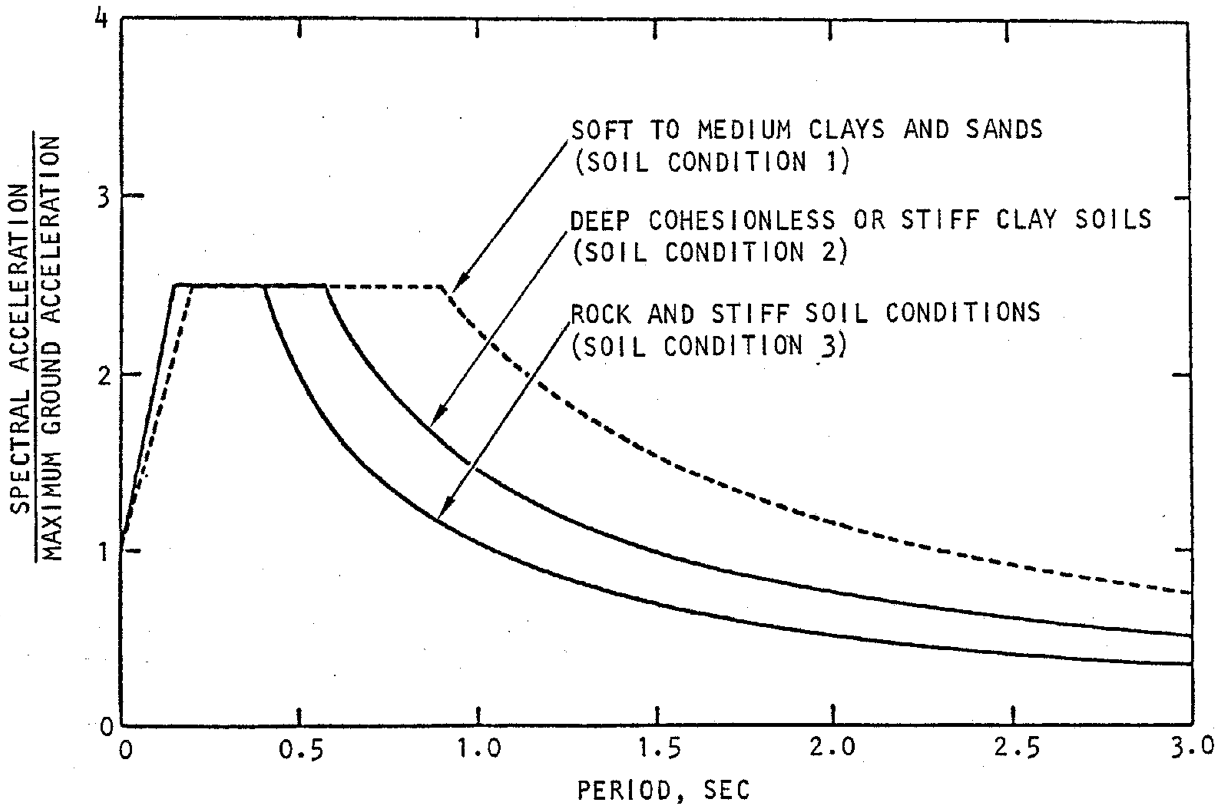

FIGURE 3-8. NORMALIZED SPECTRAL CURVES RECOMMENDED FOR USE IN BUILDING CODE

describing the design ground shaking. A significant deficiency of the response spectrum is that it does not by itself say anything about duration of the shaking. It might be better to use a set of four or more acceleration time histories, whose average elastic response spectrum is similar to the design spectrum. This approach may be desirable for buildings of special importance or for research studies of the seismic response of buildings.

SECTION 4

SEISMIC ANALYSIS OF UNREINFORCED MASONRY BUILDINGS

This section describes the analytical methods that can be used for the seismic analysis of unreinforced masonry (URM) structures and how these methods can be used to estimate the response of critical elements. In addition, the adequacy of the analysis methods and corresponding modeling assumptions are discussed.

4.1 METHODS OF ANALYSIS

The analytical methods that are available for the seismic analysis of URM structures can be divided into three basic categories:

- Static
- Pseudodynamic
- Dynamic

In each of these categories, either linear or nonlinear analyses can be performed. A description of these methods and some important subcategories are given in the following subsections.

4.1.1 STATIC ANALYSIS

The response of URM structures to seismic environments is a dynamic phenomenon, and the use of static methods is only approximate. In the case of reinforced masonry, building codes have established criteria for the magnitude and distribution of seismic forces to be applied in static analyses. Although the magnitude of these forces is specified as a function of the structural frequencies, they are only an approximation of the inertial forces that would result in a dynamic environment.

However, in some cases, relatively stiff or rigid structures will respond as a rigid body and can be analyzed using equivalent static forces. In the case of a stiff structure sited on a good soil, the structure will respond with the free field, and equivalent static forces can be determined from the structural weight and the peak ground acceleration. For a stiff structure sited on soft soil, some amplifications of the peak ground acceleration can be expected due to the rocking response.

In general, static analyses are useful only if the dynamic response of the structure is known.

4.1.2 PSEUDODYNAMIC ANALYSIS

Pseudodynamic analyses are approximate methods and should be viewed as a refinement of the equivalent static method. In these analyses, simple mathematical models are employed to estimate the dynamic response of the structure. Inertial loads determined from the response are applied as equivalent static loads.

4.1.3 DYNAMIC ANALYSES

There are three subcategories of dynamic analyses methods, as given below:

1. Response spectrum
2. Modal time history
3. Direct integration time history

Each of these methods can be utilized with one-, two-, or three-dimensional mathematical models. All three methods can be used for linear elastic models. However, nonlinearities can be treated in an approximate way with the first two methods. When nonlinearities are important, the direct integration method must be employed.

In the response spectrum method, the seismic input is defined in the form of a response spectrum. The input response spectrum defines the peak responses to a specific seismic or loading environment of several linear single-degree-of-freedom (SDOF) oscillators with various values of equivalent viscous damping. The peak responses are defined as the relative displacements, pseudorelative velocities, or absolute pseudoaccelerations. However, the exact time at which the peak responses occur is not specified. Based on a limited number of normal modes of the structure, the peak structural response in each mode can be obtained from the response spectrum. The response of the complete structure is determined by combining the contributions from each mode. The peak modal responses do not necessarily occur at the same instant of time, and the response spectrum does not provide information on phase relationships. Accordingly, the complete structural response is estimated by combining the peak modal responses in a probabilistic manner. Several procedures are available, such as--

- Square root of the sum of the squares (SRSS)
- Peak (or peaks) plus the SRSS of the rest
- Absolute sum

The procedure selected will depend on the modes obtained. Equivalent viscous damping can be included to simulate energy dissipation and account for nonlinearities in an approximate way.

The modal time-history analysis method uses a time history input rather than a response spectrum. Based on a limited number of normal modes of the structure, the structural response time history in each mode is obtained by direct integration. The response time history of the complete structure is determined directly by combining the contributions from each mode. As in the response spectrum method, equivalent viscous damping can be included to simulate energy dissipation and account for nonlinearities in an approximate way.

The direct integration time-history method is the most general method for the seismic analysis of structures. It provides the time-dependent response to a time-history input. In this scheme, the numerical integrations are carried out directly on the coupled set of simultaneous differential equations of motion in the structural system's physical coordinates. This method allows for the inclusion of nonlinearities that can be very important for URM structures.

4.2 ANALYSIS MODELS

A mathematical model is a mathematical representation of a structural system in terms of its significant characteristics. The type and complexity of the model selected will depend on the response to be determined and the importance of structural interactions. There is a wide range of mathematical models that may be used to represent a structure:

- Simple one-dimensional cantilever beam models
- Two-dimensional frame and shear wall models
- Pseudo-three-dimensional building models
- Three-dimensional structural models

as shown in Figure 4-1. In addition, the soil can be included in each of these models, either as one-dimensional spring elements or two- and three-dimensional continuum elements.

Some typical mathematical models for the nonlinear analysis of diaphragms and wall rocking are given in Section 5. These are very simple lumped parameter models for the analysis of critical elements of a URM structure. Depending on the information required, more complex three-dimensional finite element models can be used.

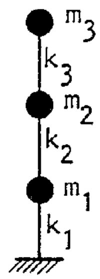

(a) One-dimensional

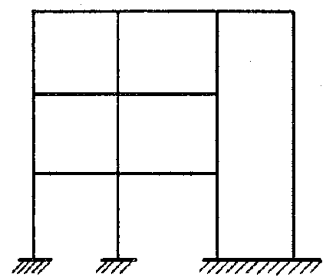

(b) Two-dimensional single frame

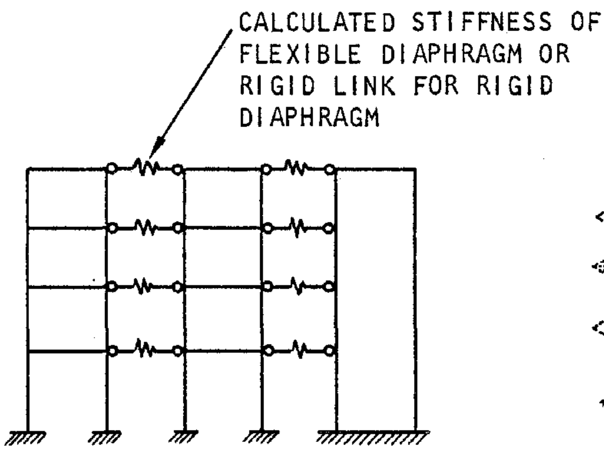

(c) Two-dimensional multiple frames

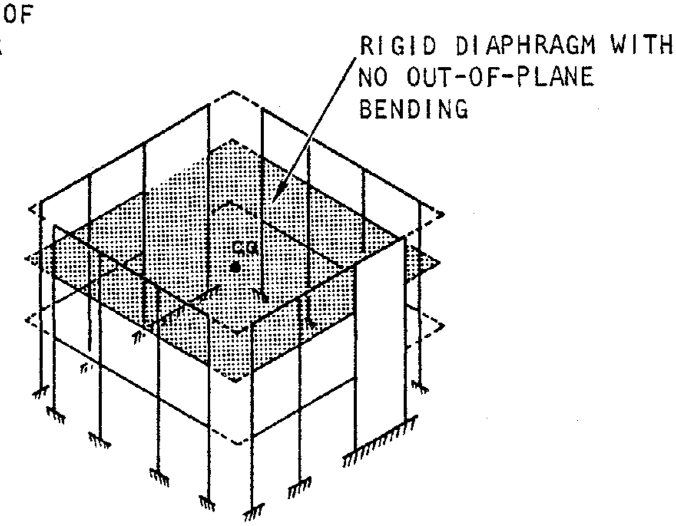

(d) Pseudo-three-dimensional

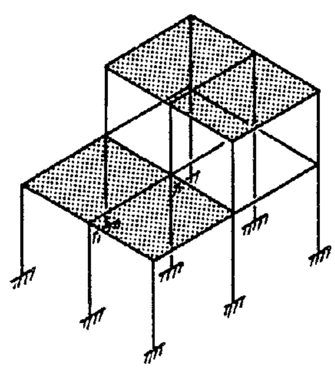

(e) Three-dimensional

FIGURE 4-1. TYPES OF MATHEMATICAL MODELS OF STRUCTURES (Source: SEAOC, Electronic Computation Committee, *Seismic Analysis by Computer*, Los Angeles, 1977.)

4.3 ADEQUACY OF CURRENT ANALYSIS ASSUMPTIONS

The review of the analytical methods and models indicate that the response of critical elements can be predicted using finite element and lumped parameter models. In general, the performance prediction of a URM structure in a seismic environment will require nonlinear analyses, since these structures are not expected to respond in the elastic range. The adequacy of these analyses depend on the availability of data on the nonlinear characteristics of the various components of a URM structure.

Analysis of existing test data is necessary to develop criteria for the nonlinear characteristics of several elements including piers, panels, and masonry joints. Additional test data are necessary for the out-of-plane characteristics of walls, the nonlinear properties of diaphragms, masonry panel strength and stiffness, and anchorage characteristics.

Once these data are available, reasonable upper and lower bound performance prediction of URM structures can be made using dynamic nonlinear parameter and finite element models.

SECTION 5

EXAMPLE ANALYSES OF ROOF DIAPHRAGMS AND MASONRY-WALL ROCKING DUE TO EARTHQUAKE EXCITATION

This section represents results obtained by using the STARS computer program for the analysis of two examples:

a. A simple one-story building with a wood diaphragm roof supported on masonry walls. The purpose of these calculations was to demonstrate (1) some basic phenomena and the potential effect that the energy-absorption capacity of wood diaphragms will have on the response of existing unreinforced masonry buildings, (2) the effect that stiffening these diaphragms will have on the response of masonry buildings to earthquake loading, and (3) the usefulness of the STARS computer program as a tool for studying these effects.

b. In-plane masonry-wall rocking. The purpose of these calculations was to study (1) whether the wall would detach from its supporting soil at the response levels used in this study, (2) the relationship of the H/D ratio and supporting soil stiffness to the rocking of such walls, (3) the effect that rocking will have on the response of these walls to seismic excitations, and (4) the usefulness of the STARS computer program as a tool for studying these effects.

These analyses were performed in close collaboration with the firms of KK&A and SB&A.

5.1 ANALYSIS OF ONE-STORY BUILDING WITH WOOD-DIAPHRAGM ROOF SUPPORTED ON MASONRY WALLS

5.1.1 SYSTEM DESCRIPTION

The one-story building considered in the following calculations consists of a wood diaphragm roof supported at four sides by 13-in. solid masonry walls as illustrated in Figure 5-1. The uniform load of the roof is assumed to be 30 lb/sq ft and the wall uniform load as 130 lb/sq ft.

The roof diaphragm is modeled as a deep shear beam (Fig. 5-2a). This beam is divided into a series of segments, as shown in Figures 5-2b and 5-2c. The 100-ft-long masonry wall will crack when subjected to shaking normal to its plane. Therefore, only its weight will be included in the model.

For the present phase of the analysis the two end walls are assumed rigid. Earthquake input motions are assumed to be transmitted from the foundation level (Levels C and D) to the top of the end shear walls (Levels A and B) without any modification (Fig. 5-2a).

The four-segment model is shown in Figure 5-3; the eight-segment model is shown in Figure 5-4.

5.1.2 MATERIAL PROPERTIES

From full-scale tests on plywood diaphragms (Ref. 38) it appears that for cyclic monotonic loading, the deflection may be expressed by

$$\Delta = CWL \tag{5-1}$$

where

- Δ = Midpoint diaphragm deflection in inches (Total deflection is attributed to in-plane shear deformation.)
- C = Flexibility coefficient
- W = Total load in kips in diaphragm assumed uniformly distributed over diaphragm length
- L = Diaphragm span in feet

Use of a single constant C to describe flexibility appears to be applicable for diaphragm span/depth ratios of 2 to 4.

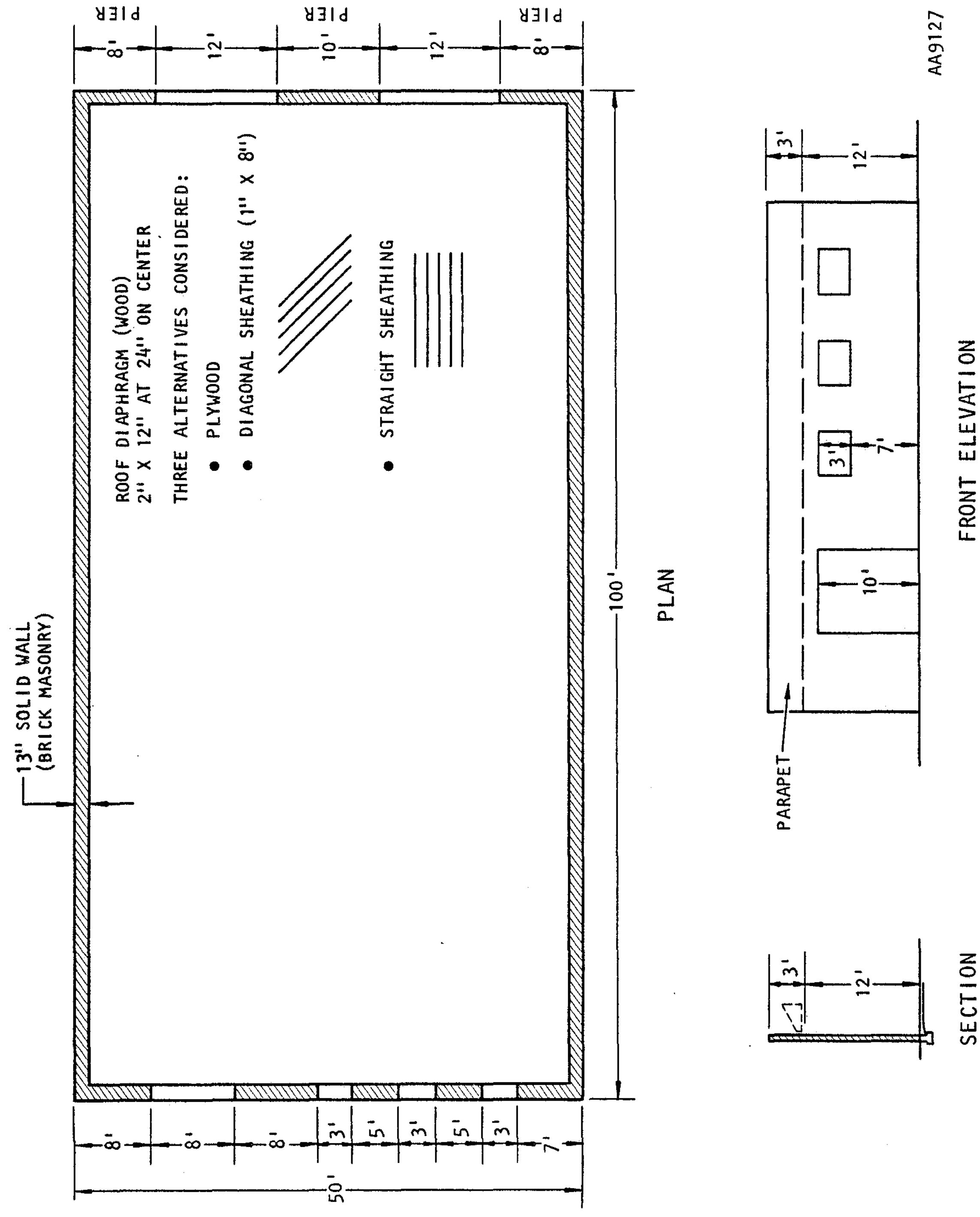

FIGURE 5-1. ONE-STORY UNREINFORCED MASONRY BUILDING WITH A WOOD DIAPHRAGM ROOF.

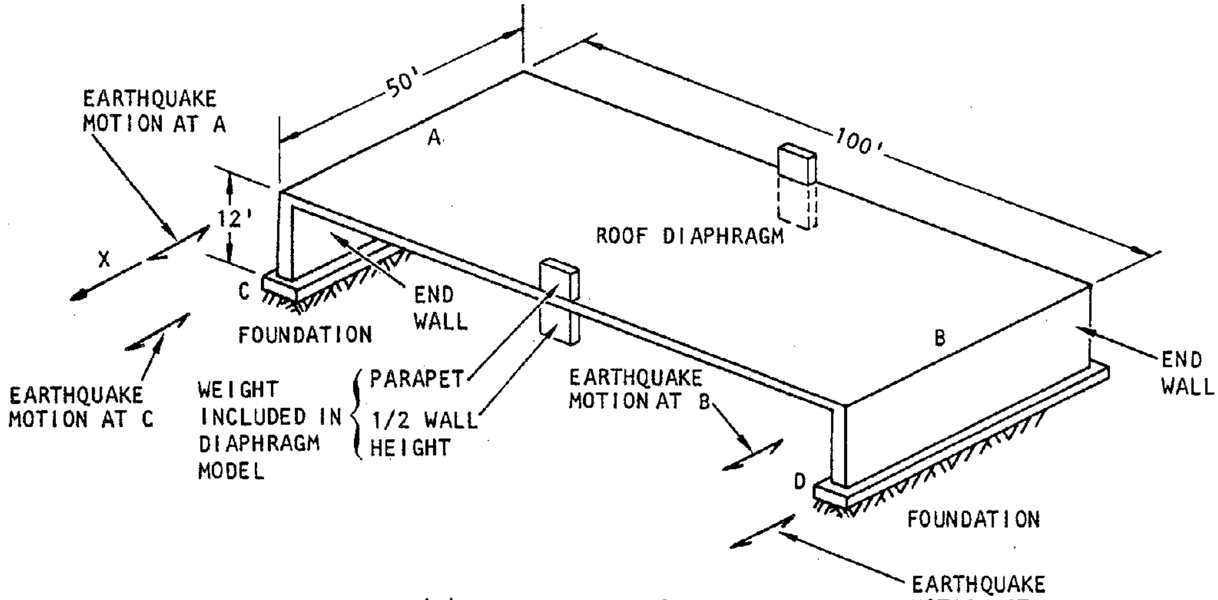

(a) System configuration

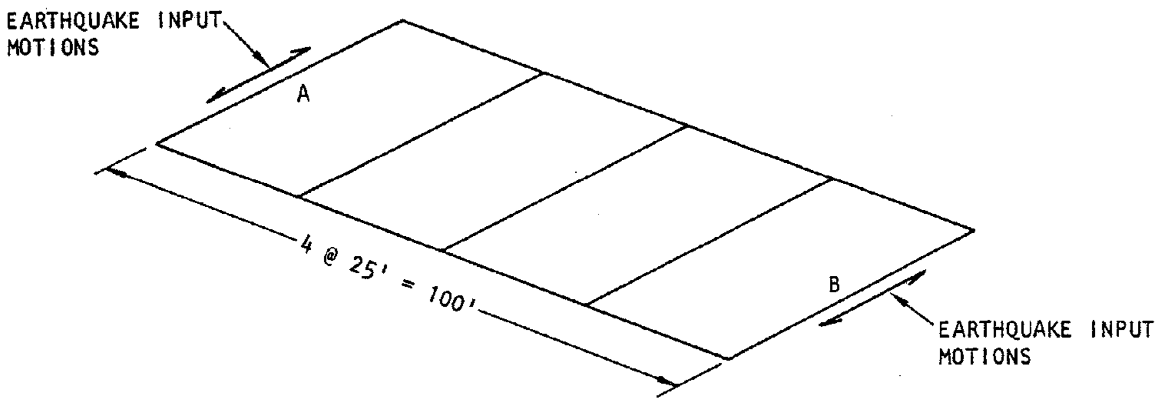

(b) Four-segment diaphragm model

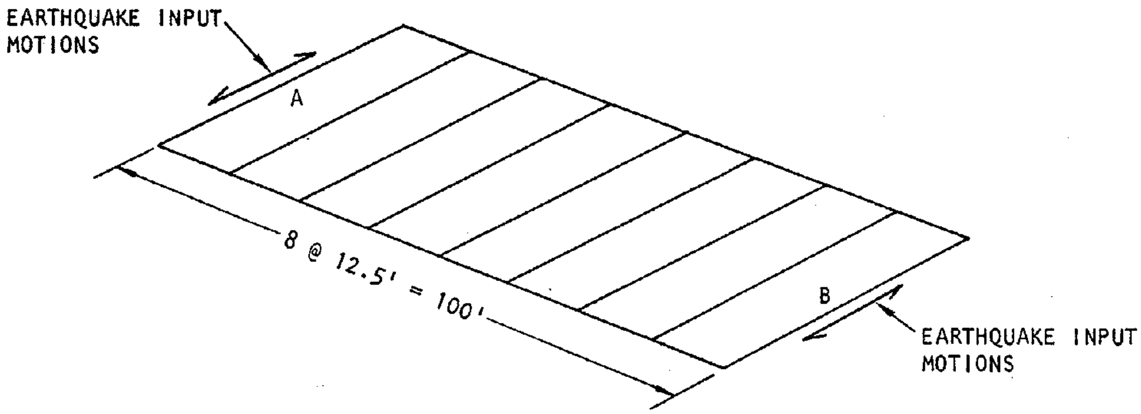

(c) Eight-segment diaphragm model AA9133

FIGURE 5-2. DIAPHRAGM/WALL CONFIGURATION AND MODEL CONSIDERED IN EXAMPLE ANALYSIS

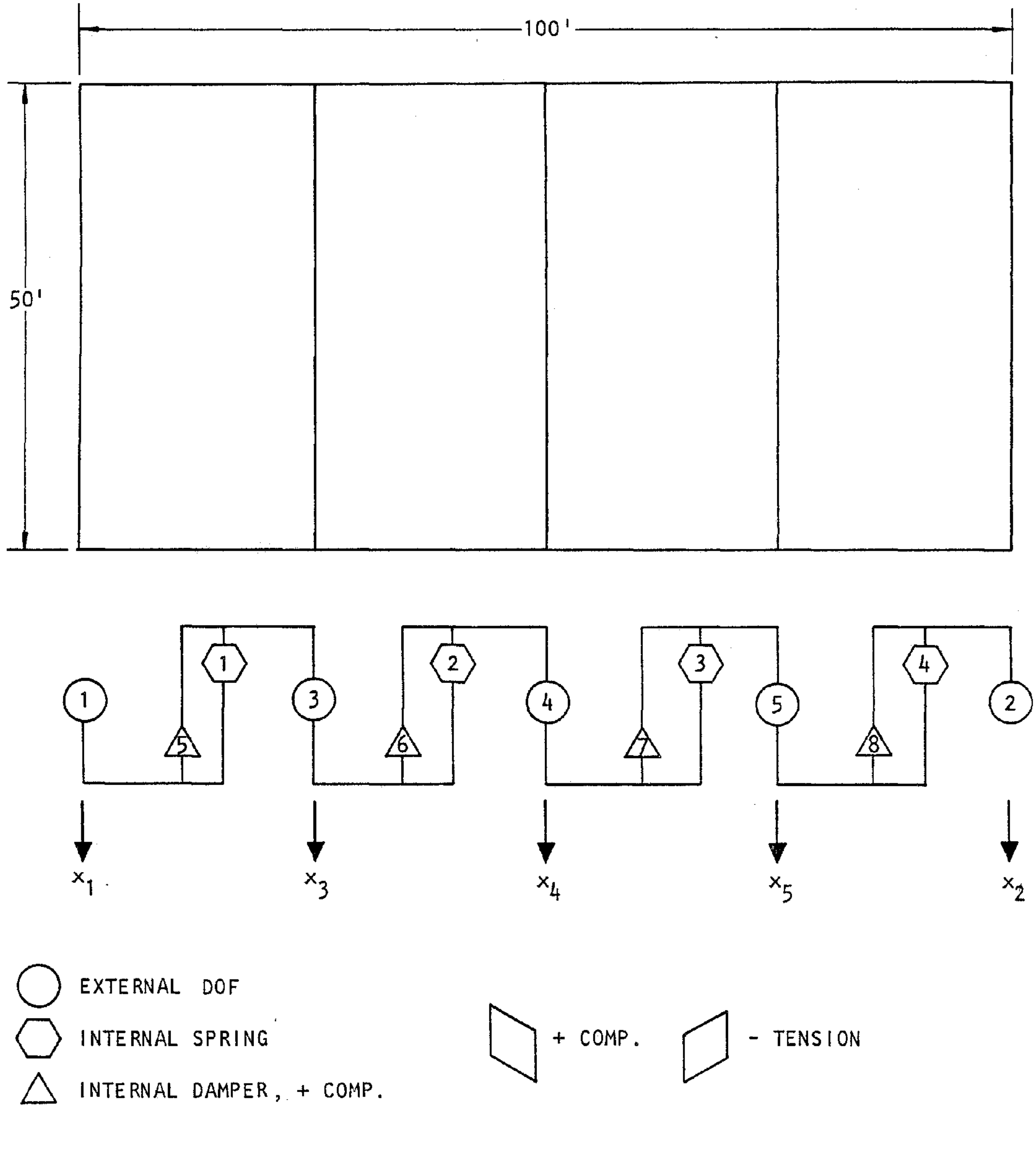

FIGURE 5-3. LUMPED PARAMETER MODEL (4 SEGMENTS — MODEL 1)

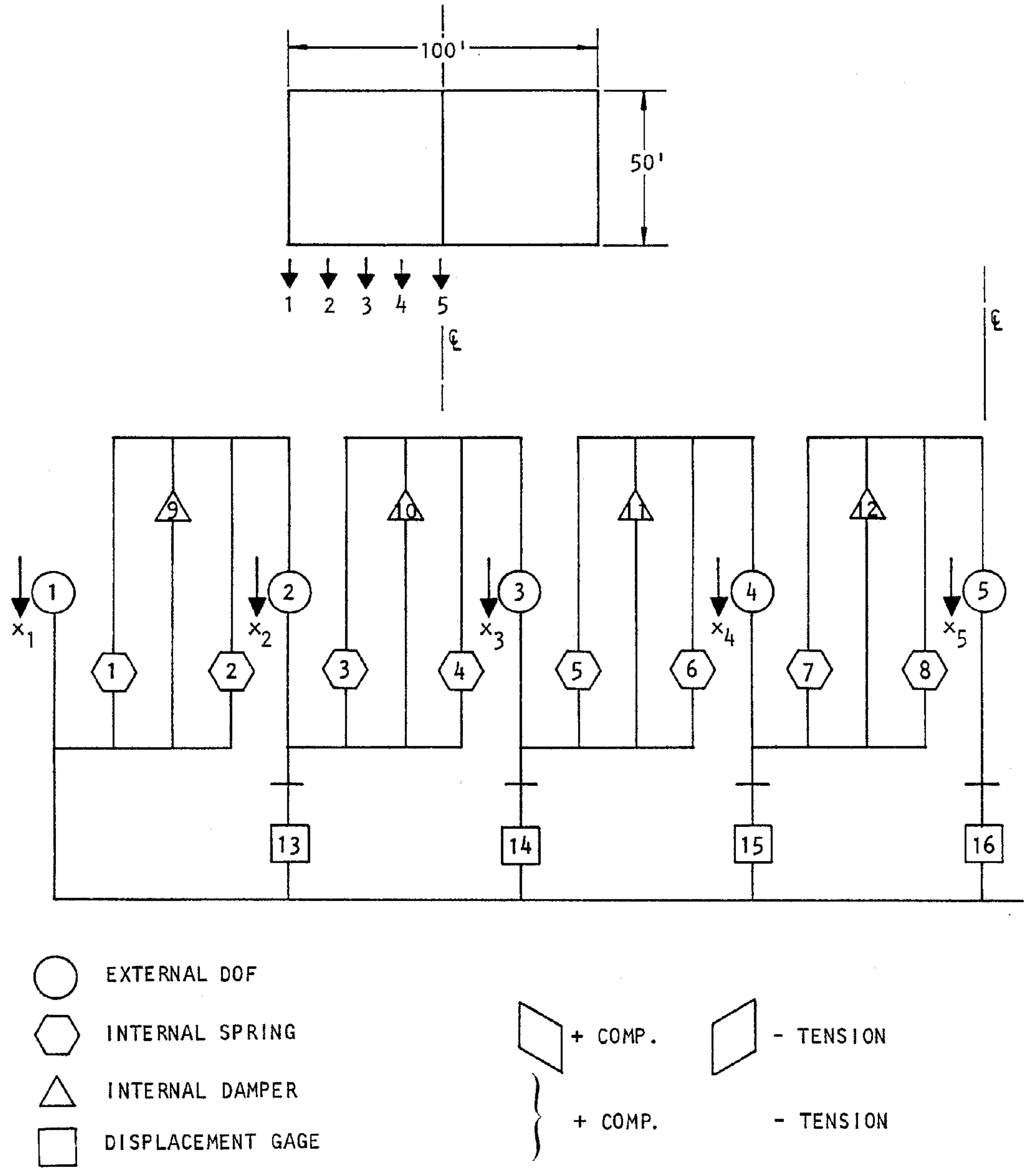

FIGURE 5-4. LUMPED PARAMETER MODEL (8 SEGMENTS — HALF MODEL, MODEL 2)

The plot on Figure 5-5 indicates that the diaphragm will cycle at a constant deflection for repetitions of reloading. This is generally confirmed by the plots of tests shown in Figure 5-6.

The simple idealized load deflection relation, shown in Figure 5-7, describes a monotonically increasing loading curve in compression and an image relationship in tension. The hysteretic curve indicates a permanent set of 0.5 Δ. This idealization was included in the present analysis.

As illustrated in Figure 5-7, the data on plywood was presented by the relation

$$\Delta = 5 \times 10^{-4}\ WL \tag{5-2}$$

for

$$W = 5 \text{ kips}$$

and

$$L = 100 \text{ ft}$$

$$\Delta = 0.25 \text{ in.}$$

If K represents the stiffness of the plywood diaphragm

$$K = \frac{1}{CL}$$

or

$$K = \frac{1}{5 \times 10^{-4}\ L}$$

or

$$K = 20 \text{ kips/in.}$$

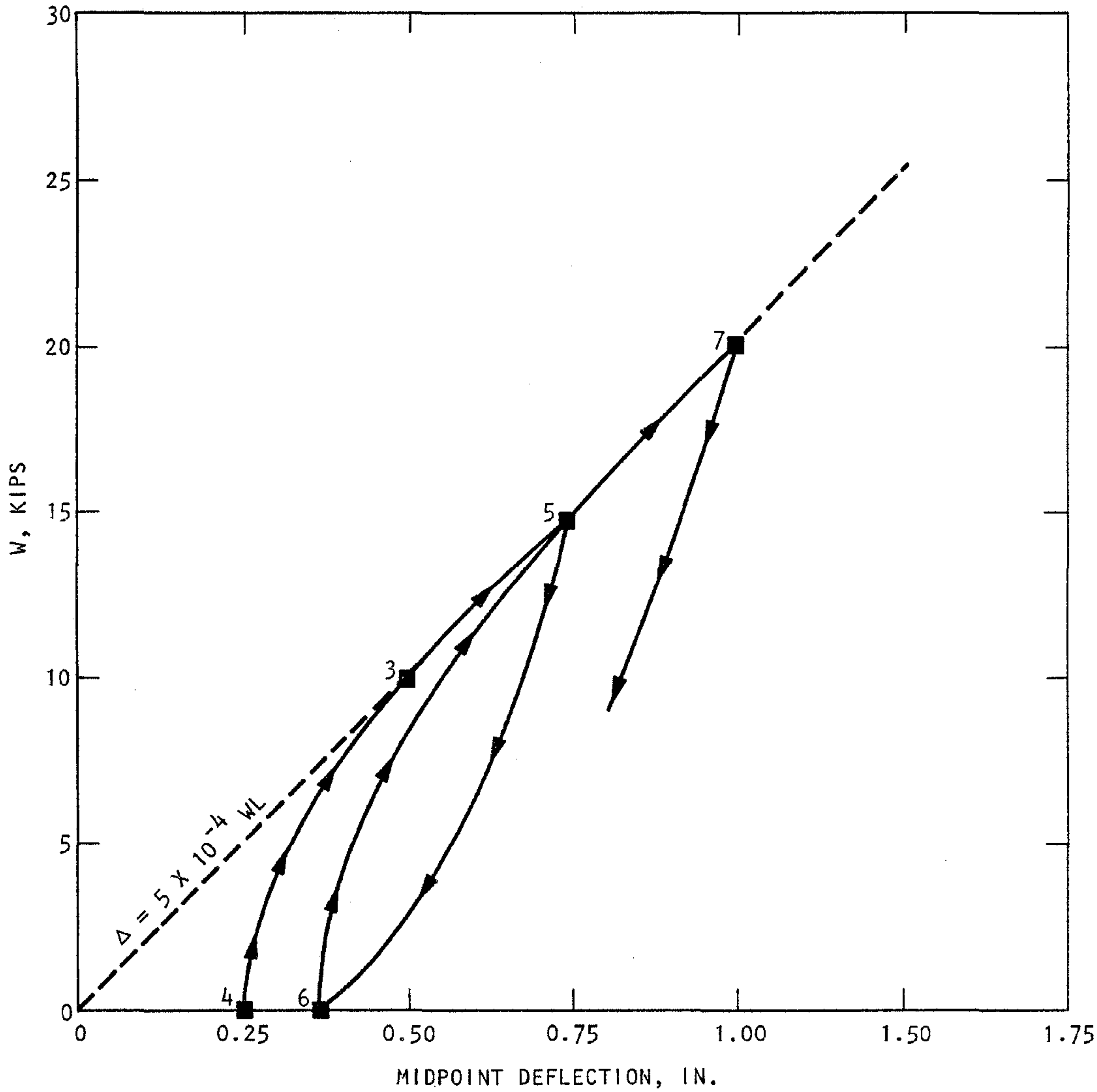

FIGURE 5-5. CYCLIC LOAD DEFLECTION RELATIONS AT APPROXIMATELY CONSTANT DEFLECTION (Ref. 38)

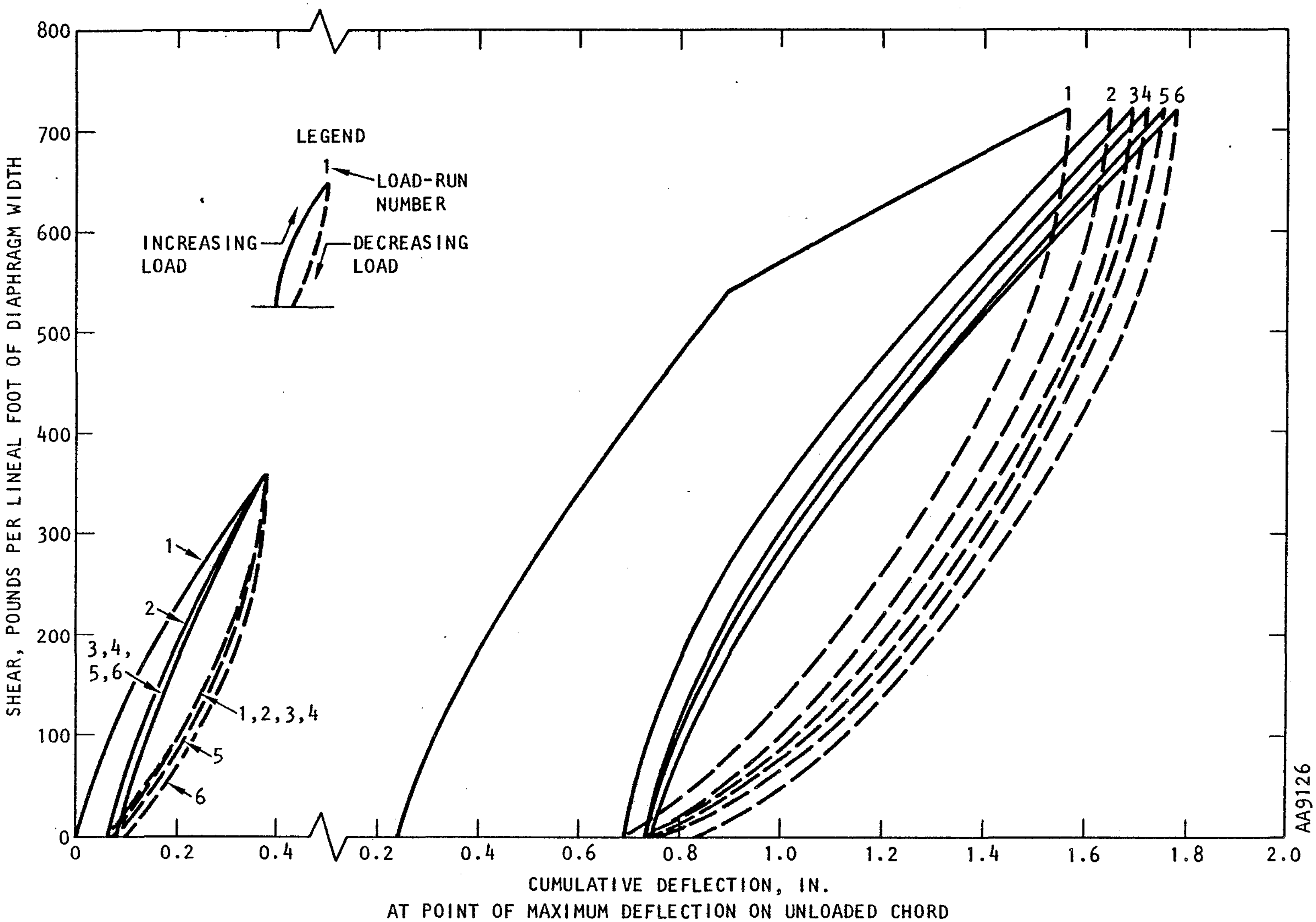

FIGURE 5-6. REPETITIVE LOADING AT 360 AND 720 PLF (12 x 60 ft diaphragm sheathed with 1/2 in. plywood) (Ref. 38)

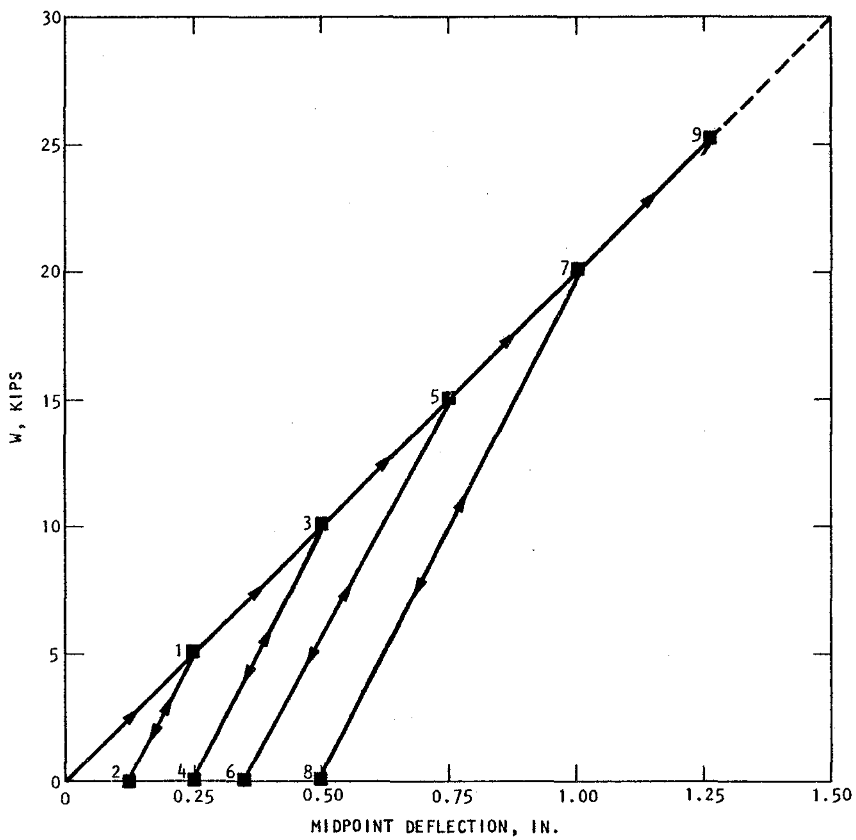

$\Delta = 5 \times 10^{-4}$ WL FOR DEFLECTION OF EACH CYCLE
PERMANENT SET ON LOAD REVERSAL = 1/2
PLOTTED FOR PLYWOOD: 100' SPAN, 50' DEPTH

(a) Simple load deflection model for plywood diaphragms

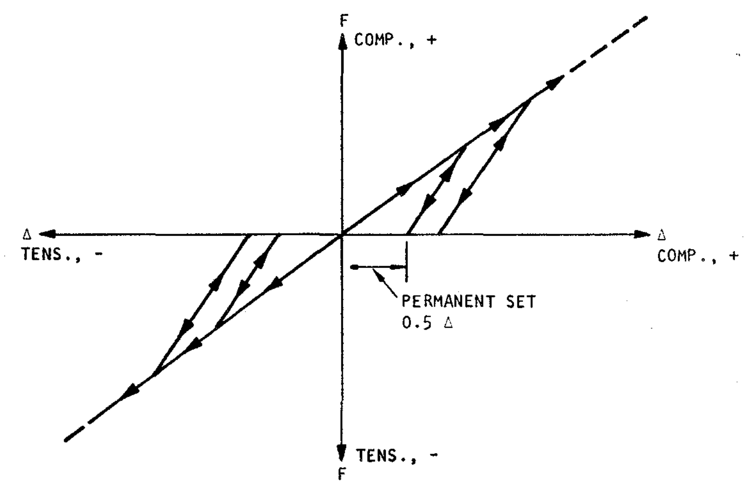

(b) Loading-unloading cycle

FIGURE 5-7. IDEALIZED LOAD DEFLECTION RELATIONS USED IN DIAPHRAGM MODELS OF THIS STUDY

For the four-segment model, the stiffness per segment is

$$k = \frac{K}{4} = 5 \text{ kips/in.}$$

For the eight segment model

$$k = \frac{K}{8} = 2.5 \text{ kips/in.}$$

A summary of material properties used for the diaphragms analyzed in this study is given in Table 5-1.

TABLE 5-1. STIFFNESS OF ROOF DIAPHRAGM USED IN THE PRESENT ANALYSIS

Roof Diaphragm	Load-Deflection Relation	Diaphragm Stiffness, kips/in.	Stiffness/Segment, k, kips/in.	
			Model 1 4 Segments	Model 2 8 Segments
Plywood	$\Delta = 5 \times 10^{-4}$ WL	20	5	2.5
Diagonal	$\Delta = 2.5 \times 10^{-3}$ WL	4	1	0.5
Straight	$\Delta = 10 \times 10^{-3}$ WL	1	0.25	0.125

In addition to the hysteretic damping provided by the hysteretic cycles of Figure 5-7, a 10% critical damping was used in the analyses of some cases to account for viscous damping provided by the roofing materials (viscous damping shown in Table 5-2).

5.1.3 INPUT MOTIONS

The intensity of ground shaking used in this study represents the level of shaking expected in a highly seismic area such as Los Angeles. Effective peak acceleration for such an area is 0.40 g (Ref. 36). Two earthquakes can be specified to represent bounding conditions for the earthquake shaking at the site. The first condition corresponds to a local earthquake with high-frequency content. The second condition corresponds to a large earthquake event centered some 40 miles from the site. This earthquake would have a long duration and a wide band of dominant frequencies.

The N69W component of the 1971 Castaic record was selected for the nearby event. The time history record was scaled to the 0.40 g level and used as the first earthquake input to the diaphragm analysis. The response spectra for this record are shown in Figure 5-8.

The N-S component of the 1940 El Centro record was selected for the distant event. The time history record was scaled to the 0.40 g level and used as input to both diaphragm and wall-overturning models. The response spectra for this record are shown in Figure 5-9.

For the diaphragm analysis, the critical orientation of earthquake input motions is shown in Figure 5-2. In this analysis, the scaled time-history motions discussed above were applied directly at the ends of the roof diaphragm (Levels A and B).

5.1.4 DISCUSSION OF RESULTS OF DIAPHRAGM ANALYSES

A number of parametric cases were run as summarized in Table 5-2. Cases 1, 2, and 3 were subjected to the 1971 Castaic N69W component. A

TABLE 5-2. SUMMARY OF DIAPHRAGM ANALYSIS RESULTS

Case No.	Diaphragm	No. of Segments	Earthquake Input*	Material Property	Type of Damping	Calculated Period T, sec	Acceleration at Center, g	Relative Peak Displacement at Center, in.†
1	Plywood	4	Castaic 1971 N69W Component	Elastic	Viscous	1.73	0.15	3.9
2	Diagonal Sheathing					3.35	0.03	4.2
3	Straight Sheathing					9.30	0.01	6.5
4	Plywood		El Centro 1940 N-S Component			1.80	0.20	6.2
5	Diagonal Sheathing					3.00	0.06	7.4
6	Straight Sheathing					9.30	0.02	12.0
7	Plywood	8	El Centro 1940 N-S Component	Elastic	No Damping	2.80	0.20	11.0
8	Plywood			Elastic	Viscous	2.80	0.14	10.4
9	Plywood			Hysteretic	Hysteretic	3.00	0.20	8.0
10	Plywood			Hysteretic	Hysteretic & Viscous	3.00	0.12	10.7‡
11	Straight Sheathing			Hysteretic	Hysteretic	10.60	0.02	11.0
12	Straight Sheathing			Hysteretic	Hysteretic & Viscous	11.50	0.006	9.0‡

*Earthquake input motions scaled to 0.40g peak ground acceleration
†Relative peak displacements were calculated by subtracting the absolute input displacement from the absolute peak midpoint displacement.
‡30-sec record used for cases 10 and 12

NOTES:
3-sec record used for cases 1 and 2
15-sec record used for cases 3 through 9 and case 11

AA9070

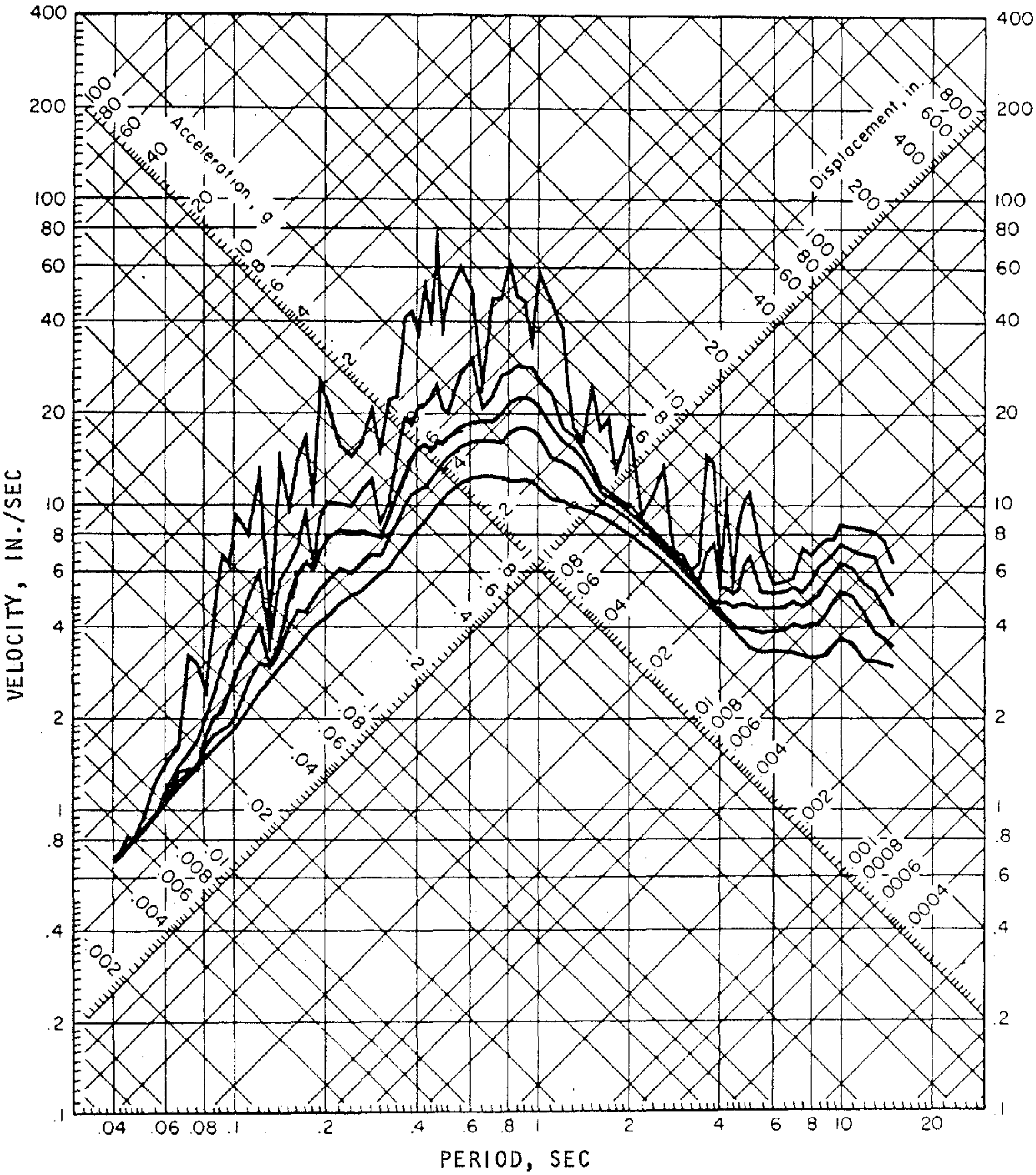

FIGURE 5-8. RESPONSE SPECTRUM OF SAN FERNANDO EARTHQUAKE, 9 FEBRUARY 1971: CASTAIC OLD RIDGE ROUTE, COMP N69W (Damping values are 0, 2, 5, 10 and 20 percent of critical--unscaled)

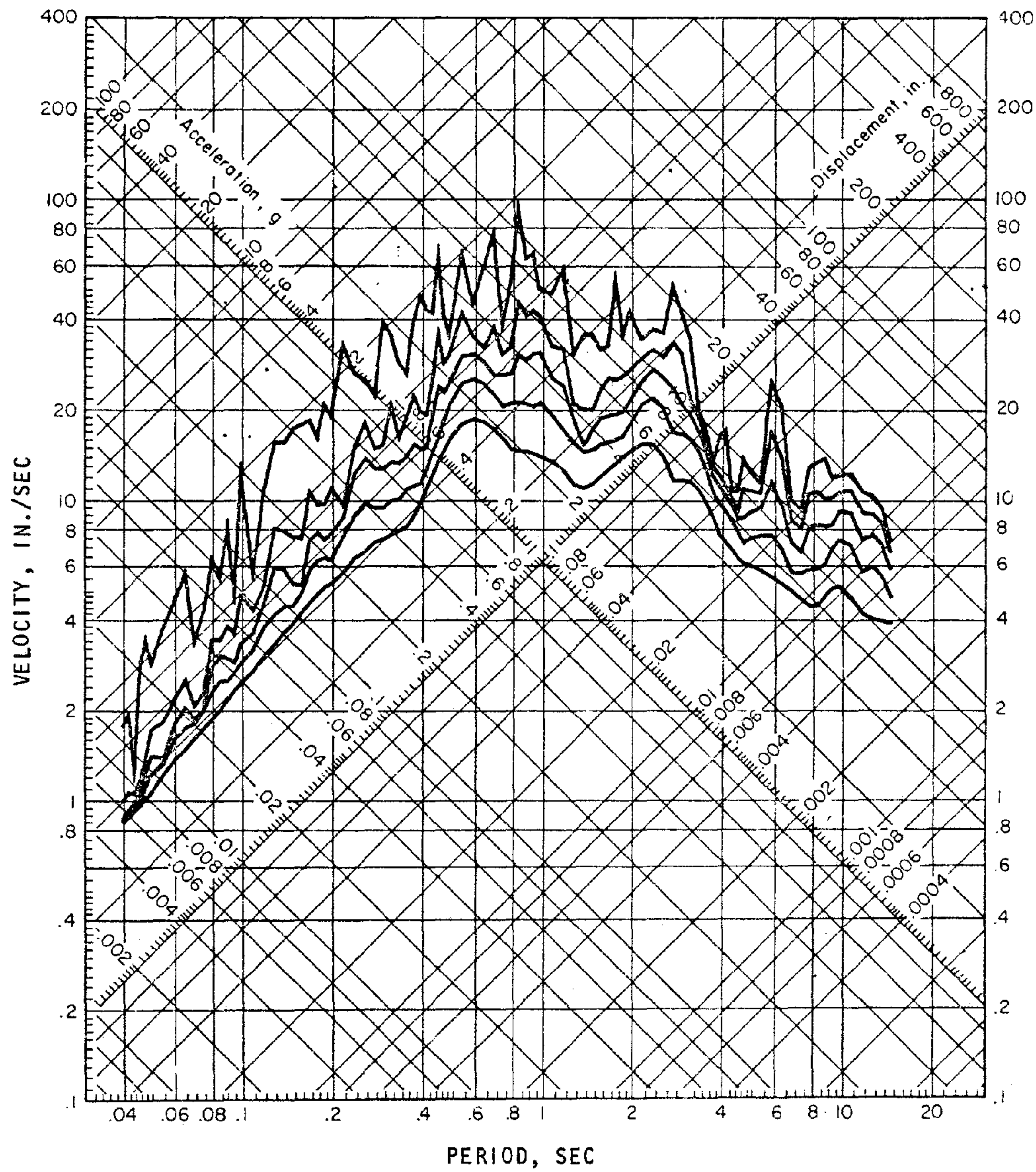

FIGURE 5-9. RESPONSE SPECTRUM OF IMPERIAL VALLEY EARTHQUAKE, 18 MAY 1940: EL CENTRO SITE, IMPERIAL VALLEY IRRIGATION DISTRICT, COMP SOOE (Damping values are 0, 2, 5, 10 and 20 percent of critical--unscaled)

3.5 sec record was used for cases 1 and 2, whereas a longer record of 15 sec was used for the longer-period diaphragm of case 3. The 1940 El Centro N-S component was used as input to cases 4 through 12. The length of the record used for cases 4 through 9, in addition to case 11, was 15 sec. The length of record used for cases 10 and 12 was 30 sec.

Both elastic and hysteretic material properties were assumed in the analysis. Viscous and hysteretic damping were included in 11 cases, as illustrated in Table 5-2. The results of the calculations are presented in Table 5-2 and Figures 5-10 through 5-17. They are provided at the middle of the diaphragm (DOF 4 in Fig. 5-3 and DOF 5 in Fig. 5-4). The relative peak displacements shown in Table 5-2 are determined by calculating the maximum difference between input displacements and the absolute displacements of the midpoint of the diaphragm at the same instant of time.

The first set of results corresponds to cases 1 through 3. The results from the diagonal-sheathing model (case 2) show response periods that are longer than those of the plywood model (case 1), as was shown in Table 5-2. As a result, the peak acceleration at the middle of the case 2 diaphragm is lower than that of the case 1 diaphragm (0.03 g vs. 0.15 g). However, the relative peak displacement of case 2 is only slightly higher than that of case 1 (4.2 in. vs. 3.9 in.), as illustrated in Figure 5-10.

The straight-sheathing diaphragm (case 3) has the longest period among the three diaphragms studied (9.30 sec). Maximum acceleration of 0.01 g (Fig. 5-10) and relative peak displacement of 6.5 in. were calculated at the midpoint.

The second set of results corresponds to cases 4 through 6 subjected to the 1940 El Centro input motions with a longer duration (15 sec). The results of case 4 indicate that the fundamental period is 1.80 sec, about the same as case 1. The peak acceleration of 0.20 g is slightly higher than the 0.15 g calculated for case 1. The major differences can be seen in peak displacements for case 4 as compared to case 1. A peak

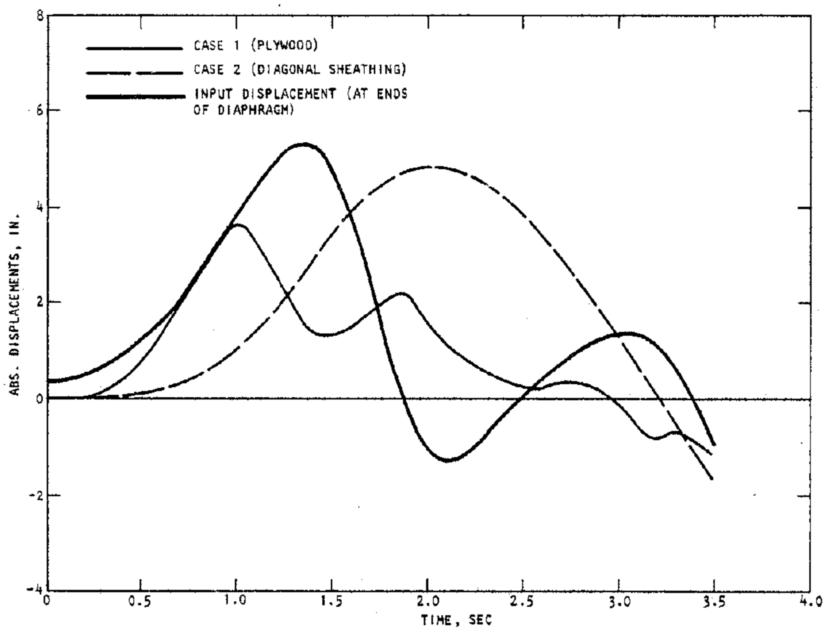

(a) Cases 1 and 2

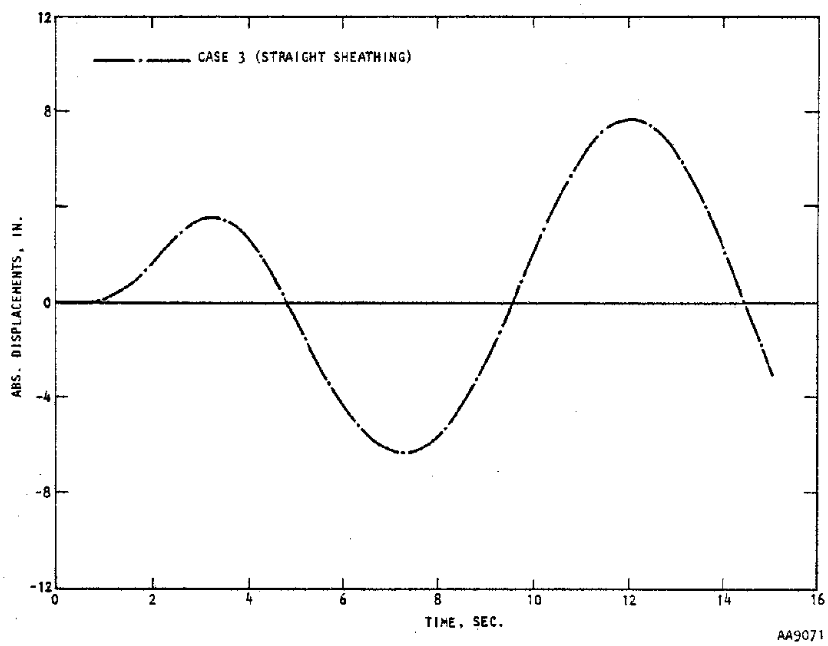

(b) Case 3

Relative peak displacements were calculated by subtracting the absolute input displacement from the absolute peak midpoint displacement.

FIGURE 5-10. ABSOLUTE DISPLACEMENTS AT MIDPOINT OF DIAPHRAGM MODELS, CASES 1, 2, 3 relative displacement of 6.2 in. is shown in Figure 5-11. This higher displacement is attributed to the strong long-period content of the El Centro record.

The response time-history for case 5 indicates that the period of the system is 3.0 sec. The peak acceleration of 0.06 g is slightly higher than the peak acceleration of case 2, associated with the Castaic input record. The case 5 relative peak displacement of 7.4 in. (Fig. 5-11) is higher than that of case 2. However, due to phasing of the response, the peak displacement appears not much greater than that of case 4.

From the results of cases 1 through 5 and the results of the first 15 sec of case 6, it is estimated that for case 6 the maximum acceleration will reach around 0.02 g. The peak displacement is estimated to be 12 in. (Fig. 5-11), which is the same as the peak displacement of input motions.

The third set of results corresponds to cases 7 through 10. Four diaphragms of varying material properties and damping were analyzed. Figure 5-12 and Table 5-2 illustrate how the response of the diaphragm is affected by increasing the number of segments in the diaphragm model. The results of case 8 indicate that the second and third natural modes provide a considerable contribution to the response. The 6.2 in. peak displacement of case 4 was increased to 10.4 in. in case 8 by including the contribution of the second mode (Fig. 5-12). This resulted in shifting the response to a lower acceleration region. The contribution of the higher modes, particularly the second mode, to the acceleration is minimal; and the final result was a reduction in peak acceleration from 0.20 g for case 4 to 0.14 g for case 8 (Fig. 5-13). Therefore, the four-segment model behaves like a stiffer structure with a higher acceleration (0.2 g), shorter period (1.8 sec), and smaller displacement (6.2 in.); whereas the eight-segment model performs like a more flexible structure with a lower acceleration (0.14 g), longer period (2.8 sec), and larger displacement (10.4 in.). It is also observed that the El Centro input, with its strong long period content, when applied to the eight-segment model, provides the most interaction with the periods of the plywood diaphragm (Fig. 5-14).

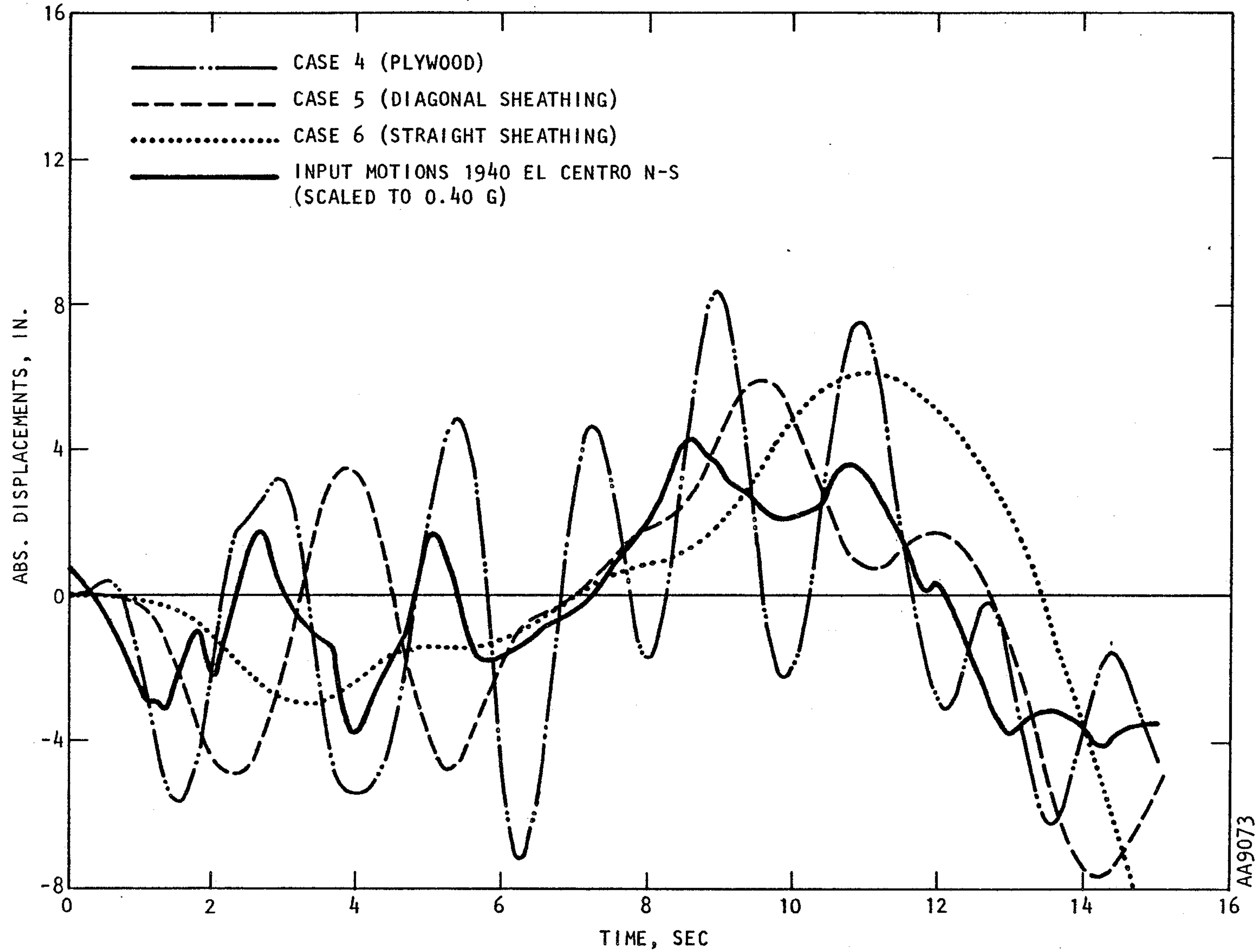

Relative peak displacements were calculated by subtracting the absolute input displacement from the absolute peak midpoint displacement.

FIGURE 5-11. COMPARISON OF ABSOLUTE DISPLACEMENTS AT MIDPOINT OF DIAPHRAGM MODELS, CASES 4, 5, 6

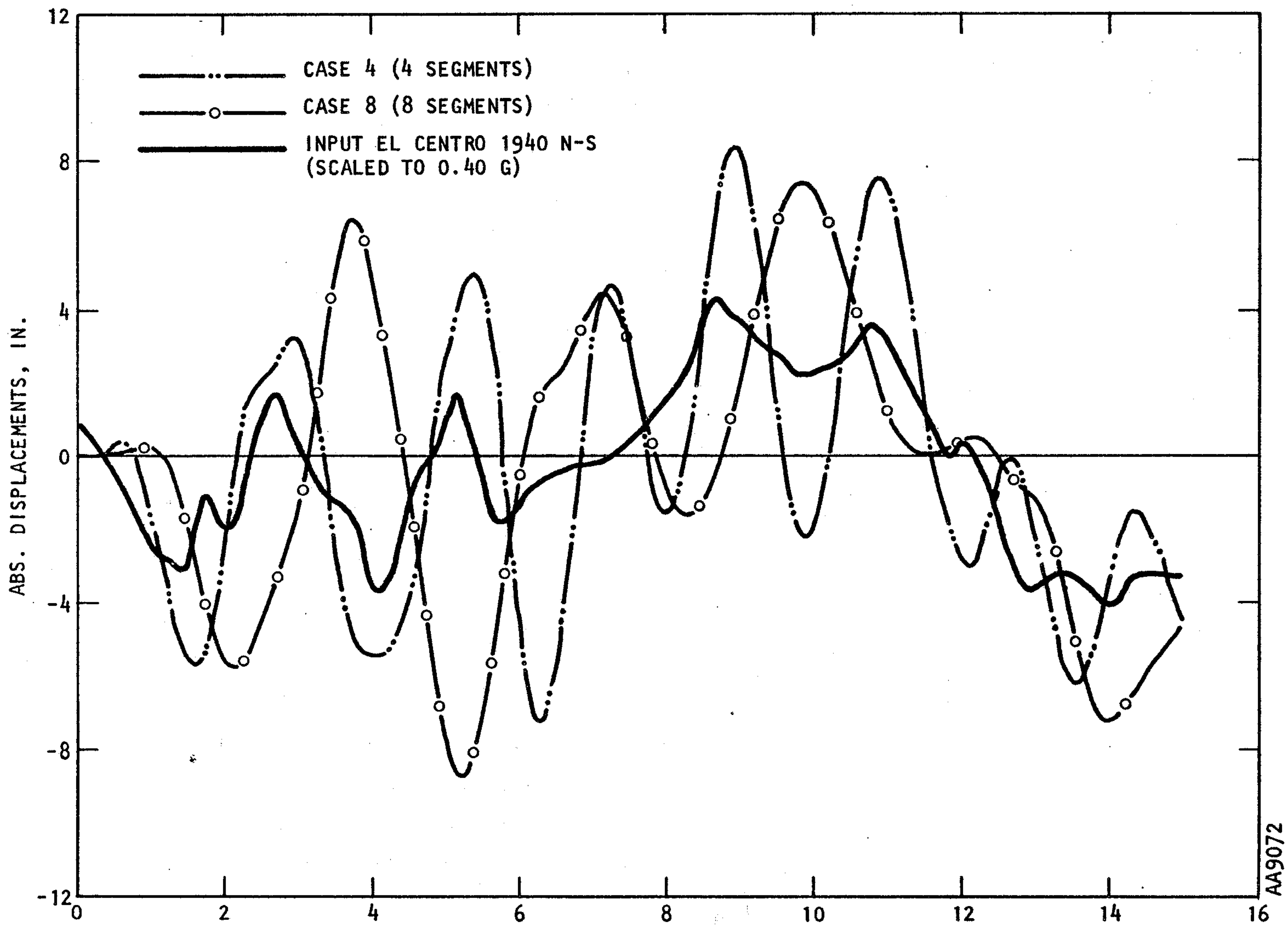

Relative peak displacements were calculated by subtracting the absolute input displacement from the absolute peak midpoint displacement.

FIGURE 5-12. COMPARISON OF ABSOLUTE DISPLACEMENTS AT MIDPOINT OF PLYWOOD DIAPHRAGM MODELS, CASES 4 AND 8

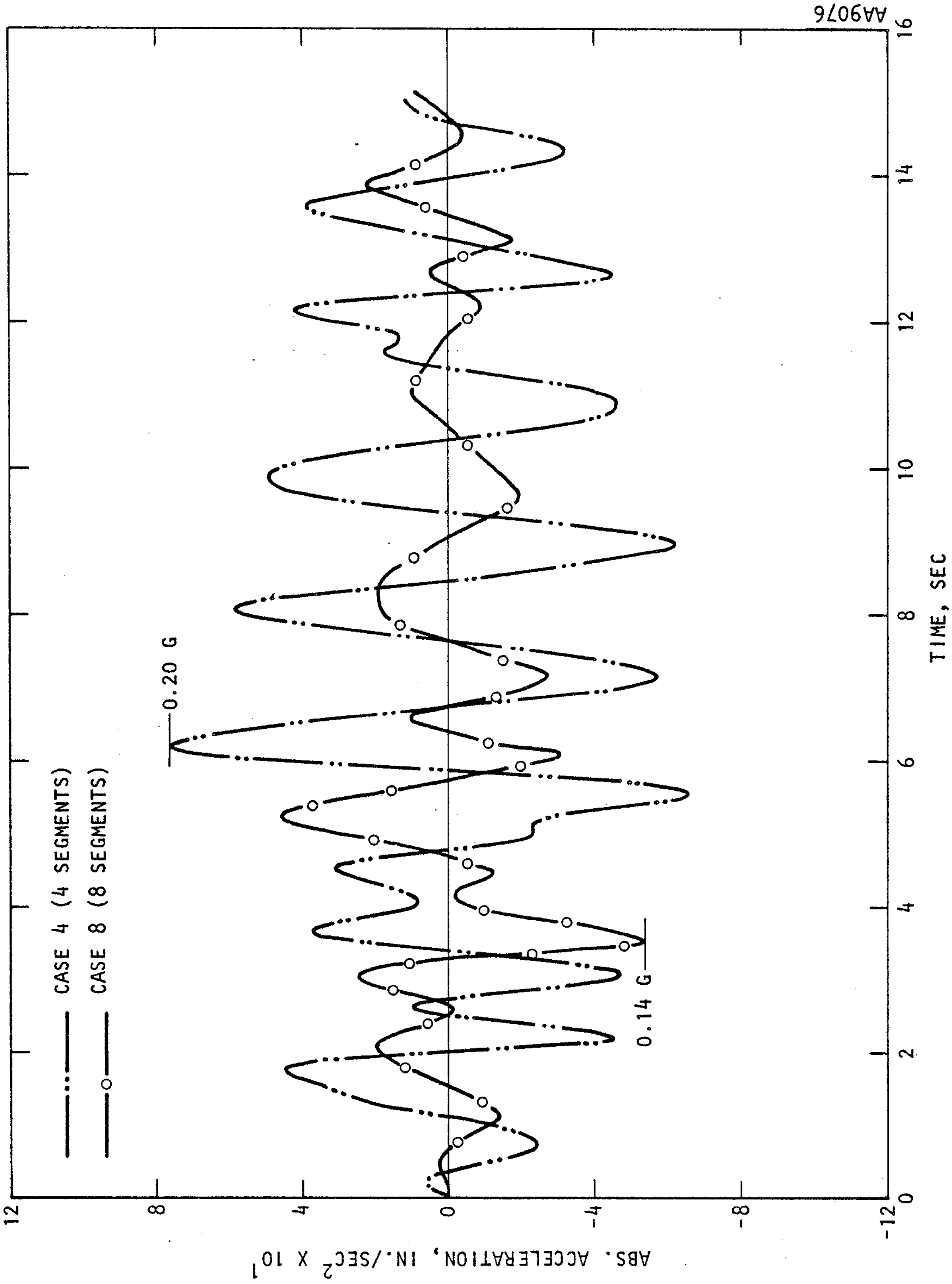

FIGURE 5-13. COMPARISON OF ACCELERATION TIME-HISTORY RESPONSES AT MIDPOINT OF PLYWOOD DIAPHRAGM MODELS, CASES 4 AND 8

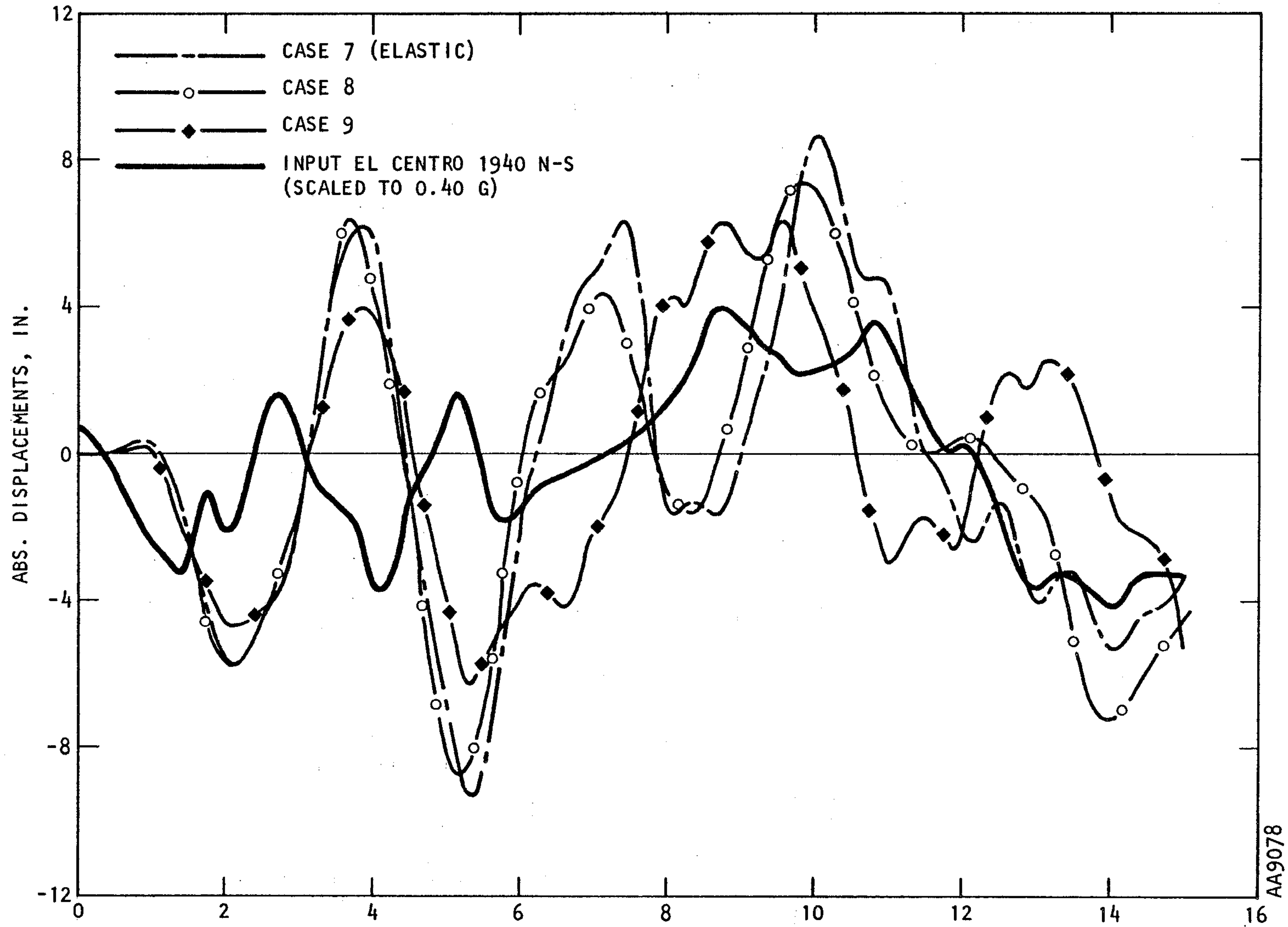

Relative peak displacements were calculated by subtracting the absolute input displacement from the absolute peak midpoint displacement.

FIGURE 5-14. COMPARISON OF ABSOLUTE DISPLACEMENTS AT MIDPOINT OF PLYWOOD DIAPHRAGM MODELS, CASES 7, 8, 9

When the diaphragm material is represented by hysteretic characteristics, as shown in case 9, the structural response corresponds to contributions from a band of diaphragm frequencies, bounded by values related to the slopes of the loading and unloading curves (Fig. 5-15). The period of the diaphragm is lengthened from 2.8 sec (case 7) to 3.0 sec (case 9) for the plywood diaphragm. Because of the combination of higher damping and more frequency contribution to the response, the relative peak accelerations are about the same for cases 7 and 9, as illustrated in Figure 5-16 (0.2 g). However, the peak displacement for case 9 is 8 in., which is smaller than that of case 7, due to the damping effect.

The difference between cases 9 and 10 is that the latter has viscous damping in addition to the hysteretic characteristics. In addition, case 10 was run to 30 sec, whereas case 9 was run for only 15 sec. The peak acceleration for case 9 is 0.20 g as compared to 0.12 g for case 10. Therefore, viscous damping appears to have a considerable effect on attenuating peak accelerations in these diaphragms. The relative peak displacement for case 10 is 10.7 in., compared to 8 in. for case 9 (Table 5-2). However, case 9 may show higher displacements if run for an additional 15 sec.

For the straight sheathing diaphragm, the natural periods are 10.6 and 11.5 sec for cases 11 and 12, respectively. The effect of the additional viscous damping in case 12 results in a reduction of the response of the diaphragm from 11.0 in. for case 11 to 9.0 in. for case 12. The peak acceleration of the midpoint is 0.02 g and 0.006 g for cases 11 and 12, respectively. These values indicate no significant changes in the peak acceleration calculated for the four-segment model of case 6. The results illustrate the considerable attenuation of peak acceleration that is provided by these relatively soft diaphragms. The shear force transmitted to the ends of these diaphragms is reduced from 7.5 kips for the plywood diaphragm (case 10) to 0.54 kips for the straight-sheathing diaphragm (case 12).

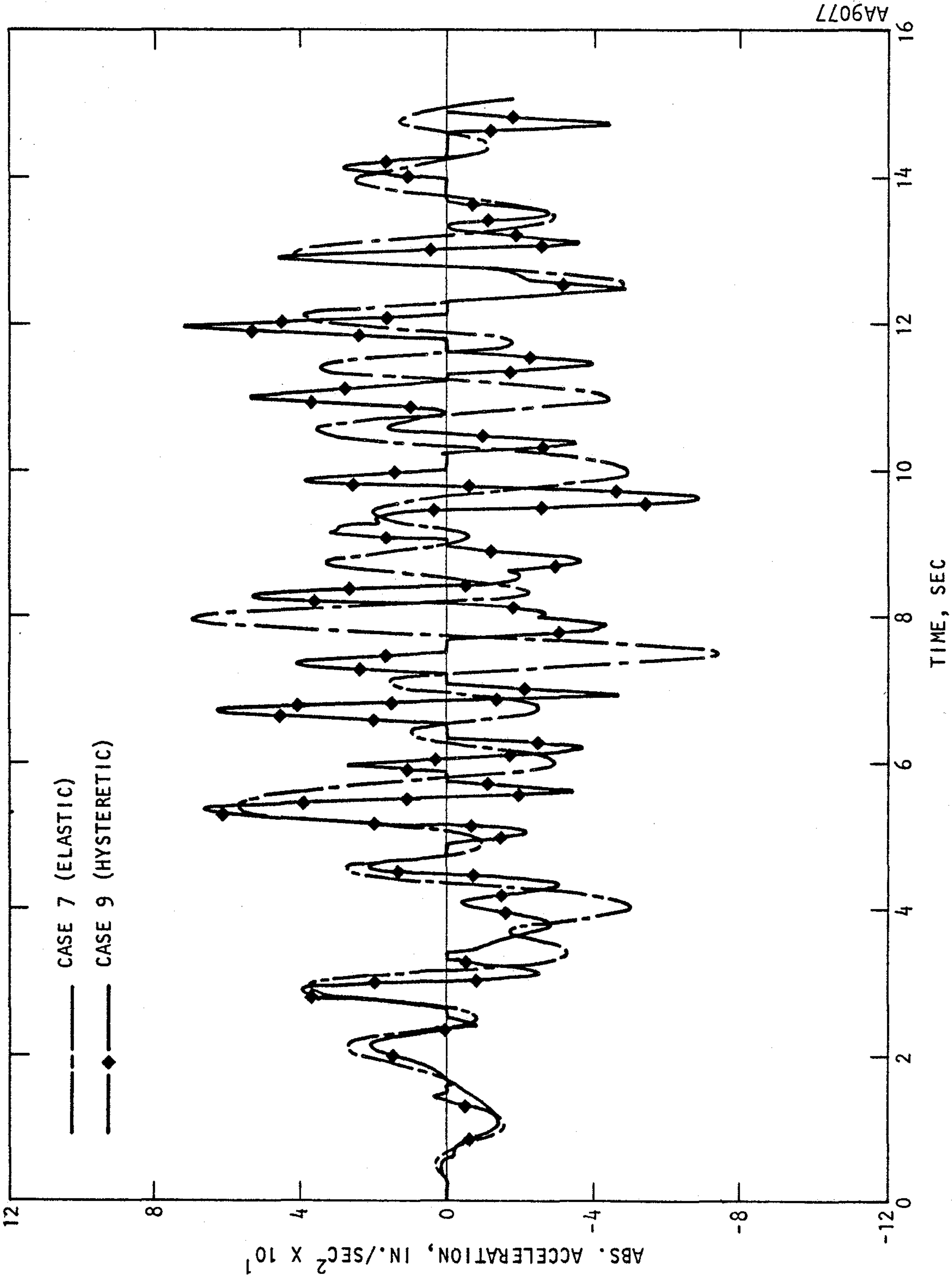

FIGURE 5-15. COMPARISON OF ACCELERATION TIME-HISTORY RESPONSES AT MIDPOINT OF PLYWOOD DIAPHRAGM MODELS, CASES 7 AND 9

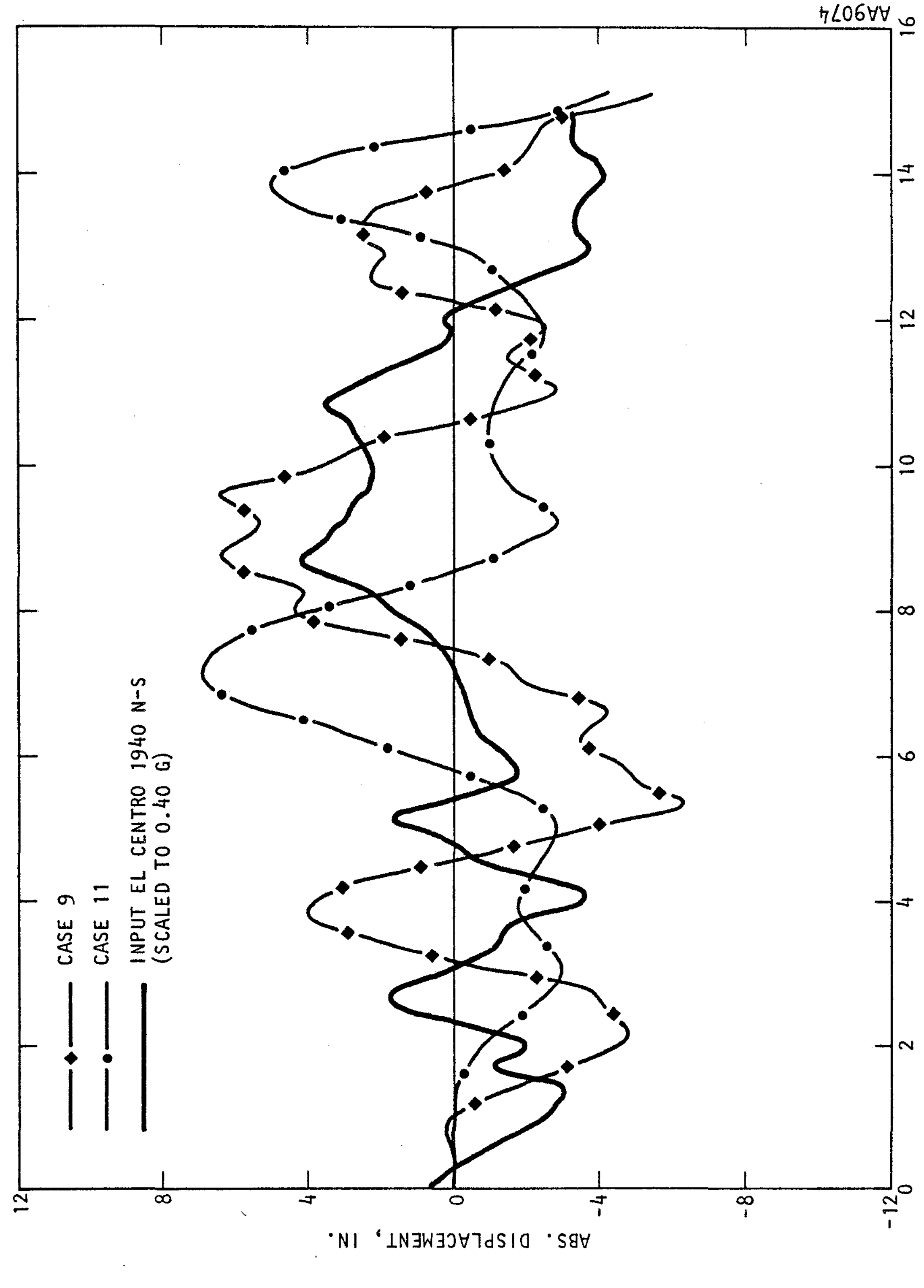

Relative peak displacements were calculated by subtracting the absolute input displacement from the absolute peak midpoint displacement.

FIGURE 5-16. COMPARISON OF ABSOLUTE DISPLACEMENTS AT MIDPOINT OF PLYWOOD AND STRAIGHT-SHEATHED DIAPHRAGM MODELS, CASES 9 AND 11

A comparison of the response of the plywood and straight-sheathed diaphragms indicate that the periods of the latter are much longer, whereas the peak accelerations are much lower. The peak displacements vary between 8 and 11 in. for both diaphragms (Figs. 5-16 and 5-17).

The above results indicate that the eight-segment model provided a better representation of the response of the diaphragms. Addition of the second-mode contribution resulted in a more intense response with longer periods and larger displacements.

The results also indicate that the El Centro record, when compared to the Castaic record, has a wider and stronger long-period content. Therefore, this input was found to be more critical for studying the response of the above diaphragms. However, the El Centro record has strong long-period peaks and valleys. Therefore, its use must be substantiated by other records with strong long-period content. The results also indicate that the viscous damping effect of roofing materials reduced both the acceleration and the displacement of the diaphragm

It is of interest to note that the results of this study indicated diaphragm periods ranging from 1.73 sec for case 1 to 11.5 sec for the softest diaphragm of case 12. These results are in contrast to those obtained by Blume, et al. (Refs. 12, 13) and Rea, et al. (Ref. 14), where relatively shorter periods ranging between 0.17 and 0.75 sec were obtained from low amplitude testing of full-scale school buildings. This discrepancy is probably a result of the highly nonlinear character of these diaphragms, which results in lengthening the periods of these diaphragms when they are subjected to the input level of the 0.40 g scaled El Centro used in this study. Therefore, the preliminary analysis conducted in this study would indicate that stiffening the softer wood diaphragms may not improve the performance of these diaphragms in highly seismic areas.

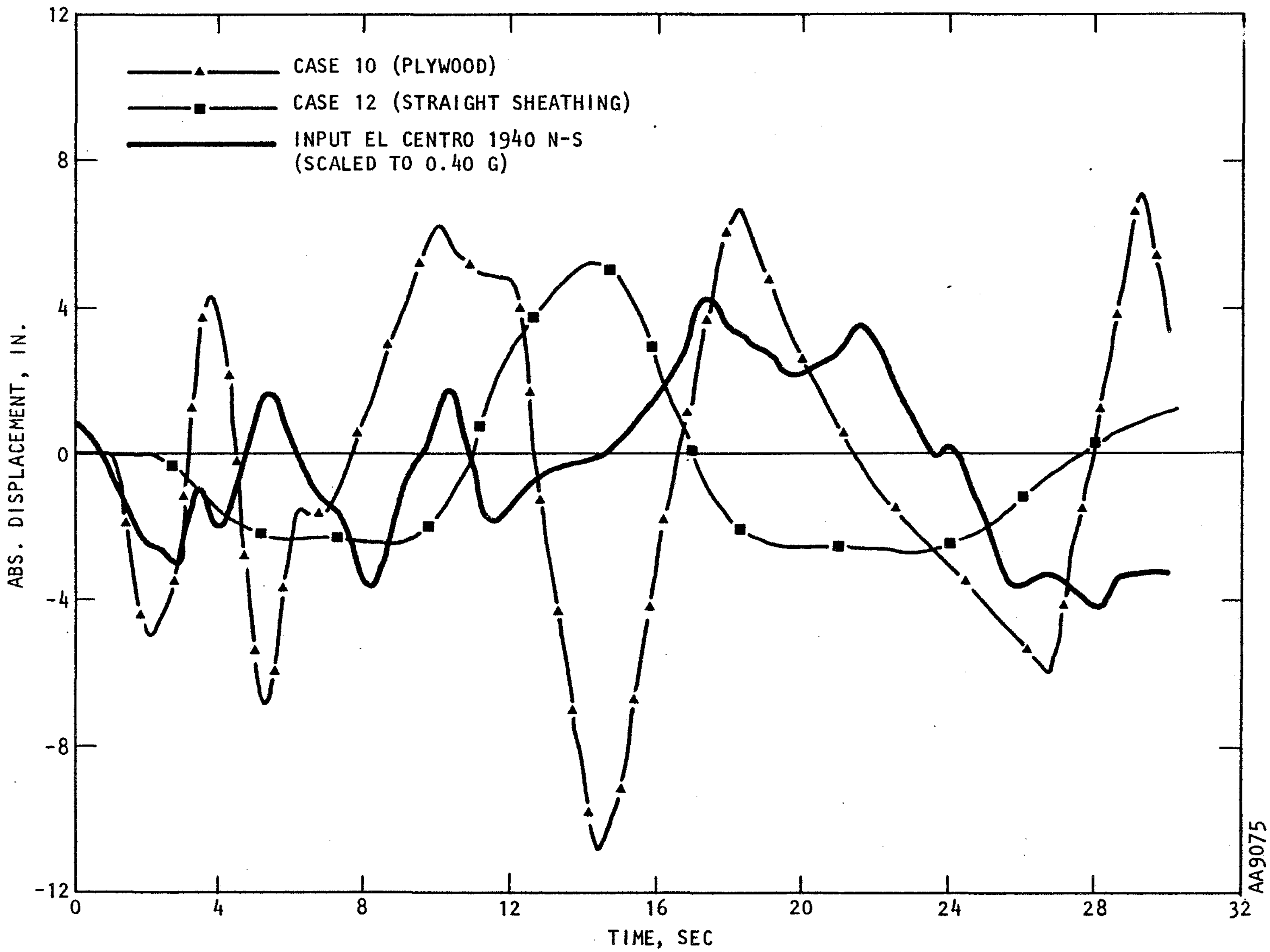

Relative peak displacements were calculated by subtracting the absolute input displacement from the absolute peak midpoint displacement.

FIGURE 5-17. COMPARISON OF ABSOLUTE DISPLACEMENTS AT MIDPOINT OF PLYWOOD AND STRAIGHT-SHEATHED DIAPHRAGM MODELS, CASES 10 AND 12

5.2 ANALYSIS OF IN-PLANE MASONRY-WALL ROCKING

5.2.1 SYSTEM DESCRIPTION

The wall considered in the following calculations is shown in Figure 5-18. The wall is modeled as a rigid rectangular shear panel of height H and width D (Fig. 5-19). The following assumptions are made in the analysis.

a. Horizontal earthquake motion is applied to degree-of-freedom 1.

b. Wall is driven horizontally through the horizontal inter-actor spring 11. This spring is tuned to a high frequency so that it will transmit the ground motion to the base of the wall.

c. Wall responds at degrees-of-freedom 2, 3, and 4.

d. Soil is represented as 10 one-way, bilinear, hysteretic springs (i.e., compression only).

e. Output consists of wall motions at degrees-of-freedom 2, 3, and 4, in addition to forces and deformation in the soil springs, Nos. 1 through 10, and wall motions at the top and bottom of the wall centerline.

Parameters used in the analyses are

$H = 40$ ft $= 480$ in.

$t_w = 9$ in.

$t_f = 18$ in.

$\rho = 0.10$ kips/ft^2 $= 100$ lb/ft^2

$H/D = 0.25$, 1.0, and 1.5

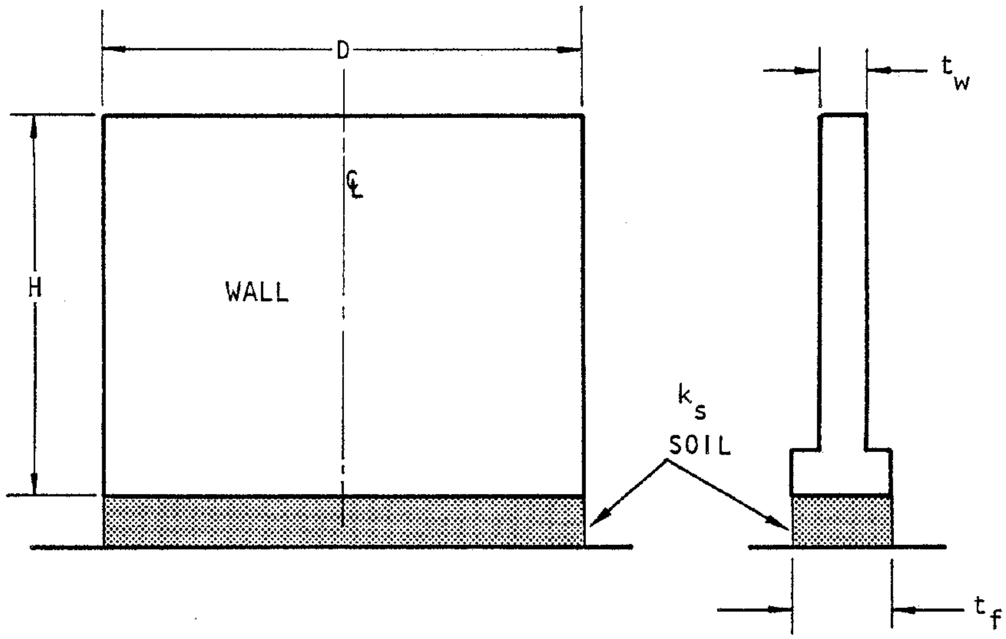

H = WALL HEIGHT
D = WALL WIDTH
t_w = WALL THICKNESS
t_f = FOUNDATION WIDTH
k_s = SOIL STIFFNESS

H/D = 0.25 → 1.5
t_w/t_f = 0.5 (t_w = 9 IN.)
ρ = WEIGHT OF WALL = 100 LB/FT^2
k_s = 100 to 800 PSI/IN.
η = DUCTILITY COEFFICIENT FOR SOILS

FIGURE 5-18. MASONRY WALL AND SUPPORTING FOUNDATION

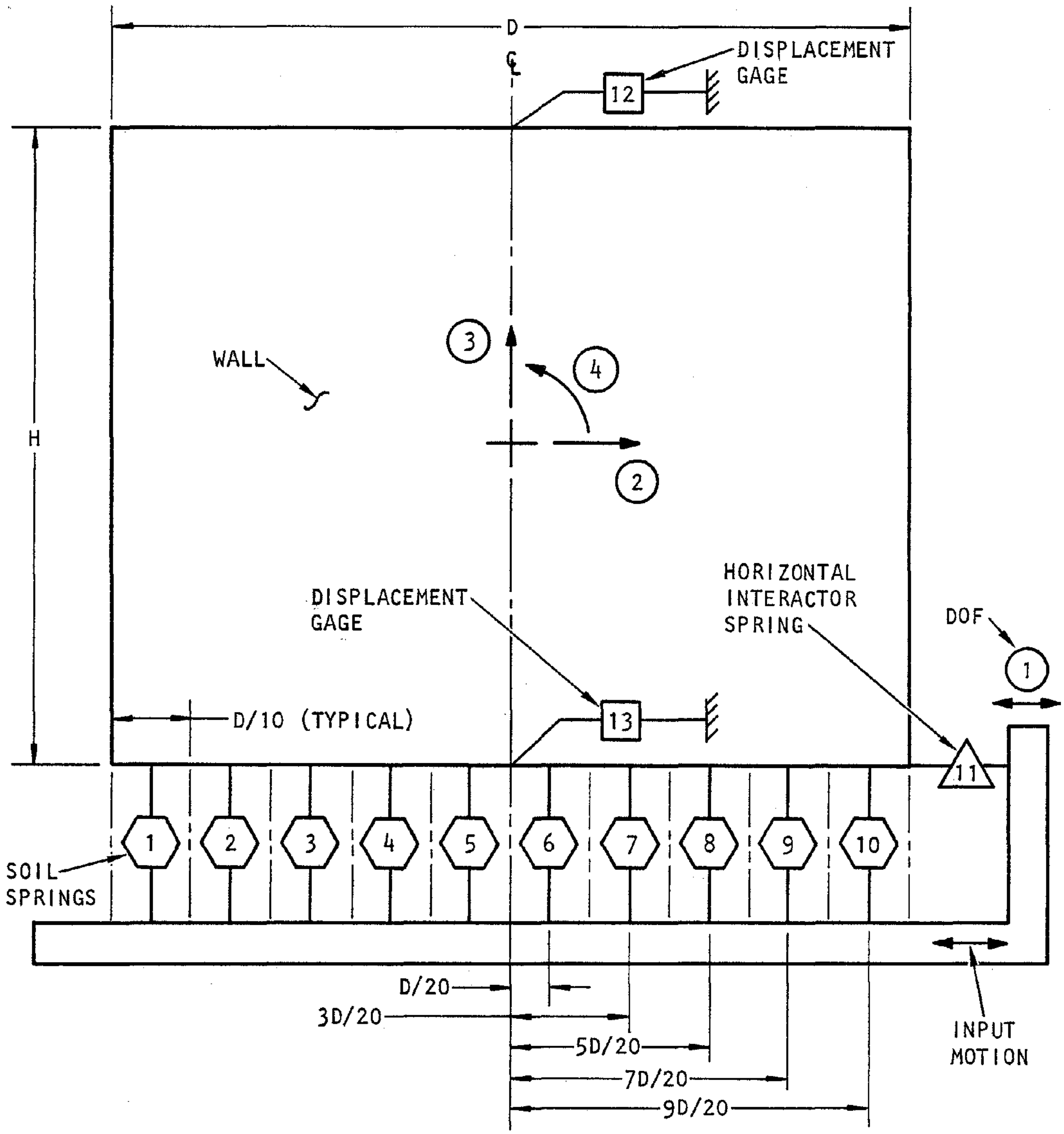

FIGURE 5-19. LUMPED-PARAMETER WALL MODEL CONSIDERED IN WALL-ROCKING ANALYSIS

Soils data for

$$k_s = 100 \text{ psi/in.} \qquad \eta = 0.5$$

and for

$$k_s = 800 \text{ psi/in.} \qquad \eta = 0.0 \qquad \text{(Fig. 5-20)}$$

Inelasticity occurs at $e = 1.0$ in. and

$$F_y = \frac{1}{12} k_s \quad (\text{lb/ft}^2)$$

The mass of the wall is calculated from the relation

$$M = H \cdot D \cdot \rho/g = \frac{\rho}{g} H^2 \left(\frac{D}{H}\right)$$

The polar moment of inertia, J, of the wall is given by the equation

$$J = \frac{M}{12} (H^2 + D^2) = \frac{M}{12} H^2 \left(1 + \frac{D^2}{H^2}\right)$$

$$= \frac{\rho}{12g} H^4 \left(\frac{D}{H}\right) \left[1 + \left(\frac{D}{H}\right)^2\right]$$

The soil-spring stiffness is calculated as follows:

$$k_s = 100 \text{ psi/in.} , \qquad \eta = 0.5$$

$$K_s = \frac{k_s}{10} t_f \cdot H\left(\frac{D}{H}\right) = \frac{100}{10} \times 18 \times 480 \ (D/H)$$

$$K_s = 8.64 \times 10^4 \ (D/H) \text{ lb/in.}$$

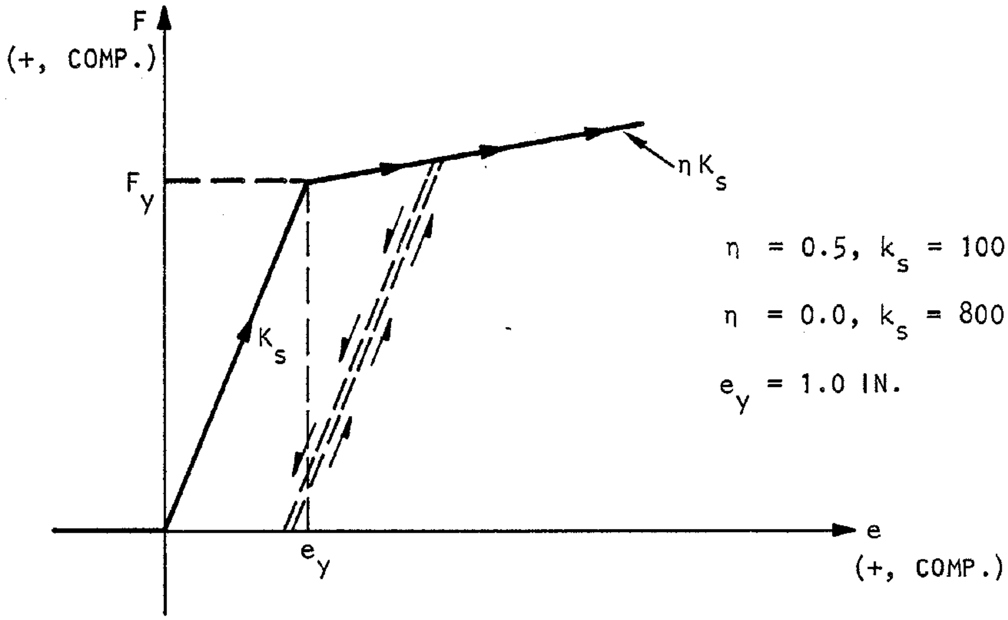

BILINEAR HYSTERETIC SPRING (COMPRESSION ONLY)

K_s = INITIAL ELASTIC STIFFNESS, LB/IN.

$k_s \cdot t_f \cdot D/10$

k_s = 100 TO 800 PSI/IN.

F_y = YIELD LOAD (i.e., soil yield strength)

η = DUCTILE COEFFICIENT FOR SOILS

FIGURE 5-20. SOIL SPRING CHARACTERISTICS and for

$$k_s = 800 \text{ psi/in.} \quad , \qquad \eta = 0.0$$

$$K_s = 6.912.\text{x } 10^5 \text{ (D/H) lb/in.}$$

Table 5-3 provides properties of the lumped mass wall model for three H/D ratios.

The intensity of ground shaking used in the study of wall rocking is the same as the intensity used earlier in this section for diaphragm analysis. The N-S component of the 1940 El Centro record is scaled to 0.40 g and used as input to the model. The first three seconds of the record were used in the analyses. Damping was provided as viscous or hysteretic effects. A 1% critical damping was considered for the vertical springs while a high damping of 10% was specified for the sway spring.

5.2.2 DISCUSSION OF RESULTS OF WALL-ROCKING ANALYSES

A number of parametric cases were run as summarized in Table 5-4. The case of a wall of H/D = 0.25 and k_s = 100 psi/in. did not result in any modification of the input motions. Therefore, this case was not pursued. The results of case 1 indicate that for soft soils (k_s = 100 psi/in.) and H/D = 1.0, there is approximately 15% amplification of the motion at the top of the wall (Displacement Gage 12). The motion of three points at the middle line of the wall are plotted in Figure 5-21, which illustrates the change in motion from the bottom of the wall (point 13) to the top of the wall (point 12). This amplification is caused by the rocking and lifting of the two bottom corners of the wall, as illustrated by the vertical displacements of springs 1 and 10 in Figure 5-22.

TABLE 5-3. LUMPED MASS MODEL PROPERTIES FOR SELECTED H/D RATIOS

H/D	0.25	1	1.50
D/H	4	1	0.66
D	1920 in.	480 in.	320 in.
M, $lb\text{-}sec^2/in.$	1658	414.5	276.3
J, $lb\text{-}sec^2/in.$	5.413×10^8	1.592×10^7	7.665×10^6
K_s (of k_s = 100 psi/in.), lb/in.	3.456×10^5	8.64×10^4	5.76×10^4
F_y (of k_s = 100 psi/in.), lb	3.456×10^5	8.64×10^4	5.76×10^4
K_s (of k_s = 800 psi/in.), lb/in.	2.765×10^6	6.912×10^5	4.608×10^5
F_y (of k_s = 800 psi/in.), lb	2.765×10^6	6.912×10^5	4.608×10^5

TABLE 5-4. SUMMARY OF WALL-ROCKING ANALYSIS RESULTS

Case No.	H/D	Soil Stiffness, psi/in.	Peak Vertical Uplift, in.	Horizontal DOF (2)			Vertical DOF (3)		Rocking DOF (4)		Bottom of Wall (13)		Top of Wall (12)	
				Peak Displ., in.	Peak Accel., g	Amplif. Ratio	Peak Displ., in.	Peak Accel., g	Peak Displ., in.	Peak Accel., g	Peak Displ., in.	Amplif. Ratio	Peak Displ., in.	Amplif. Ratio
1	1.0	100	0.34	-3.35	0.44	1.10	0.24	0.32	0.0018	0.002	+2.85	0.88	+3.75	1.15
2	1.0	800	0.05	-3.35	0.47	1.17	0.015	0.29	0.0003	0.001	-3.35	1.0(no ampl.)	3.35	1.0(no ampl.)
3	1.5	100	1.70	+4.5	0.52	1.30	0.47	0.60	0.009	0.002	+2.80	0.62	+6.10	1.36

AA9130

- Earthquake input at (1) 1940 El Centro N-S component scaled to 0.40 g peak ground acceleration--3 sec record
- Damping in vertical springs--1%
- Damping in sway spring--10%
- The displacements shown in this table are peak *absolute* displacements

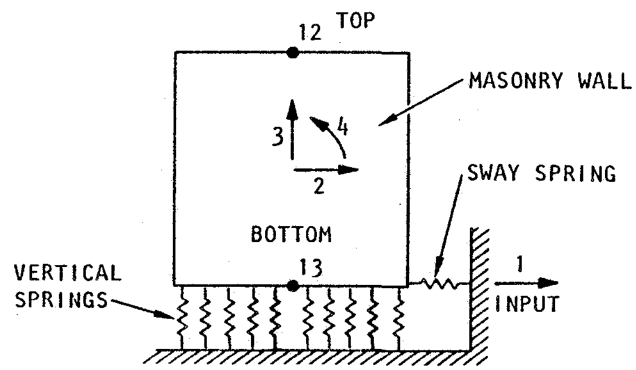

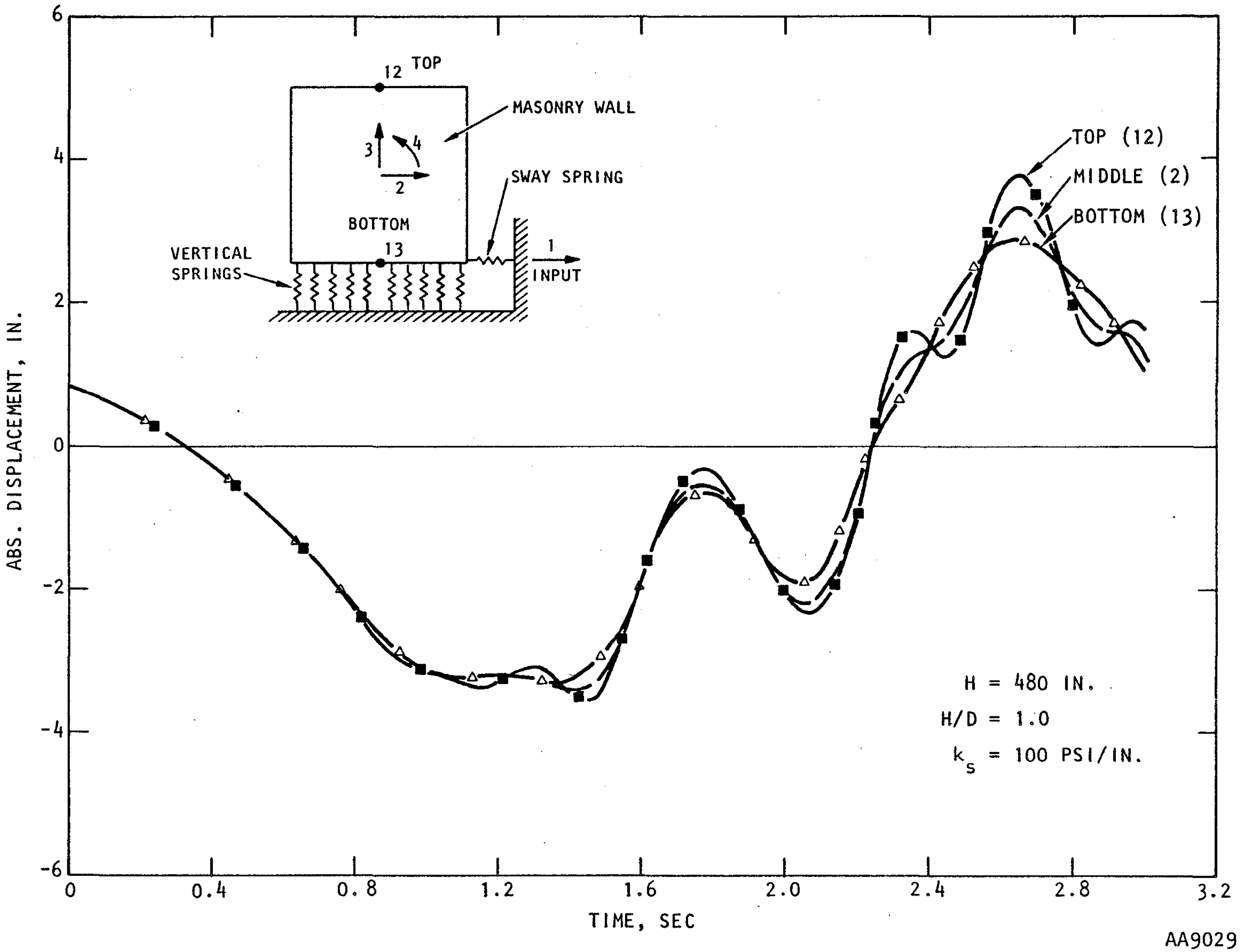

FIGURE 5-21. COMPARISON OF ABSOLUTE DISPLACEMENTS OF WALL, CASE 1

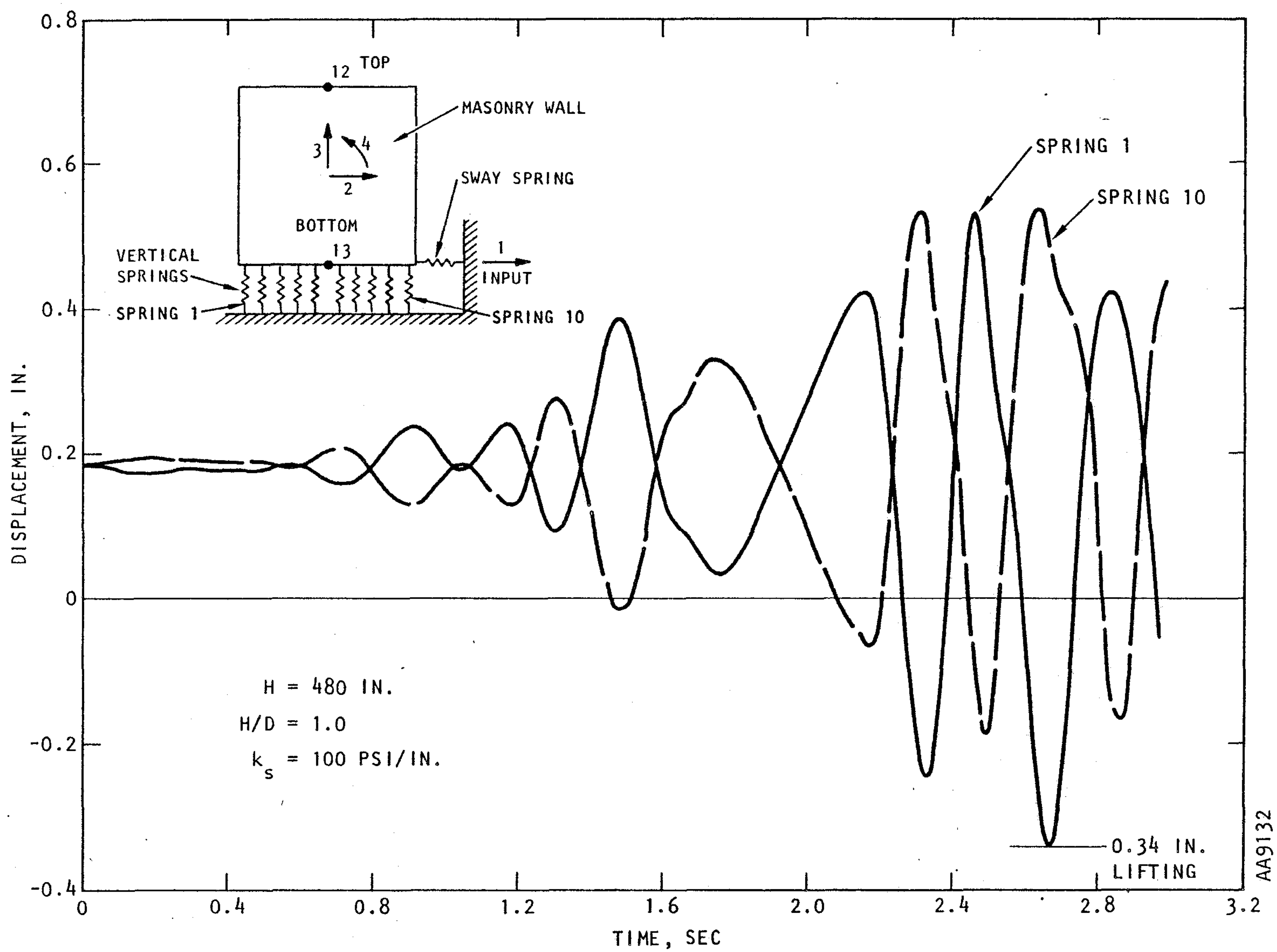

FIGURE 5-22. LIFTING OF TWO BOTTOM CORNERS OF WALL, CASE 1

The continuous rocking of the wall and lifting of the corners resulted in a gradual buildup of response in the vertical direction, where peak absolute displacement reached 0.24 in. while peak acceleration was 0.32 g (Table 5-4). However, the rocking displacements and accelerations were very small due to the large rotary inertia that was associated with the assumption of a 40 ft x 40 ft rigid wall.

The results of case 2 for $H/D = 1$ and k_s of 800 psi/in. indicate that increasing the stiffness of the soil from 100 to 800 psi/in. created very stiff supporting springs. No rocking, lifting, or amplifying of the motion was observed. This indicates that, for such a model, input motions are transmitted through the structure with virtually no change.

The results of case 3, where H/D was increased to 1.5 and k_s was held at 100 psi/in., indicate a larger lifting and higher amplification than those reported for case 1. The response at the top of the wall (point 12) indicate approximately 36% amplification, as illustrated by Figure 5-23. A peak lifting of 1.70 in. is shown in Figure 5-24. The peak vertical displacement was 0.47 in. while the peak vertical acceleration was 0.60 g.

Figure 5-25 illustrates the effect that increasing H/D and k_s has on the response at the top of the wall (point 12). This comparison indicates that large amplifications would be expected for higher H/D values associated with soft soil springs. It should be emphasized that the rotational displacements in the above three cases were very small and would indicate that the rigid body mathematical model must be modified to include both internal deformations and soil deformations. However, these preliminary studies indicate that the response of the vertical element of the selected representative building is strongly affected by the stiffness of the supporting soil and the height to width ratio of the element. Further research with a model that includes wall deformations is needed to determine bounds of the response and to study other effects such as variations of input motion.

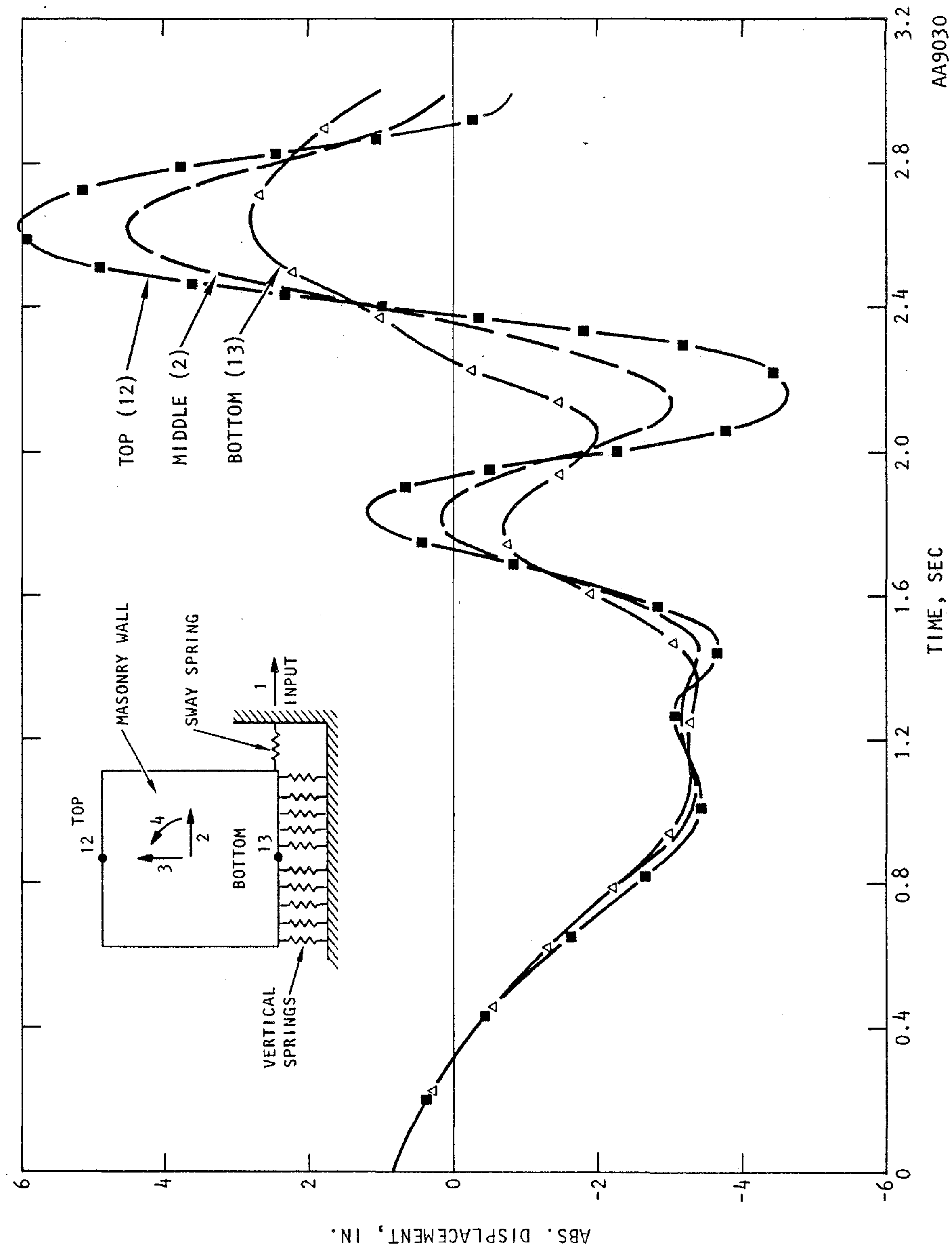

FIGURE 5-23. COMPARISON OF ABSOLUTE DISPLACEMENTS OF WALL, CASE 3

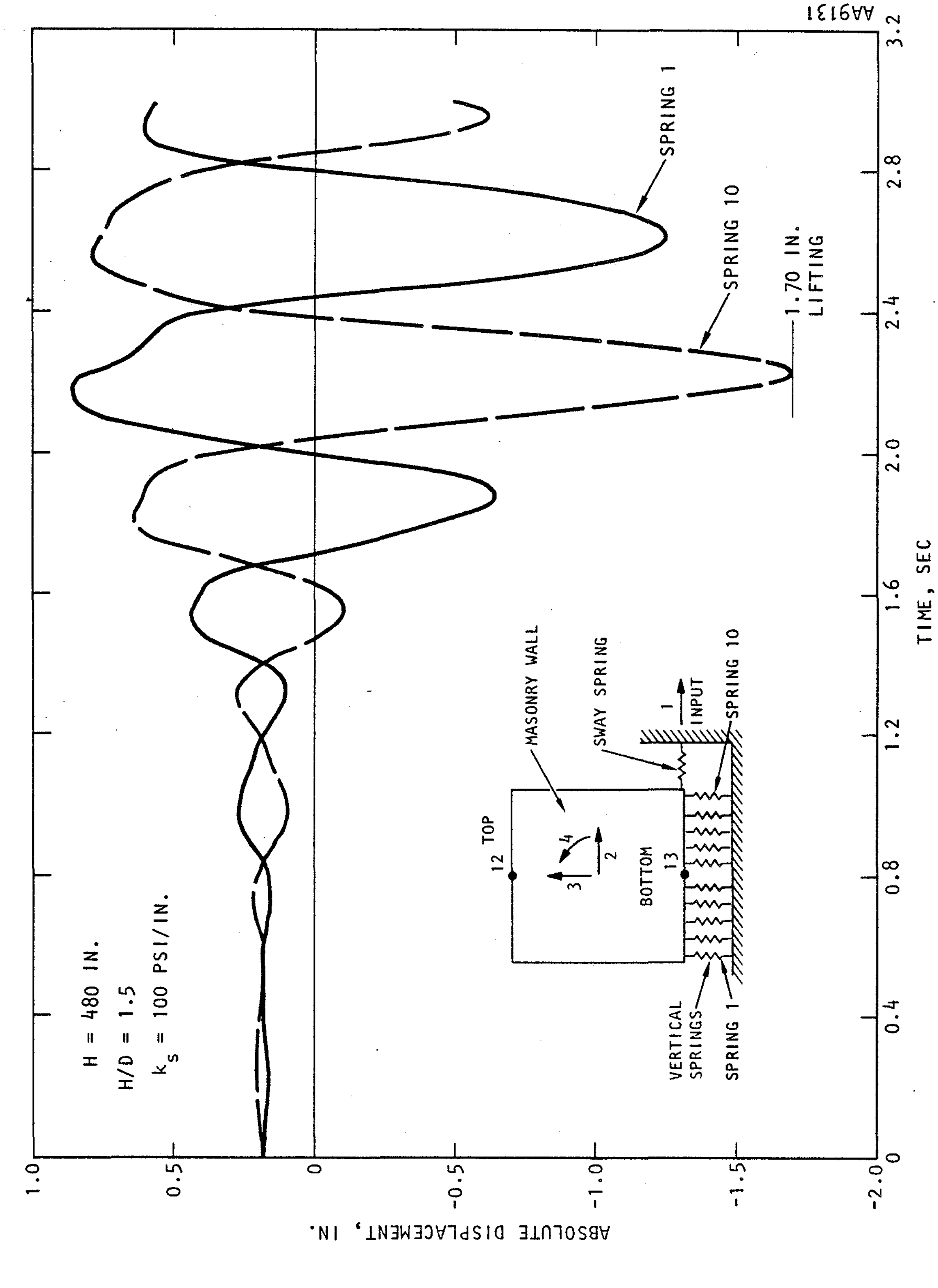

FIGURE 5-24. LIFTING OF TWO BOTTOM CORNERS OF WALL, CASE 3

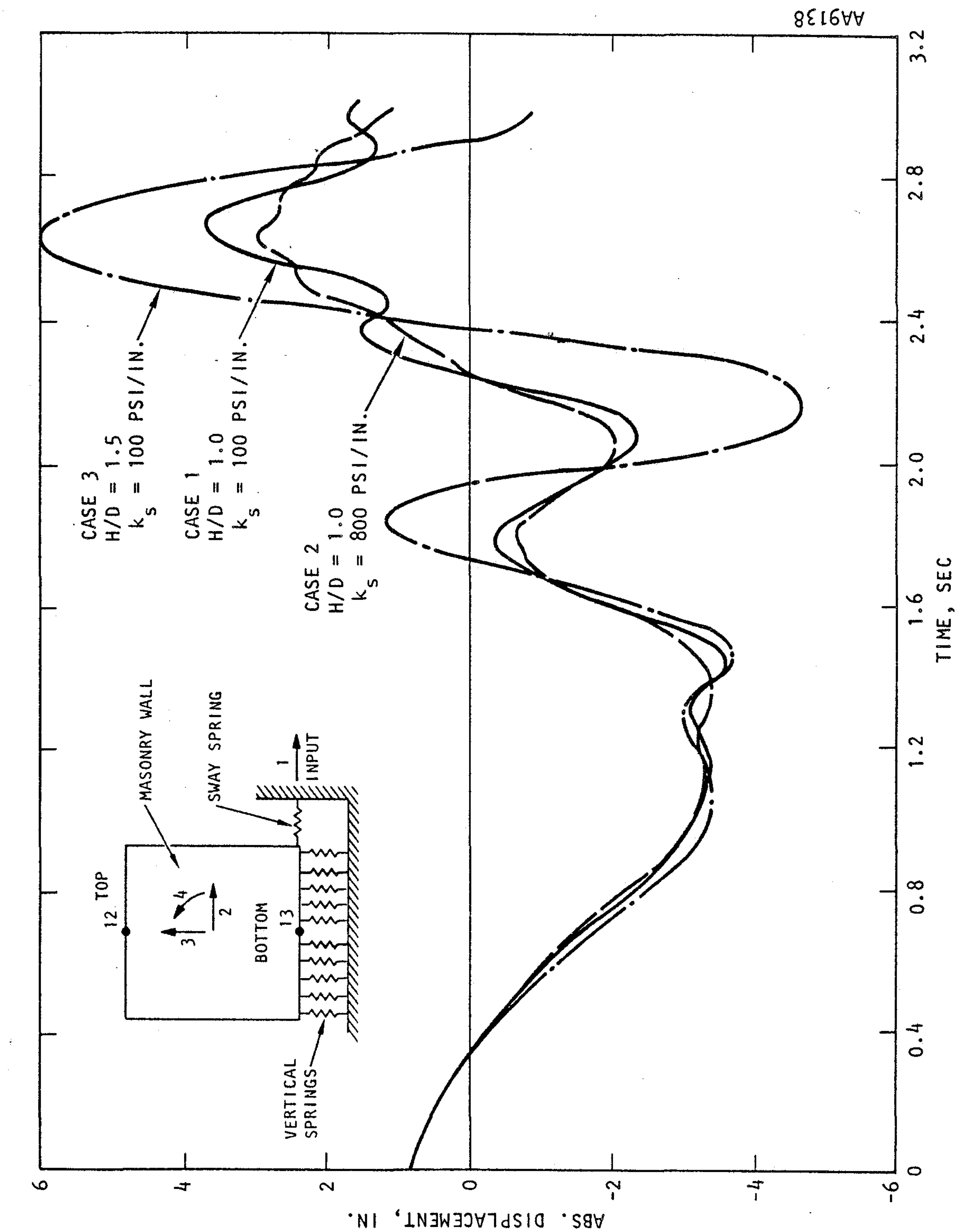

FIGURE 5-25. COMPARISON OF ABSOLUTE DISPLACEMENTS OF TOP OF WALL FOR CASES 1, 2, AND 3

SECTION 6

CONCLUSIONS OF PHASE I STUDY AND RECOMMENDATIONS FOR PHASE II STUDY

6.1 CONCLUSIONS OF PHASE I STUDY

1. Most masonry research programs have been directed towards studying masonry for new construction. Research programs for mitigation of earthquake hazards in existing unreinforced masonry buildings are meager and still in the early stages.

2. ATC-3 is the state-of-the-art tool for describing the ground shaking at various sites across the United States. However, the smooth elastic response spectrum recommended in ATC-3 is not the ideal means for describing the design ground shaking input needed in the present study for evaluating the response of various components of existing unreinforced masonry buildings.

3. The response of wood diaphragms is highly nonlinear when subjected to the level of shaking expected in highly seismic zones. Therefore, low-amplitude tests are not adequate to predicting the response of these diaphragms in highly seismic zones.

4. The wood diaphragms studied in Phase I have periods that range between 1.73 and 11.5 sec and are strongly influenced by earthquake ground motions that have a strong long-period content.

5. Overturning effects of in-plane forces on masonry walls are important, and are strongly dependent on the height-to-width ratio (H/D) of these walls and the stiffness of the supporting soil. Walls with $H/D \geq 1$ on soft soild would amplify the input earthquake motions.

6.2 RECOMMENDATIONS FOR PHASE II STUDY

In order to further evaluate and extend the findings of Phase I, the following recommendations are given.

1. ATC-3 should be used to describe the intensity of earthquake shaking at various sites to be studied in Phase II.

2. An ensemble of time-history ground motions would be selected at each site based on the above criteria. These records should have response spectra that relate to the standard spectra proposed by ATC-3.

3. Additional analyses of diaphragms are needed. These analyses would include a larger number of segments and a variety of earthquake input motions. In addition, the effects of retrofit methods on the response of these diaphragms should be studied.

4. An experimental program of diaphragms that includes a pseudo-static and -dynamic series of tests is needed. Pseudo-static tests would account for loading and unloading under load reversal. Dynamic tests would be performed for low-amplitude and large-amplitude earthquake forces. These tests would provide data for correlation with the results of the analyses conducted in the Phase II study and for confirmation of the trends described in the Phase I study.

5. Further investigation is needed for the overturning effects of in-plane forces on masonry walls. This would include a model that accounts for wall deformations and supporting soil stiffness. In addition, various earthquake input ground motions would be used. Bounds on the response of walls with different H/D ratios and various supporting soil stiffnesses would be provided.

6. Analyses of the one-story building studied in Section 5 should be extended to include both wall and diagphragm response in the model.

7. A model of a multistory building should be analyzed for various time histories. Response of critical elements should be evaluated.

8. Torsional capabilities of diaphragms and existing unreinforced masonry buildings need to be studied.

9. The effect of out-of-plane earthquake forces on the response of unreinforced masonry walls of different height-to-thickness ratios needs to be investigated, both analytically and experimentally.

10. The effect of coupling probable vertical motions with horizontal time histories on the response of the above models needs further investigation.

11. A simple method of determining upper and lower bound properties of existing unreinforced masonry walls is needed. Results of pin tests, bed joint tests, and 4 ft x 4 ft prism tests should be correlated with masonry wall strength.

12. Effect of various retrofit methods on the response of existing URM buildings should be studied both analytically and experimentally.

13. Experimental data on joints, panels, piers, and walls, from previous studies by others, should be analyzed and evaluated. This step would extend the data base provided by the present program to include all available pertinent data.

SECTION 7

REFERENCES

1. Hegemier, G.A. "Mechanics of Reinforced Concrete Masonry: A Literature Survey," AMES-NSF-TR-75-5. San Diego, CA: Univ. of Calif., 1975.

2. Mayes, R.L. and Clough, R.W. "A Literature Survey-Compressive, Tensile, Bond and Shear Strength of Masonry," EERC 75-15. Berkeley, CA: Univ. of Calif., 1975.

3. Agbabian Assoc. *The Response of an Eleven-Story Reinforced-Concrete Masonry Building to Earthquake Ground Motion,* R-3200-2211. El Segundo, CA: AA, 1972.

4. Young, G.A.; Adham, S.A.; and Ts'ao, H.S. *Response of Two Multistory Reinforced-Concrete Masonry Buildings to Earthquake Ground Motion,* P72-131-2410. El Segundo, CA: Agbabian Assoc., 1972.

5. Hegemier, G.A. *Earthquake Response and Damage Prediction of Reinforced-Concrete Masonry Multistory Buildings: A Consortium Proposal for Continued Research to be Conducted under the Sponsorship of the National Science Foundation.* UCSD-8237. San Diego, CA: Univ. of Calif., Oct 1975.

6. Barclay, B.; Clark, J.M.; and Ewing, R.D. *Earthquake Response and Damage Prediction of Reinforced Concrete Masonry Multistory Buildings: Experimental Studies, Numerical Studies, and Computer Program Modifications,* R-7512-1-3908. El Segundo, CA: Agbabian Assoc., Jul 1975.

7. Hegemier, G.A.; Krishnamoorthy, G.; and Nunn, R.O. "An Experimental Study of Concrete Masonry under Seismic Type Loading," NBS Building Sci. Series 106. *Earthquake Resistant Masonry Construction: National Workshop.* Washington, DC: Nat'l Bureau of Standards, Sep 1977.

8. Mayes, R.L. and Clough, R.W. "Cyclic Tests on Concrete Masonry Piers," *Proc. 44th Annual Convention, Struct. Eng. Assn of Calif.* San Francisco: SEAC, 1975, p 26.

9. Esteva, L. "Behavior under Alternating Loads of Masonry Diaphragms Framed by Reinforced Concrete Members," presented at the *Int. Symp. on the Effects of Repeated Loading of Materials and Struc. Elements, R.I.L.E.M., Mexico City, Mexico, Sep 15-17, 1966.*

REFERENCES (CONTINUED)

10. Fattal, S.G. and Cattaneo, L.E. *Structural Performance of Masonry Walls Under Compression and Flexure*. Washington, DC: Nat'l Bureau of Standards, Jun 1976.

11. Mayes, R.L. and Galambos, T.V. "Large-Scale Dynamic Shaking of Eleven-Story Concrete Buildings," in *Proc. 46th Annual Convention of the Struct. Eng. Assoc. of Calif.*, Coronado, Calif., 1977.

12. Blume, J.A.; Sharpe, R.L.; and Elsesser, E. *A Structural-Dynamic Investigation of Fifteen School Buildings Subjected to Simulated Earthquake Motion*. Sacramento, CA: State of Calif. Dept. of Public Works, 1961.

13. Blume, J.A. *The Earthquake Resistance of California School Buildings-Additional Analyses and Design Implications*. Sacramento, CA: State of Calif. Dept. of Public Works, 1962.

14. Rea, D.; Bouwkamp, J.G.; and Clough, R.W. *Dynamic Properties of McKinley School Buildings*, EERC 68-4. Berkeley, CA: Univ. of Calif., Nov 1968. (PB 187 902)

15. Forest Products Lab (FPL). *Diaphragm Action of Full-Scale Diagonally Sheathed Wood Roof or Floor Panels*. Madison, WI: FPL, Apr 1955.

16. Atherton, G.H. and Johnson, J.W. *Diagonally Sheathed Wood Diaphragms*. Corvallis, OR: Oregon Forest Research Lab, Oct 1951.

17. Stillinger, J.R.; Johnson, J.W.; and Overholser, J.L. *Lateral Tests on Full-Scale Lumber-Sheathed Diaphragms*. Corvallis, OR: Oregon Forest Products Lab., Oct 1952.

18. Stillinger, J.R. *Lateral Tests on Full-Scale Lumber-Sheathed Roof Diaphragms*. Corvallis, OR: Oregon Forest Research Lab., Oct 1953.

19. Johnson, J.W. *Lateral Tests on Full-Scale Lumber-Sheathed Roof Diaphragms of Various Length-Width Ratios*. Corvallis, OR: Oregon Forest Research Lab., Oct 1954.

20. Johnson, J.W. *Lateral Tests on 12-by-60 ft and 20-by-80 ft Lumber-Sheathed Roof Diaphragms*. Corvallis, OR: Oregon Forest Research Lab., Oct 1955.

21. Burrows, C.H. and Johnson, J.W. *Lateral Test on Full-Scale Roof Diaphragm with Diamond-Pattern Sheathing*. Corvallis, OR: Oregon Forest Research Lab., Oct 1956.

REFERENCES (CONTINUED)

22. Stillinger, J.R. "Lateral Tests on Full-Scale Lumber and Plywood-Sheathed Roof Diaphragms," in *Symp. on Methods of Testing Building Construction*, ASTM-STP-166. New York: Amer. Soc. of Mech. Eng., 1955.

23. Oregon Forest Labs. (OFL). *Lateral Tests on Full-Scale Lumber and Plywood-Sheathed Roof Diaphragms*. Corvallis, OR: OFL, Mar 1956.

24. Countryman, D. *Lateral Tests on Plywood Sheathed Diaphragms*. Tacoma, WA: Douglas Fir Plywood Assoc. Lab., Mar 1952.

25. Oregon Forest Research Lab. (OFRL). *Lateral Tests on Full-Scale Plywood-Sheathed Roof Diaphragms*. Corvallis, OR: OFRL, Oct 1953.

26. Countryman, D. and Colbenson, P. *1954 Horizontal Plywood Diaphragm Tests*. Tacoma, WA: Douglas Fir Plywood Assoc. Lab., Oct 1954.

27. Douglas Fir Plywood Assoc. (DFPA). *1954 Horizontal Plywood Diaphragm Tests*. Tacoma, WA: DFPA, Jan 1955.

28. Johnson, J.W. *Lateral Test on a 12-by-60 ft Plywood Sheathed Roof Diaphragm*. Corvallis, OR: Oregon Forest Research Lab., Jan 1955.

29. Clark, W.B. and Hange, C.J. "When...the Earth Quakes...You Can Reduce the Danger," *California Geology*, 24:11, 1971, p 203.

30. Lew, H.S.; Leyendecker, E.V.; and Dikkers, R.D. *Engineering Aspects of the 1971 San Fernando Earthquake*, Bldg. Sci. Series 40. Washington, DC: Nat'l Bureau of Standards, Dec 1971.

31. Hudson, D.E. "Strong Motion Seismology," in *Proc. Int. Conf. on Microzonation for Safer Construction Res. and Appl. Seattle, Nov. 1972*, Vol. 1, pp 29-60.

32. Schnabel, P.B. and Seed, H.B. *Acceleration in Rock for Earthquakes in the Western United States*, EERC-72-2. Berkeley: Univ. of Calif. Earthquake Eng. Res. Center, 1972. (PB 213 100)

33. Schnabel, P.B. et al. *SHAKE, A Computer Program for Earthquake Response Analysis of Horizontally Layered Sites*, EERC-72-12. Berkeley: Univ. of Calif. Earthquake Eng. Res. Center, Dec 1972. (PB 220-207)

REFERENCES (CONCLUDED)

34. Shannon & Wilson (SW) & Agbabian Assoc. (AA). *Procedures for Evaluation of Vibratory Ground Motions of Soil Deposits at Nuclear Power Plant Sites*. Seattle, WA: SW & El Segundo, CA: AA, Jun 1975. (NUREG-75/072)

35. Seed, H.B., et al. *Site-dependent Spectra for Earthquake Resistant Design*, EERC-72-12. Berkeley: Univ. of Calif. Earthquake Eng. Res. Center, Nov. 1974. (PB 240-953)

36. Applied Technology Council (ATC). *Recommended Comprehensive Seismic Design Provisions for Buildings, Final Review Draft*, ATC-3-05. Palo Alto, CA: ATC. Jan 1977.

37. Newmark, N.M. and Hall, W.J. "Seismic Design Criteria for Nuclear Reactor Facilities," *Proc. 4th World Conf. on Earthquake Eng., Santiago, Chile*, 1969.

38. Tissel, J.R. *Horizontal Plywood Diaphragm Tests*, Tacoma, WA: Plywood Assoc, 1966.